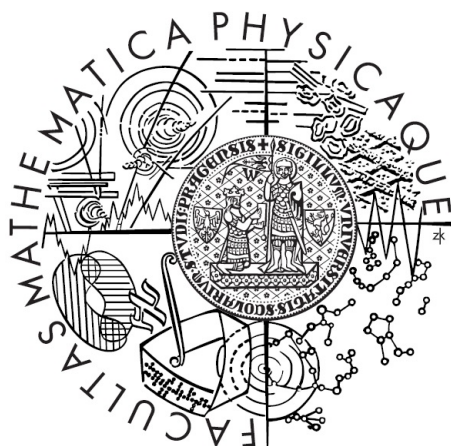


Charles University in Prague  
Faculty of Mathematics and Physics

## BACHELOR THESIS



Miroslav Rapčák

## Ising Model Boundary States from String Field Theory

Institute of Particle and Nuclear Physics

Supervisor of the bachelor thesis: Mgr. Martin Schnabl, Ph.D.

Study programme: Physics

Specialization: General physics

Prague 2013



## **Acknowledgements**

I would like to thank my advisor, Martin Schnabl, for his guidance, useful discussions, and motivating explanations. I am also grateful Matěj Kudrna for discussions and explanation of his code. This thesis is dedicated to my family for their sustained support, especially to my parents, Lenka, and also to my friends.

I declare that I carried out this bachelor thesis independently, and only with the cited sources, literature and other professional sources.

I understand that my work relates to the rights and obligations under the Act No. 121/2000 Coll., the Copyright Act, as amended, in particular the fact that the Charles University in Prague has the right to conclude a license agreement on the use of this work as a school work pursuant to Section 60 paragraph 1 of the Copyright Act.

In ..... date .....

signature of the author

Název práce: Okrajové Stavy Isingova Modelu z Teorie Strunných Polí

Autor: Miroslav Rapčák

Katedra: Ústav jaderné a částicové fyziky

Vedoucí: Mgr. Martin Schnabl, Ph.D., Fyzikální ústav AV ČR

Abstrakt: Isingův model je jedním z nejstudovanějších modelů statistické fyziky. V této práci shrnujeme metody užívané k jeho řešení a soustředíme se na stav při kritické teplotě, kdy je systém popsitelný metodami konformní teorie pole (CFT). Konformní teorie pole vnáší nový vhled do problému a umožňuje klasifikaci tříd univerzality či relativně snadný výpočet korelačních funkcí v případě dvou dimenzí. CFT také umožňuje studium okrajových efektů a defektů na mřížce. Kritický systém s hranicí lze obvykle popsat metodami CFT s konformně invariantní okrajovou podmínkou. Klasifikace všech konformních teorií pole s hranicí zůstává stále otevřeným problémem.

Diskutujeme detailně metodu vyvinutou nedávno ve strunové teorii pole (SFT) přicházející s novým přístupem a ilustrujeme ji na příkladu Isingova modelu. Z každého řešení pohybových rovnic SFT lze zkonstruovat okrajový stav popisující konzistentní okrajovou podmínku. V této práci formulujeme SFT Isingova modelu, numericky nalezneme nová řešení a zkonstruujeme jim odpovídající okrajové stavy. Vyhneme se tak řešení komplikovaných sešívacích podmínek a získáme velmi dobrou shodu s exaktním řešením. Narozdíl od metody renormalizační grupy limitované  $g$ -teorémem ukazujeme, že lze zkonstruovat také stavy s vyšší energií. Konformní defekty a korespondence dvojitého Isingova modelu s bosonem na  $S^1/Z_2$  orbifoldu je také diskutována. Práce rozšiřuje diskuzi připravovaného článku [1].

Klíčová slova: Isingův model, hranice, konformní teorie pole, teorie strunných polí

Title: Ising Model Boundary States from String Field Theory

Author: Miroslav Rapčák

Department: Institute of particle and nuclear physics

Supervisor: Mgr. Martin Schnabl, Ph.D., Institute of physics AS CR

Abstract: The Ising model is widely studied model in statistical physics. In this thesis, we review methods used to solve it and we concentrate on the state at the critical temperature, where the system exhibits phase transition and can be described by means of conformal field theory (CFT). This description comes with a new insight into the problem and enables to study boundary effects. Critical behavior for systems with boundaries is often described by conformally invariant boundary conditions. Classification of all boundary CFTs still remains an open problem.

We discuss methods developed recently in string field theory (SFT) proposing a new approach and we illustrate it on the Ising model. Knowing a solution to the SFT equations of motion, one can construct corresponding boundary state describing consistent conformally invariant boundary condition. We have formulated SFT for the Ising model, found new solutions numerically, and constructed corresponding boundary states. This procedure avoids solving difficult sewing constraints and results agree with exact values. Unlike the renormalization group approach, where we are limited by the  $g$ -theorem, we can construct also states with higher energy. Conformal defects and correspondence with free boson on  $S^1/Z_2$  orbifold is also discussed. This thesis is based on forthcoming paper [1].

Keywords: Ising model, boundary, conformal field theory, string field theory

# Contents

<b>Introduction</b>	<b>3</b>
<b>1 The Ising model</b>	<b>7</b>
1.1 Critical phenomena . . . . .	7
1.2 Models of ferromagnetism . . . . .	7
1.3 Renormalization group . . . . .	14
1.4 Solution to the 1D model . . . . .	16
1.5 Ising model in two and higher dimensions . . . . .	18
1.6 Boundary problems . . . . .	20
<b>2 Conformal field theory</b>	<b>25</b>
2.1 Quantum field theory description . . . . .	25
2.2 Conformal invariance . . . . .	27
2.3 Primary operators . . . . .	30
2.4 Stress-energy tensor . . . . .	32
2.5 Operator formalism . . . . .	36
2.6 Examples of CFTs . . . . .	42
2.6.1 Free boson . . . . .	42
2.6.2 Free fermion . . . . .	45
2.6.3 bc-ghost system . . . . .	46
2.7 The Ising model as a minimal model . . . . .	47
2.8 Double Ising and bosonization . . . . .	50
<b>3 Boundary CFT</b>	<b>53</b>
3.1 Boundary conditions and Ishibashi states . . . . .	53
3.2 Boundary fields . . . . .	55
3.3 Sewing constraints . . . . .	57
3.3.1 Crossing symmetry . . . . .	58
3.3.2 Modular invariance . . . . .	59
3.3.3 Cardy's condition . . . . .	61
3.3.4 Boundary crossing symmetry . . . . .	62
3.3.5 Open-open-closed amplitude . . . . .	63
3.3.6 Open-closed-closed amplitude . . . . .	63
3.4 Solving the Ising model BCFT . . . . .	64
3.5 Folded models . . . . .	67
<b>4 String Field theory</b>	<b>71</b>
4.1 Bosonic open string theory . . . . .	71
4.2 Witten's cubic string field theory . . . . .	72
4.3 Boundaries and Sen's conjectures . . . . .	74
4.4 Ellwood invariants . . . . .	75
4.5 Level truncation method . . . . .	78
4.6 Conservation laws . . . . .	80

<b>5</b>	<b>Boundary states construction</b>	<b>87</b>
5.1	The Ising model SFT . . . . .	87
5.2	Truncated action for the Ising model . . . . .	88
5.2.1	Solutions on the $\sigma$ -brane . . . . .	89
5.2.2	Solutions on the $\mathbb{1}$ -brane and $\epsilon$ -brane . . . . .	93
5.3	Algorithm details . . . . .	95
5.4	Double Ising model . . . . .	98
	<b>Conclusion</b>	<b>103</b>
	<b>Bibliography</b>	<b>105</b>
	<b>List of Abbreviations</b>	<b>113</b>



# Introduction

The Ising model [2] is widely studied statistical model of ferromagnetism. Even though it is quite a simple model, it undergoes a phase transition at the critical temperature and therefore serves as a useful toy model for the study of critical phenomena. A lot of progress has been made in the past (see textbooks [3, 4]), but still many open questions remain. Physicists often claim that solving the Ising model in three dimensions is one of the most challenging tasks in modern physics. Critical phenomena is an attractive subject since standard methods of statistical physics, such as perturbative expansions, break down and new interesting features appear. Key feature is the universality. Different models share the same critical behavior. At the critical temperature a model can be characterized by just a few parameters in contrast with variety of possible couplings of the original model [6]. At the critical point many quantities become divergent, such as correlation length. Fluctuations spread up, and the model originally defined on a lattice with nearest neighbor interactions suddenly develops long range correlated behavior [5]. In this mode a theory becomes scale invariant and with some other natural assumptions the symmetry extends to the full conformal invariance. The whole theory can be then formulated in the language of conformal field theory (CFT) [7].

CFT becomes most powerful in 2 dimensions, where the conformal group is infinite dimensional and the conformal invariance thus restrictive enough to enable solving exactly even nontrivial interacting models [8]. Apart from the applications in statistical physics, CFT is an interdisciplinary subject with connections to many other branches of physics and mathematics. CFT provides fundamental background for studying string theory [9] and even its intrinsic mathematical structure is interesting in its own. Using CFT in two dimensions, one can study two dimensional interacting quantum field theories nonperturbatively and thus get some insight into the physics of strongly interacting systems.

One can add a boundary to a given bulk CFT and impose some boundary condition on this boundary [10]. Inclusion of such a boundary is necessary when studying finite size lattices in statistical physics and it is also important for the formulation of the string theory in covariant gauge. An open string can be stretched between different D-branes corresponding to different boundary conditions for the worldsheet bosons [11]. Moreover, studying boundaries in the tensor products of simple CFTs (folded models) is related to the defects in lattices. In CFT with a boundary (often called boundary conformal field theory or BCFT) new features appear. One of the most interesting question is classification of all possible consistent boundary conditions preserving conformal invariance for a given bulk CFT. The previous statement can be reformulated as classifying all possible BCFT's for a given CFT. Precisely this question will be addressed here in detail.

Different consistent boundary conditions can be associated with different boundary states [12]. In the past, Cardy found the solution for boundary states in the case of rational models, and in particular for the Ising model. Unfortunately, a solution for the irrational models (e.g. free boson on the torus, or the tensor product of minimal models) has not yet been found in general. An important exception is the case of the folded Ising model, where one can use The only progress in this direction has been made in the case of folded Ising model, where one can

use a duality with the free boson on the orbifold to find the boundary states [13].

Assume that we are given a CFT with particular boundary condition and we know all 2-point and 3-point functions in the theory (we have solved the model in given BCFT background). With the use of the renormalization group (RG), one can construct other consistent boundary conditions deforming the theory by a relevant boundary operator and flowing to the infrared, or by marginal deformations of the original theory [14]. Many methods, such as thermodynamical Bethe ansatz, scattering matrices or truncated conformal space approach, have been developed to address this issue [15]. All the methods based on the RG flows have huge limitation given by g-theorem. It states that boundary entropy must decrease along the RG flow. It leads to inability to find all the theories with higher boundary entropy than the entropy of the original background.

String field theory[16] (SFT) comes with new methods to address these problems. In 1999, Sen conjectured that solitonic solutions in SFT correspond to different D-brane configurations [17, 18]. If we believe in consistency of SFT, these solutions must correspond to consistent boundary conditions (D-branes) and due to recent developments in string theory, we can construct corresponding boundary states. Moeller, Sen, Zwiebach [81] developed a numerical method that is powerful in attempts to find solutions to the SFT equations of motion. Having a solution we wish to find corresponding boundary state. The progress has been made by construction of gauge invariant observables [20, 21] in open string field theory, proposing Ellwood's conjecture [22] and its recent generalization due to Maccaferri, Schnabl and Kudrna [23]. Thanks to these tools, we can give physical interpretation to an arbitrary solution by computing coefficients of its boundary state.

This thesis is based on the paper with collaborators, Matěj Kudrna and Martin Schnabl, where we construct all boundary states for the Ising model numerically by means of string field theory and illustrate the recently developed methods on this simple model [1]. The first numerically stable solution with positive energy has been found. We briefly address extension to the double Ising model. Even though the presented results are known only numerically, there has been a huge progress in finding analytic solutions since 2005 following [24] and we believe that analytic solutions of string field theory describing different boundary conditions of the Ising model will be found soon. Here we will extend discussion from [1] and give detailed discussion of the computations starting from very elementary notions of CFT, the Ising model and string theory. In addition to the content of our paper, we discuss conservation laws for higher weight primaries in folded models that can lead to the identification of the other boundary states in the double Ising model. The existence of new solutions is hinted and the discussion is supported by many pictures, graphs, and tables.

This thesis is organized as follows. In the first chapter we elaborate on the importance of the Ising model and briefly discuss some methods used to deal with the model. In the second chapter we present necessary notions from CFT. We also give brief discussion of the free boson, free fermion, and bc-ghost system as examples. The Ising model CFT is discussed at the end of this chapter. The third chapter is dedicated to discussion of BCFT. We give Cardy's solution for the boundary states and discuss folded models briefly. In the fourth chapter, we address basic ideas of SFT constructing its action, describing level truncation

method and Ellwood invariants. In the last chapter we formulate SFT for the Ising model, comment on the computation of truncated action, find solutions and determine its Ellwood invariants that lead to the interpretation of the discovered solutions. We also discuss the double Ising model and give numerical results obtained by our C++ code.



# 1. The Ising model

## 1.1 Critical phenomena

During a phase transition, a system undergoes huge changes in its properties. Phase transitions are interesting phenomena with many peculiarities that are not yet well understood despite enormous progress in this field throughout the twentieth century. There is enormous literature considering this topic, for example [3, 4, 5]. This section reviews basic notions in this field.

Phase transitions can be divided into two broad categories. To the first category of so called *first order phase transitions*, belong processes involving a latent heat, that is absorbed or released precisely at the transition point. Correlation length of the system that characterizes fluctuations and long-range behavior remains finite. There exist mixed-phase regimes, in which some parts of the system have completed the transition and the rest part is still in the initial configuration. For example, freezing of water or Bose-Einstein condensation are examples of the first order phase transition.

Second class consists of the *continuous* (sometimes called second order or critical) *phase transitions*. There is nothing like latent heat for these phenomena and correlation length (together with heat capacity, isothermal susceptibility and other quantities) becomes divergent at the critical point. These systems are often more difficult to be described. Ferromagnetic transitions, superconductors or superfluid transitions belong to this category.

One of the most interesting features of the critical phenomena is its *universality* (see nice review [6]). Systems that seems to be totally different have often the same critical behavior. Criticality erases many possible inputs in the model and only a few relevant quantities are enough to describe criticality. All physical systems fall into a few universality classes characterized by different critical exponents.

Another feature of the critical phenomena is the scaling hypothesis. It has been introduced by Fisher, Kadanoff, and others and it was supported by wide range of experiments and computations on the model systems [25, 26]. Scaling hypothesis states that singular part of the free energy is degree  $a$  homogenous function of its variables. Since thermodynamical potential is homogenous function of degree  $a$  and all the other properties can be found as derivatives of this potential, they are also degree  $a'$  homogenous function for some  $a' \neq a$ . We will come back to this hypothesis later, when focusing on ferromagnetic materials and the Ising model. Scaling hypothesis gives us relations between critical exponents and only few parameters remain to be relevant and cannot be computed using this hypothesis. To find the remaining critical exponents and even to find the critical point, renormalization group (RG) is widely used tool [27, 28].

## 1.2 Models of ferromagnetism

As a model system of the critical phenomena we will use a magnetic material. Atoms of a crystal lattice carry a magnetic moment, due either to the spin of the electron or to electron's motion around the atom nucleus. At the high

temperature phase, these magnetic moments are randomly oriented and average magnetization of the lattice is zero. If we lower the temperature and reach the critical point  $T_c$  (Curie temperature), new phase occurs. In the so-called ferromagnetic materials, magnetic moments tend to get aligned and the total magnetization of the material is non-vanishing below the critical temperature  $T_c$ . At the temperature  $T_c$  the material undergoes second order phase transition.

To describe the phase transition, one needs an *order parameter* that enables us to recognize the phase of the system. In the case of magnetic dipoles  $\vec{\sigma}_i$  on the lattice, total magnetization  $\vec{M} = \sum_i \vec{\sigma}_i$  plays the role of the order parameter since it vanishes at high temperatures and becomes nonvanishing below the critical temperature.

The simplest model of the phase transitions that can be solved analytically at least in one and two dimensions and is still quite realistic is the Ising model. The simplification is obtained by considering only one direction and two discrete values of the spin  $\sigma_i = \pm 1$  in this direction. Naturally, the Ising model Hamiltonian has following form

$$\mathcal{H}(\{\sigma_i\}) = -J \sum_{(i,j)} \sigma_i \sigma_j - B \sum_i \sigma_i, \quad (1.1)$$

where the first sum runs over all nearest neighbors  $(i, j)$ ,  $J$  is interaction constant and  $B$  external magnetic field. For the ferromagnetic materials  $J > 0$  unlike in the case of anti-ferromagnetics. One configuration of two-dimensional Ising model is visualized in the figure 1.1.

The Ising model was originally introduced by Wilhelm Lenz (1920) and solved in one dimension by his PhD student Ernst Ising in 1925 [2]. Since that time, many scientists have been involved in studying properties of this beautiful model. Big progress has been made by Kramers and Wannier [29] who managed to determine the critical temperature of the two dimensional Ising model and thus proved existence of the phase transition at nonzero temperature. Fundamental contribution

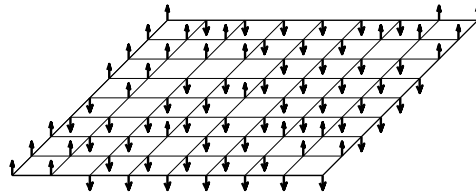


Figure 1.1: Ising model lattice with random configuration of spins.

came in 1944 with Lars Onsanger [30], who found the solution for the partition function with zero external magnetic field in two dimensions. Onsanger's solution has been simplified by others, like Kaufmann and Baxter. Computation of spontaneous magnetization, magnetic susceptibility, correlation functions, and analysis of general lattices followed. Since 1990, new progress in solving Ising model appeared with the help of quantum field theory methods and S-matrix formalism originally proposed in this context by Zamolodchikov [31]. With these methods, a spectrum of excitations of two-dimensional Ising model with external magnetic field has been found and correlation functions calculated (Delfino, Mussardo, Simonetti) [32, 33].

Unfortunately, despite numerous attempts, solution for the model in three dimensions is still lacking. Many physicists consider the problem of solving the Ising model in three dimensions to be one of the most interesting open problems in theoretical physics. Due to computer advances in recent years, numerical

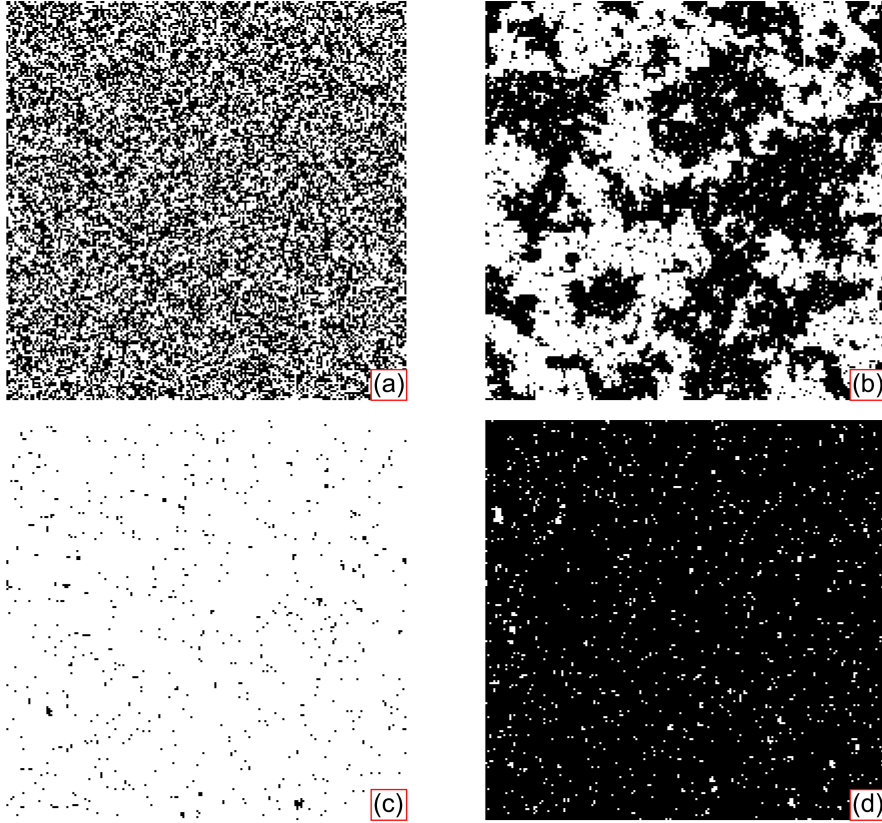


Figure 1.2: Configurations of spins on the Ising lattice under four different circumstances obtained by Monte Carlo simulation on the lattice of  $200 \times 200$  spins. The first picture (a) shows high temperature disordered phase. The upper-right picture (b) shows the critical phase with long-ranging clusters of the same spins. The two bottom pictures (a) and (b) shows the system near the two energy minima in the low temperature regime.

simulations and series expansions enabled to predict properties of the critical behavior with very good accuracy.

Numerically, the Ising model is commonly studied by means of Monte Carlo simulations [34]. Having a lattice of  $N \times N$  spins and starting from arbitrary initial configuration we can generate a sequence of new configurations (Markov process). The simulation consists of two steps that are still repeating:

1. suggesting a flip of random spin and
2. accepting it with probability  $e^{-\beta \Delta \mathcal{H}}$ ,

where we have denoted  $\Delta \mathcal{H}$  the energy difference caused by the flip and  $\beta$  is the inverse temperature. When the thermodynamical equilibrium is reached (the dependence on the initial configuration is suppressed), one can measure current quantities on the simulated system and compute its time average after performing a few steps. New configurations are then generated with Boltzmann distribution and the time average is precisely the Boltzmann-weighted statistical average.

We have created a program simulating the Ising model in 2D and performed the simulation on the lattice of  $200 \times 200$  spins with periodic boundary conditions. Main features of the model can be easily understood on the simulated system.

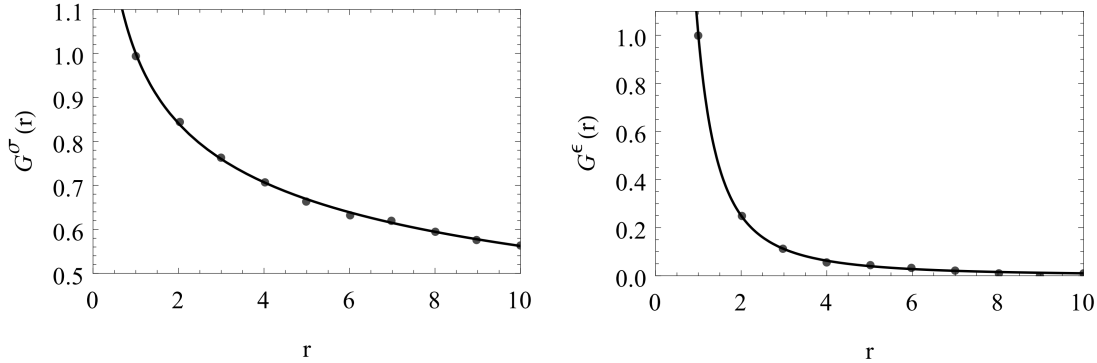


Figure 1.3: Two-point functions of the spin  $\sigma$  and energy density  $\epsilon$ . The points showing values obtained on the simulated system and corresponding exact curve for the model in the thermodynamic limit.

With the help of these simulations, average magnetization, susceptibility, energy density, heat capacity, and other quantities can be easily computed as time average of corresponding quantities currently measured on the simulated systems.

In the figure 1.2, four different states of the simulated systems are shown. Black points correspond to the spin up and the white points correspond to the spin down. There is a high temperature phase, where all the spins are almost random. In this phase, the entropy maximization is the leading effect. The second picture shows the system at the critical temperature. We can see long range domains spreading almost along the whole lattice. The behavior of the spins becomes collective, correlation length diverges, and the system is scale invariant at scales much bigger than the lattice spacing. The system undergoes fractal-like behavior. The last two cases correspond to the low temperature phase. At low temperatures the system tends to be in the minimum energy configuration. There are two such configurations if no external field is switched on. The energy minimum is then degenerated and the system can fall into the configuration with all spins up or all spins down. These two cases are visualized in the last two pictures. Since the temperature is not precisely zero, some spins can be excited.

We have also measured the correlation functions for the spin variable  $\sigma$  and the energy density  $\epsilon$ . The results are shown in the figure 1.3. We have performed regression with the function of the form

$$G^i(r) = a + \frac{b}{r^{2\Delta_i}} \quad (1.2)$$

where  $\Delta_i$  has been kept fixed to precise value and parameters  $a$  and  $b$  have been found. We performed normalization of the two-point function to set  $b = 1$ .  $\Delta_i$ s are scaling dimensions of the operators. These values  $\Delta_\sigma = \frac{1}{8}$  and  $\Delta_\epsilon = 1$  are exactly computable using methods of statistical physics and we will see how they emerge in the conformal field theory. We can see quite a good agreement of the simulated data and exact values despite finite size effects and finite number of sites in the simulated system. To obtain our results, we took an average of 50 000 current values at 10 different lattice points.

It is evident that description of the system near the absolute zero or at high temperatures can be easily performed using perturbative expansions. There is wide range of tools to study this cases generally and we will make a comment



on them later. Much more interesting is the critical phase, where new features emerge and the perturbative treatment fails.

Apart from the description of magnetic properties, the Ising model can be reinterpreted as a model of gas on the lattice. The Ising model is thus a toy model of gas atoms with short-range interaction. The Ising model is very universal and one can also find its applications going beyond the physics. For example, it is a model used in economics to explain correlations in the social structures.

Many generalizations of the Ising model are known [5]. Let us name some of them. Direct extension of the Ising model is the Potts model. Spin at each site can have  $q$  discrete values, i.e.  $1, 2, \dots, q$  and contribution of the neighboring pairs to the energy is non-vanishing only if their spins equal. More realistic generalization is the  $O(n)$  model, where spin  $\vec{\sigma}_i$  is an  $n$ -component unit vector and interaction of two spins in the Hamiltonian is given by the inner product of the two vectors. Another important model is the tri-critical Ising model describing a magnetic material with vacancies. There are 3 possible configurations at each site  $\sigma_i = \pm 1, 0$  and a new term  $-\mu \sum_i (\sigma_i)^2$  is added to the Ising model Hamiltonian (1.1). There have been many models invented, but their description is behind the scope of this thesis. Many methods developed for solving the Ising model can be extended to these generalizations.

There are many quantities characterizing the ferromagnetic material. They usually diverge with some power as the temperature approaches the critical value  $T \rightarrow T_c$ . Exponents in this dependence are called *critical exponents*. We will denote relative displacement from the critical point as  $t = (T - T_c)/T_c$ . An example of quantities characterizing ferromagnets is the spontaneous magnetization

$$\mathcal{M}(B, t) = -\frac{\partial F}{\partial B} \quad (1.3)$$

with corresponding scaling behavior

$$\mathcal{M}(0, t) \propto (-t)^\beta, \quad (1.4)$$

in the limit  $t \rightarrow 0^-$ . Another important exponent characterizing the dependence on the magnetic field  $B$  is  $\delta$ , defined as

$$|\mathcal{M}(B, 0)| \propto |B|^{1/\delta}. \quad (1.5)$$

Performing one more derivative, one finds the next thermodynamical function, magnetic susceptibility, with critical exponent  $\gamma$

$$\chi(B, t) = \frac{\partial \mathcal{M}(B, t)}{\partial B}, \quad |\chi(0, t)| \propto |t|^{-\gamma}. \quad (1.6)$$

Derivative of the internal energy  $U$  gives us heat capacity with corresponding scaling

$$C(t) = \frac{1}{T_c} \frac{\partial U}{\partial t}, \quad |C(t)| \propto |t|^{-\alpha}. \quad (1.7)$$

So far, we have defined critical exponents  $\alpha, \beta, \gamma, \delta$ . For the definition of the other two, we will need a *correlation function*. Consider an infinite lattice of spins  $\sigma_i$  associated with sites  $i$ . Average alignment of the spins situated at sites  $i$  and

---



---

$\mathcal{M}(0, t) \propto (-t)^\beta$	$ \mathcal{M}(B, 0)  \propto  B ^{1/\delta}$	$ \chi(0, t)  \propto  t ^{-\gamma}$
$ C(t)  \propto  t ^{-\alpha}$	$C_c(r, 0) \propto \frac{1}{r^{d-2-\eta}}$	$ \xi(B, t)  \propto  t ^{-\nu}$

---



---

Table 1.1: All the critical exponents introduced for ferromagnets.

$j$  is characterized by the two-point correlation function, i.e. thermal average of the product of corresponding spins

$$C^\sigma(i, j) = \langle \vec{\sigma}_i \cdot \vec{\sigma}_j \rangle. \quad (1.8)$$

For systems in the thermodynamic limit this function is usually translationally and rotationally invariant if we study it on the scales much bigger than lattice spacing  $a$ . Then we can write just  $C(r)$ , for  $r = |i - j|$ . If we are rather interested in relative fluctuations in the ordered phase, it is convenient to subtract their mean value  $\vec{\sigma}_0 = \langle \vec{\sigma}_i \rangle$  and define connected correlation function

$$C_c^\sigma(r) = \langle (\vec{\sigma}_i - \vec{\sigma}_0) \cdot (\vec{\sigma}_j - \vec{\sigma}_0) \rangle = \langle \vec{\sigma}_i \cdot \vec{\sigma}_j \rangle - |\vec{\sigma}_0|^2. \quad (1.9)$$

Clearly, for a system with local interactions, nearby sites will be correlated and the correlation will decrease with a distance. Dependence on the distance is typically exponential

$$C_c^\sigma(r) \propto e^{-r/\xi}, \quad (1.10)$$

where we have introduced the correlation length  $\xi$ . The correlation length measures typical size of the correlated domains of spins. The larger the correlation is, the larger clusters of the same spins can be suspected. Precisely at the critical temperature  $T_c$ , the correlation length diverges and the  $r$ -dependence becomes power law

$$C_c^\sigma(r) \propto \frac{1}{r^{d-2+\eta}}, \quad (1.11)$$

where  $\eta$  is the new critical exponent. Divergence of the correlation length  $\xi$  is given by the exponent  $\nu$

$$|\xi(t)| \propto |t|^{-\nu}. \quad (1.12)$$

Generally, the multiplicative constant standing in front of the right sides of (1.6), (1.6) and (1.6) can be different for positive and negative values of  $t$ .

Totally, we have defined 6 critical exponents, but they are not all independent. Due to the scaling hypothesis, there exist 4 relations between them and only two parameters remain to be determined. The 4 relations read

$$\begin{aligned} \alpha + 2\beta + \gamma &= 2, & \alpha + \beta\delta + \beta &= 2, \\ \nu(2 - \eta) &= \gamma, & \alpha + \nu d &= 2, \end{aligned} \quad (1.13)$$

and can be derived using the scaling hypothesis and fluctuation dissipation theorem. Introduction of the scaling hypothesis led to huge developments in statistical physics. It was originally introduced as consequence of experimental data and behavior of some statistical models and conjectured to be general fact for all critical phenomena. We will sketch its proof later when talking about renormalization group. Due to the scaling hypothesis, thermodynamic potential is degree

$y$  homogenous function of its variables, for some  $y \in \mathbb{R}$ . For instance, in the case of magnetic materials, density of the Gibbs energy scales as

$$g(t, B) = \lambda^{-d} g(\lambda^{y_t} t, \lambda^{y_B} B), \quad (1.14)$$

where  $d$  is dimension of the lattice and we have introduced scaling exponents  $y_t$  and  $y_B$ . Let us illustrate how the relations (1.13) emerge. Substituting  $\lambda = t^{-1/y_t}$  into the equation above, one finds

$$g(t, B) = t^{\frac{d}{y_t}} g(1, t^{-\frac{y_B}{y_t}} B) \quad (1.15)$$

and for  $h = 0$ , we get scaling

$$g(0, t) \propto t^{\frac{d}{y_t}}. \quad (1.16)$$

From this relation, one can easily obtain scaling of the heat capacity performing two derivatives with respect to  $t$ . If we look at the table 1.1 defining the various scaling coefficients, we find that scaling of the heat capacity is given by parameter  $\alpha$  and we find a relation

$$\alpha = 2 - \frac{d}{y_t}. \quad (1.17)$$

Analogously, one can find relations for the other critical exponents and eliminating  $y_t$  and  $y_B$  leads to the relation between the critical exponents. It is then clear that only two parameters (corresponding to  $y_t$  and  $y_B$ ) are relevant and different values of  $y_t$  and  $y_B$  characterize different universality classes.

Not all relations can be derived using above procedure. Some formulas relating  $r$ -dependence on the lattice and thermodynamic quantities can be derived using fluctuation-dissipation theorem relating linear response of the system and fluctuations of the local quantities in general. For example, we find that

$$\begin{aligned} \chi &= \frac{\partial \mathcal{M}(B, t)}{\partial B} = \beta \sum_{i,j} \left( \langle \vec{\sigma}_j \vec{\sigma}_i \rangle - |\langle \vec{\sigma}_i \rangle|^2 \right) \\ &= \beta \sum_{i,j} C_c^\sigma(|i-j|) \approx \int dr r^{d-1} \frac{1}{r^{d-2+\eta}} f\left(\frac{r}{\xi}\right) \\ &\propto \xi^{2-\eta}, \end{aligned} \quad (1.18)$$

where we have approximated the sum by an integral and substituted for  $C_c^\sigma$  at the critical point with regulator  $f\left(\frac{r}{\xi}\right)$  that cuts off the divergence of the integral and enables to deal with it. Finally, substituting  $\chi \propto t^{-\gamma}$  and  $\xi \propto t^{-\nu}$  one finds relation

$$\nu(2 - \eta) = \gamma. \quad (1.19)$$

With a similar procedure, one can derive critical exponent also for the energy density  $\epsilon_i = \sum_j J_{ij} \sigma_i \sigma_j + h \sigma_i$ , where

$$C_c^\epsilon(r) = \langle \epsilon_i \epsilon_j \rangle - |\epsilon_0|^2 \propto \frac{1}{r^{2\Delta_\epsilon}}. \quad (1.20)$$

Performing the same procedure one finds a relation

$$\nu = 2 - \Delta_\epsilon. \quad (1.21)$$

These two relations will lead us to the identification of the Ising model in conformal field theory.

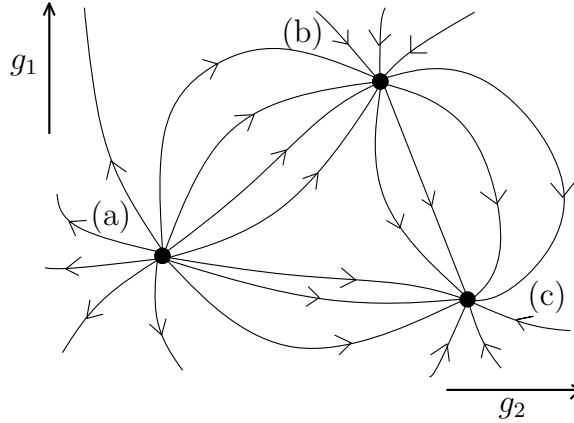


Figure 1.4: RG flow in the two dimensional manifold of interaction constants  $(g_1, g_2)$ . Three types of fixed points are shown: (a) corresponds to an unstable point with all directions relevant, (b) corresponds to a mixed fixed point, and (c) corresponds to a stable fixed point with all directions irrelevant.

### 1.3 Renormalization group

In this section, we will introduce powerful tool to study critical points of a system, i.e. the *renormalization group* (RG) [6, 27, 28]. One can think of it as a process during which we are looking at the system with different magnifying glasses. Studying a system at some length-scale one can integrate out degrees of freedom playing role on much smaller distances and obtain effective description on the new length scale with some new effective Hamiltonian.

Starting from the initial lattice, one can group together some amount of neighboring spins and assign to each such a group one new spin obtained from the original spins. We get new lattice with new spins that effectively describe the original system on larger distances. It is not difficult to construct a projection from the original lattice to the new one, but there are many possibilities and it is not at first sight clear, whether they are equivalent. It can be shown that (up to some pathological cases) results do not depend on the choice of the projection. To get correct description on the new lattice we must construct new (renormalized) effective Hamiltonian for the system of new spins to get the same partition function and thus the same thermodynamics. It is necessary to extend the original Hamiltonian by adding new terms with possibly vanishing coupling constants  $g = (g_1, g_2, \dots)$  so that the renormalized Hamiltonian has the same functional form but with different coupling constants.

We wish to go on with the procedure and construct new lattices of spins using the same projection again and again. With this procedure we obtain new renormalized Hamiltonians with different coupling constants  $g^0 \rightarrow g^1 \rightarrow g^2 \rightarrow \dots$ . One can visualize this sequence as RG flow on the manifold of coupling constants as you can see in the figure 3.3, where only two coupling constants are shown for simplicity.

Since the renormalization corresponds to looking at the system within bigger length scale when lattice spacing changes as  $a \rightarrow \lambda a$ , correlation length must renormalize as

$$\xi(g') = \lambda^{-1} \xi(g) \quad (1.22)$$

since it is measured with respect to the new lattice spacing. There can exist special points on the manifold of coupling constants called RG *fixed points*  $g^*$  that are kept fixed under the action of renormalization group  $g'^* = g^*$ . In this case we have  $\xi(g^*) = \lambda^{-1}\xi(g^*)$  for  $\lambda > 1$  and correlation length must vanish or it must be divergent. The points in the first case are called trivial fixed points whereas the other category contains *critical points*, since correlation length is divergent. Finding all the critical points for a given system now reduces to finding all fixed points of the RG on the manifold of coupling constants.

Fixed points can be divided into three categories by their stability. After a small displacement from the fixed point, the RG can flow back to the original fixed point (attractive points), it can move away to a different point (repulsive fixed point) or it can be mixed, i.e. attractive in some directions and repulsive in the others. We wish to characterize the directions at fixed points.

Consider a small perturbation of coupling constants  $g = g^* + \delta g$ . If we denote RG transformation as  $g' = \mathcal{R}(g)$ , then after performing the RG transformation, one finds infinitesimal transformation

$$g^* + \delta g' = g^* + \mathcal{K}\delta g. \quad (1.23)$$

We obtained linearized version of the RG transformation with matrix of coefficients

$$\mathcal{K}_{ab} = \frac{\partial \mathcal{R}_a}{\partial g_b}. \quad (1.24)$$

Denoting  $k^i$  its eigenvalues and  $\Delta_a^i$  its left eigenvectors, we can define so-called *scaling variables*

$$u_i = \sum_a \Delta_a^i \delta g_a \quad (1.25)$$

that have nice scaling transformation properties under the action of the RG

$$u'_i = \sum_a \Delta_a^i \delta g'_a = \sum_{a,b} \Delta_a^i \mathcal{K}_{ab} \delta g_b = \sum_b k^i \Delta_b^i \delta g_b = k^i u_i. \quad (1.26)$$

Since we have denoted  $b$  the scaling parameter of the lattice spacing, it is usual to parametrize  $k^i$  as  $k^i = \lambda^{y_i}$ . Quantities  $y_i$  determine critical exponents that can be computed from the knowledge of the matrix  $\mathcal{K}$ . Scaling variables  $u_i$  can be divided into the three classes with the help of the formula (1.26)

1.  $y_i > 0$  Relevant variables corresponding to the unstable directions.
2.  $y_i < 0$  Irrelevant variables corresponding to the stable directions.
3.  $y_i = 0$  Marginal variables that do not change under the RG action.

If we wish to construct new critical points, we can make a perturbation of the original Hamiltonian by some relevant variable and flow to the infrared. If we deform the theory by a marginal variable, one gets continuous spectrum of critical points and the corresponding set on the manifold of coupling constants is called *critical surface*. Irrelevant perturbations do not change properties of the critical behavior and if we study criticality, we can restrict our attention only to the relevant and marginal perturbations.

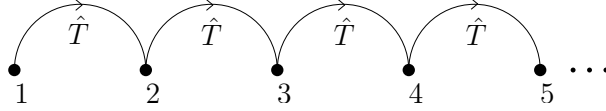


Figure 1.5: Transfer matrix performing a transfer between neighboring sites.

Now, we will prove scaling hypothesis in the case of magnetic material with relevant parameters  $t$  and  $h$ . Partition function does not depend on the renormalization and we can write

$$e^{-\beta N f(g)} = Z = Z' = e^{-\beta' N \lambda^{-d} f(g')}, \quad (1.27)$$

where  $f$  is the free energy density,  $N$  is the number of sites in a lattice, and the third equality introduces the renormalized free energy. Since we know the scaling properties of coupling constants  $t' = \lambda^{y_t} t$  and  $B' = \lambda^{y_B} B$  at the critical point, we find the scaling hypothesis

$$f(t, B) = \lambda^{-d} f(\lambda^{y_t} t, \lambda^{y_B} B). \quad (1.28)$$

RG provides a technique how to determine  $y_i$ . Looking at the table 1.1 and relations similar to (1.17), we find that RG enables us to find all the critical exponents.

## 1.4 Solution to the 1D model

There are many approaches to solve a linear chain of Ising spins. One can solve it recursively or by series expansion which we will discuss in the next section in the case of 2D model briefly. Here, we will review transfer matrix method discussed in [5], which also generalizes to the two-dimensional case. The other approaches are discussed for example in [3, 4, 5]. Moreover, we will come across with the problem of boundaries that will be addressed in more detail later.

Let us assume we are given a Hamiltonian of the form (1.1) for a chain of  $N$  spins and let us implement periodic boundary condition  $\sigma_i = \sigma_{N+i}$ . Our goal is the computation of partition function

$$Z = \sum_{\{\sigma_i\}} e^{-\beta \mathcal{H}(\{\sigma_i\})}. \quad (1.29)$$

It can be rewritten as

$$Z = \sum_{\{\sigma_i\}} \prod_{i=1}^N \exp \left[ \mathcal{J} \sigma_i \sigma_{i+1} + \frac{1}{2} \mathcal{B} (\sigma_i + \sigma_{i+1}) \right], \quad (1.30)$$

where we have denoted  $\mathcal{J} = \beta J$  and  $\mathcal{B} = \beta B$ . Now, let us define the transfer matrix

$$\hat{T} = \begin{pmatrix} e^{\mathcal{J} + \mathcal{B}} & e^{-\mathcal{J}} \\ e^{-\mathcal{J}} & e^{\mathcal{J} - \mathcal{B}} \end{pmatrix}, \quad (1.31)$$

whose elements are given by the factors appearing in (1.30). The transfer matrix is acting on a two dimensional space of spin up and down states. Denote  $|+\rangle$

and  $|-\rangle$  base vectors corresponding to the spin states. Partition function can be reexpressed using quantum theory notation as

$$Z = \sum_{\{\sigma_i\}} \langle \sigma_1 | \hat{T} | \sigma_2 \rangle \langle \sigma_2 | \hat{T} | \sigma_3 \rangle \cdots \langle \sigma_N | \hat{T} | \sigma_1 \rangle = \sum_{\sigma_1 = \pm} \langle \sigma_1 | \hat{T}^N | \sigma_1 \rangle = \text{Tr } \hat{T}^N, \quad (1.32)$$

where we have used insertions of the completeness relation  $I = \sum_{\sigma = \pm} |\sigma\rangle \langle \sigma|$ .

To get thermodynamic potentials for this model, we can proceed by diagonalizing the transfer matrix (1.41). Due to its Hermiticity, it can always be diagonalized and denoting  $\lambda_+$  and  $\lambda_-$  its eigenvalues one arrives at

$$Z = \text{Tr } \hat{T}^N = \lambda_+^N + \lambda_-^N. \quad (1.33)$$

Now, it is easy to find the expression for the free energy per unit spin

$$f(\beta, B, N) = -\frac{1}{\beta N} \ln Z_N = -\frac{1}{\beta} \left[ \ln \lambda_+ + \frac{1}{N} \ln \left[ 1 + \left( \frac{\lambda_-}{\lambda_+} \right)^N \right] \right]. \quad (1.34)$$

We can substitute expressions for the eigenvalues of  $\hat{T}$  that are solutions to the characteristic equation

$$(e^{\mathcal{J}+\mathcal{B}} - \lambda)(e^{\mathcal{J}-\mathcal{B}} - \lambda) - e^{-2\mathcal{J}} = \lambda^2 - 2\lambda e^{\mathcal{J}} \cosh \mathcal{B} + 2 \sinh 2\mathcal{J} = 0. \quad (1.35)$$

This equation has two independent solution and we will assume that  $\lambda_+ > \lambda_-$ . If we consider the thermodynamic limit  $N \rightarrow \infty$ , the second term in (1.34) vanishes and we simply find that

$$f(\mathcal{J}, \mathcal{B}, N) = -\frac{1}{\beta} \ln \left[ e^{\mathcal{J}} \cosh \mathcal{B} + \sqrt{e^{2\mathcal{J}} \cosh^2 \mathcal{B} - 2 \sinh 2\mathcal{J}} \right], \quad (1.36)$$

from which all the thermodynamical properties can be found.

The transfer matrix can be thought of as the exponential of the 'quantum Hamiltonian'  $\hat{T} = e^{-H}$  that brings us from one site to another as in the figure 1.5. Computation of the partition function for the original system can be then interpreted as quantum evolution with Hamiltonian  $H$ .

Now, we will derive correlation function of Ising spins. It can be easily computed using transfer matrix formalism

$$\langle \sigma_1 \sigma_{r+1} \rangle = \frac{1}{Z_N} \sum_{\{\sigma_i\}} \sigma_1 \langle \sigma_1 | \hat{T} | \sigma_2 \rangle \cdots \sigma_{r+1} \langle \sigma_{r+1} | \hat{T} | \sigma_{r+2} \rangle \cdots \langle \sigma_N | \hat{T} | \sigma_1 \rangle. \quad (1.37)$$

If  $\sigma_z$  is the Pauli matrix corresponding to the  $z$  projection, we can write

$$C^\sigma(r) = \langle \sigma_1 \sigma_{r+1} \rangle = \frac{1}{Z_N} \text{Tr } \sigma_z \hat{T}^r \sigma_z \hat{T}^{N-r}. \quad (1.38)$$

Since we already know how to diagonalize  $\hat{T}$ , the computation is now straightforward and one finds for the correlation function in the limit  $N \rightarrow \infty$

$$C^\sigma(r) = \sin^2 2\phi \left( \frac{\lambda_-}{\lambda_+} \right)^r, \quad (1.39)$$

where we have used  $\langle \sigma_1 \rangle = 0$  and  $\phi$  is a parameter in the unitary matrix

$$U = \begin{pmatrix} \cos \phi & -\sin \phi \\ \sin \phi & \cos \phi \end{pmatrix} \quad (1.40)$$

that diagonalizes  $\hat{T}$

$$U^{-1} \hat{T} U = \begin{pmatrix} \lambda_+ & 0 \\ 0 & \lambda_- \end{pmatrix} \quad (1.41)$$

and obeys the equation

$$\cot 2\phi = e^{2\mathcal{J}} \sinh \mathcal{B}. \quad (1.42)$$

From the equation (1.10) and (1.39), one can extract the correlation length

$$\xi = \frac{1}{\ln \lambda_+ - \ln \lambda_-}. \quad (1.43)$$

Looking at the values for  $\lambda_+$  and  $\lambda_-$  one immediately sees that the only divergence appears at the point  $T = 0$  and  $B = 0$ . One dimensional Ising model is in this sense trivial since no critical point appears.

## 1.5 Ising model in two and higher dimensions

Solving the Ising model in higher dimensions is much more difficult. We will sketch here basic approaches that are usually used. The Ising model can be solved in 2 dimensions exactly, but the solution for the three dimensional model is still lacking.

One can use approximative methods, such as mean field theory. This method is not very accurate, but it can provide useful insight into the problem. It is based on the approximation that every site interacts with all the other spins and the other spins form an effective magnetic field at this point. Consistency condition emerges if one requires that the value of the effective magnetic field and magnetization computed as statistical average are equal. Solving the consistency condition for the effective field leads to the solution for the critical temperature and other characteristics. Mean field theory provides qualitative predictions, but quantitatively it is rather off. One can use the Bethe-Peierls approximation to get more precise results.

One can think of the Ising model as a model of continuous spin variable  $\sigma$  with  $\delta$ -function probability distribution composed of two delta functions at  $\sigma = \pm 1$ . This probability can be substituted by new one that shares the same mean value and dispersion. For example, we can use a Gaussian distribution and obtain so-called Gaussian model approximation that can be solved exactly. Detailed description of the approximate methods goes beyond the scope of this thesis and we invite reader to read the details for example in [5].

Despite unsatisfactory result from the Ising model in one dimension, where no phase transition appeared, a critical point exists for the model in higher dimensions. It was suggested in 1936 by Peierls for the first time [35]. He argued that there exists a low temperature regime in which spontaneous magnetization is different from zero.



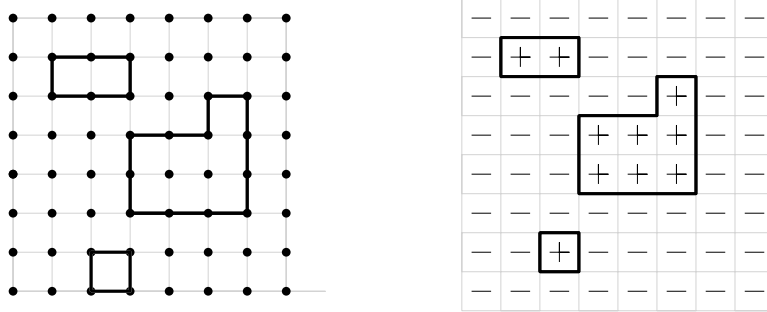


Figure 1.6: Pictures showing examples of configurations over which one has to sum when performing high-temperature and low-temperature expansion. In the high-temperature phase one needs to sum over all closed loops connecting neighboring spins. In the low temperature phase one has to sum over boundaries of all blocks of spins with the same spin value. It corresponds to the summation over all loops in the dual lattice.

The critical temperature  $T_c$  for the Ising model in 2 dimensions without the external magnetic field has been determined by Krammers and Wannier for the first time [36]. They studied low-temperature and high-temperature series for the partition function and found a duality between these two expansions. The self-dual point can then be identified with the critical point

$$\beta_c J = -\frac{1}{2} \ln(\sqrt{2} - 1) \approx 0.440686, \quad (1.44)$$

for coupling constant  $J$  and  $\beta_c$  critical inverse temperature.

We will comment on the duality argument and series expansions a bit. In the high temperature phase one can rewrite the Ising model partition function as

$$Z = \sum_{\{\sigma_i\}} \prod_{(i,j)} \cosh \mathcal{J} (1 + \sigma_i \sigma_j \tanh \mathcal{J}) \quad (1.45)$$

and expand the product on the right-hand side into a series in the small parameter  $\tanh \mathcal{J}$ . A product of some terms gives nonzero contribution only if sites incorporated in the product create closed chains as in the figure 1.6. In all the other cases, there exists another term in the expansion with all spins the same, except for one. The one differing term gives the same contribution but with opposite sign and terms differing by relative sign subtract. Contribution from such a closed chain is then  $(\tanh \mathcal{J})^l$ , where  $l$  is the length of the chain. Total partition function can be written in the form

$$Z = (2 \cosh \mathcal{J})^{N^2} \sum_{\text{loops}} (\tanh \mathcal{J})^l, \quad (1.46)$$

where  $N$  is the total number of sites in one row. As long as  $\tanh \mathcal{J}$  is small, i.e. for temperatures big enough, we can truncate the exact expansion and get approximate result.

In the low temperature phase, there are huge blocks of the same spins and only few spins are different. The energy of a configuration is then proportional to the length of the contour encircling the clusters with different spins as in the

figure 1.6. Similar procedure can be performed and we arrive at low-temperature  $\mathcal{J}' \gg 1$  expansion

$$Z = 2^{N^2 \mathcal{J}'} \sum_{\text{loops}} e^{-2\mathcal{J}'l}. \quad (1.47)$$

We can immediately see a duality between these two expansions  $e^{-2\mathcal{J}'} = \tanh \mathcal{J}$ . The self-dual point  $\mathcal{J}' = \mathcal{J}$  corresponds to the critical point given above.

There are many other methods that lead to the complete solution of the two-dimensional Ising model. Huge machinery of combinatorial techniques have been developed and their detailed discussion would take hundreds of pages [37]. These methods are based on the manipulations with the expansions and lead to the determination of the critical exponents 1.1 for the Ising model such as

$$\eta = \frac{1}{4} \quad \text{and} \quad \nu = 1, \quad (1.48)$$

others being computed from the scaling laws (1.13).

Another possible way to solve the two-dimensional Ising model is to use the transfer matrix method [3, 5]. The idea behind this method is the same as in the case of one dimension. The state space is no more two-dimensional vector space, but it is  $2^N$  dimensional space, where  $N$  is the number of sites in one row of the lattice. Each basis state  $|\psi\rangle$  from the state space corresponds to a different configuration of spins on the line and the transfer matrix  $\hat{T}$  brings us to the next row. Computing eigenvalues leads us to the partition function and thus all thermodynamic properties as in the case of the Ising model in 1D.

Key condition to solve the model in 2D is commutativity of the transfer matrices for different values of coupling constants separately in horizontal and vertical direction. In the case of the 2D Ising model, it can be proven that the transfer matrices commute if we take diagonal slicing of the square lattice and coupling constants  $\mathcal{J}_1$  and  $\mathcal{J}_2$  corresponding to different directions in the lattice keep  $\sinh 2\mathcal{J}_1 \sinh 2\mathcal{J}_2$  constant. If the matrices commute, they have the same spectra and this enables us to find the spectrum using the change of interaction constants.

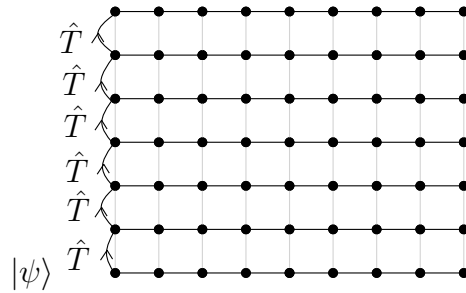


Figure 1.7: Action of the transfer matrix  $\hat{T}$  on the initial state  $|\psi\rangle$  describing a configuration of spins on a horizontal line performing a translation to the next row.

## 1.6 Boundary problems

In the section 1.4, we were considering periodic boundary conditions  $\sigma_i = \sigma_{i+N}$ . We can proceed in a bit different way changing the boundary condition. We can impose for example fixed boundary condition (spins + or -) on the two boundaries  $\sigma_1, \sigma_N = \pm 1$  or free boundary condition with no interaction for  $\sigma_1$  on the left and no interaction of  $\sigma_N$  on the right. Both spins can take both values  $\pm 1$ .

In the Hilbert space formulation, each boundary condition can be associated with a boundary state and transfer matrix evolves the initial state to the final

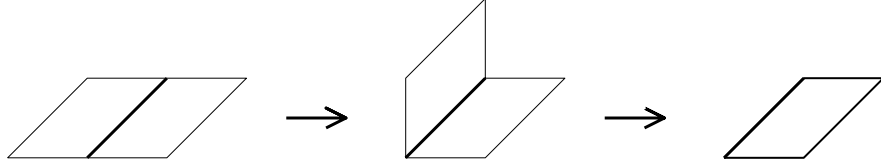


Figure 1.8: Process of folding during which a boundary emerges from a defect.

one. The partition function can be then interpreted as an amplitude between the initial state  $|a\rangle$  and the final state  $|b\rangle$ . We can find explicit expression for the three boundary states

$$|+\rangle = \begin{pmatrix} 1 \\ 0 \end{pmatrix}, \quad |-\rangle = \begin{pmatrix} 0 \\ 1 \end{pmatrix}, \text{ and } |f\rangle = \begin{pmatrix} 1 \\ 1 \end{pmatrix}. \quad (1.49)$$

Using these vectors the corresponding partition function can be written as

$$Z_N^{(a,b)} = \sum_{\{\sigma_i\}} \langle a | \hat{T} | \sigma_2 \rangle \langle \sigma_2 | \hat{T} | \sigma_3 \rangle \dots \langle \sigma_{N-1} | \hat{T} | b \rangle. \quad (1.50)$$

Performing the same diagonalization as in the case of periodic boundary conditions, we find partition functions

$$\begin{aligned} Z_N^{(+,+)} &= \lambda_+^{N-1} \cos^2 \phi + \lambda_-^{N-1} \sin^2 \phi, \\ Z_N^{(-,-)} &= \lambda_+^{N-1} \sin^2 \phi + \lambda_-^{N-1} \cos^2 \phi, \\ Z_N^{(+,-)} &= \sin \phi \cos \phi \lambda_+^{N-1} + \lambda_-^{N-1}, \\ Z_N^{(f,f)} &= \lambda_+^{N-1} + \lambda_-^{N-1} + \sin 2\phi (\lambda_+^{N-1} - \lambda_-^{N-1}). \end{aligned} \quad (1.51)$$

Different boundary conditions should not change bulk properties if the system is big enough. That is indeed true, since the boundary condition gives contribution to the free energy density of the order  $O(1/N)$ . The correction  $\Delta f$  to the free energy density  $f$  is

$$\Delta f = -\frac{1}{\beta N} \ln b(\phi), \quad (1.52)$$

where  $b(\phi) = \cos^2 \phi$  in the case of  $(+,+)$  boundary conditions,  $b(\phi) = \sin^2 \phi$  in the case of  $(-,-)$  boundary conditions,  $b(\phi) = \cos \phi \sin \phi$  for the mixed boundary conditions, and  $b(\phi) = 1 + \sin 2\phi$  for the free boundary conditions. This term is suppressed in the limit  $N \rightarrow \infty$ .

There are many interesting effects connected to the boundary. Some correlation functions may diverge if we are near the boundary. Real materials always contain a boundary and it is natural to study its effects.

Moreover, one can be interested in defect lines in the lattice. A defect line is a line, where discontinuities of local quantities can emerge. Indeed, defects are important constituents of real materials. We can study defects using so-called folding technique [13, 38]. One can fold the original model to find a doubled model with twice the number of degrees of freedom in each site than in the original model. The defect becomes a boundary in the folded model as can be seen from the figure 1.8. The two copies of the Ising lattice are not decoupled completely, but they influence each other precisely through the boundary.

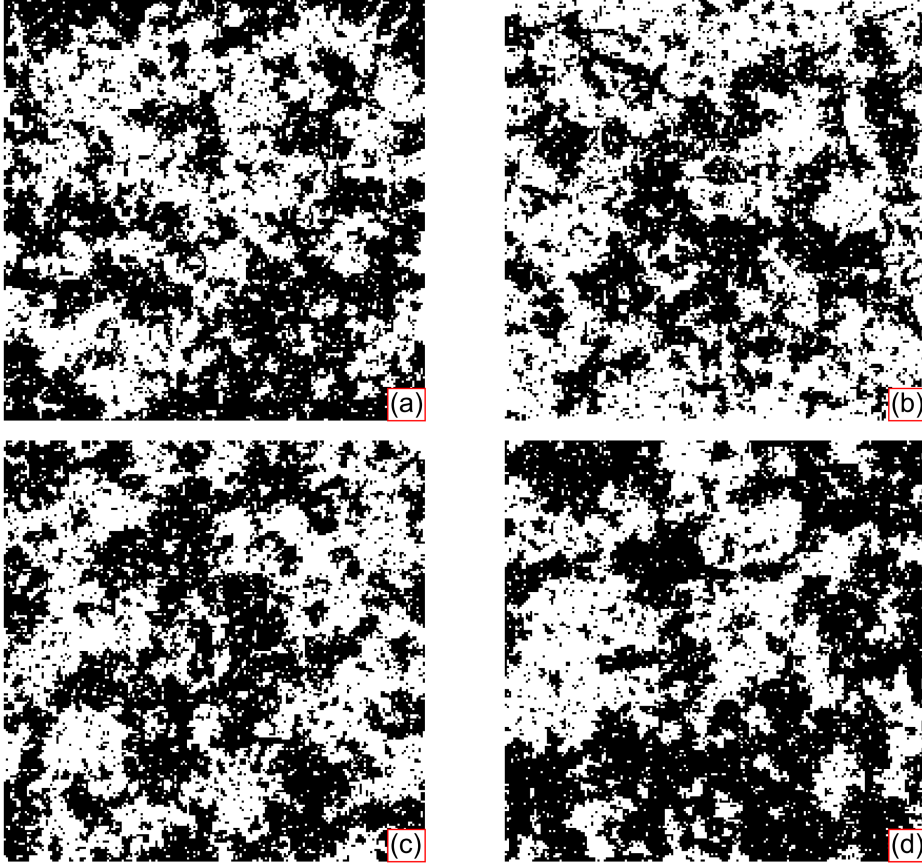


Figure 1.9: A simulation showing boundary effects for four different boundary conditions on the horizontal boundary. Picture (a) shows a boundary condition  $+$  on both sides, picture (b) shows  $-$  boundary conditions, and the two bottom pictures show free resp. periodic boundary conditions. Periodic boundary condition is imposed on the vertical boundaries in all four cases.

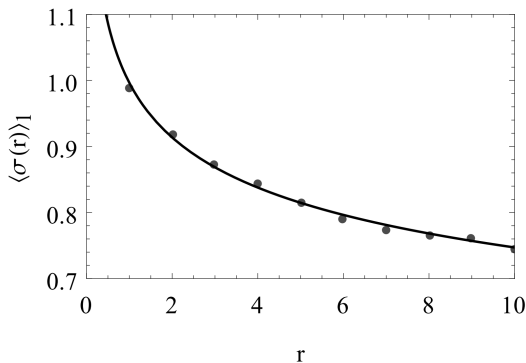


Figure 1.10: One-point function of the spin variable  $\sigma$  near the  $+$ -boundary (1-brane in the string field theory language) depending on the distance  $r$  from the boundary. Points are obtained from the simulated system and compared with the exact curve.

Ashkin-Teller model is a model of two Ising lattices coupled together.[39] The Hamiltonian of this model is

$$\mathcal{H}(\{\sigma_i\}, \{\tilde{\sigma}_j\}) = \sum_{(i,j)} [J(\sigma_i\sigma_j + \tilde{\sigma}_i\tilde{\sigma}_j) + L\sigma_i\sigma_j\tilde{\sigma}_i\tilde{\sigma}_j], \quad (1.53)$$

where a new interaction constant  $L$  coupling the two theories is introduced. The folded Ising model corresponds to the decoupling point  $L = 0$  of the Ashkin-Teller model. Studying boundary states in this model, one learns about the properties of the defects in the original model.

In two dimensions, the boundary problem is even more interesting. Boundary state is now a state in the  $2N$  dimensional space and there are many possible ways how to chose a boundary condition. Figure 1.9 shows, how the boundary condition changes behavior of spins near the boundary. At high temperatures the influence of the boundary is minimal, but if we lower the temperature, its influence becomes markable. The pictures are obtained from the simulation on the cylinder (periodic boundary condition is set on the vertical boundaries) near the critical temperature. In four different pictures, boundary conditions  $(++)$ ,  $(+, -)$ ,  $(-, -)$ , and  $(f, f)$  are imposed on the lower and upper boundary respectively. Later, boundary conformal field theory will prove useful to classify all the possible boundary conditions and to find the behavior of quantities near the boundary. In the next section, we start addressing this issues.

The boundary conditions listed above can be divided into two categories with respect to the value of the interaction constant on the boundary. Starting at the high temperature phase and lowering the temperature the boundary can undergo phase transition before the bulk or it can follow the transition of the bulk at the bulk critical temperature. The bulk transition, where the spins on the boundary are already ordered, is called *extraordinary* whereas the other boundary transitions are called *ordinary*. Extraordinary conditions can be descrtibed by fixed boundary conditions in CFT and ordinary transitions are described by free boundary conditions.

We have performed a simulation showing the behavior of spin variable  $\sigma$  and energy density  $\epsilon$  near the boundary (see figures 1.10 and 1.11). We will derive

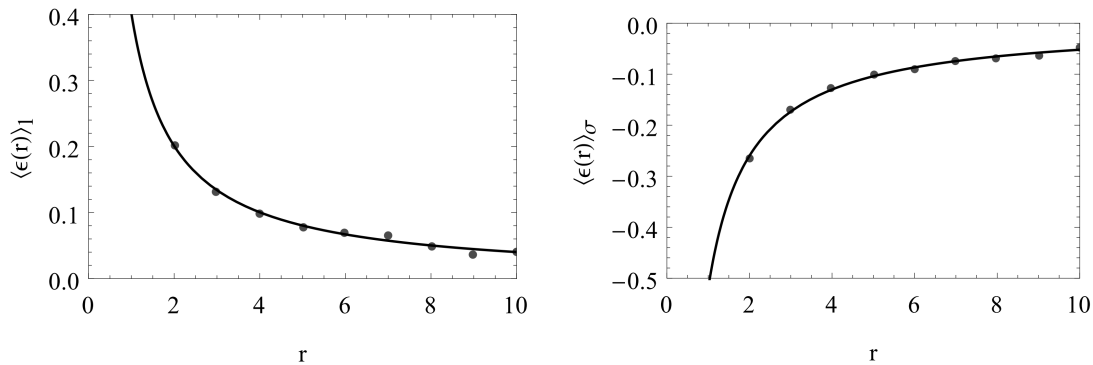


Figure 1.11: One-point functions of the energy density  $\epsilon$  near the  $+$ -boundary (1-brane) and f-boundary ( $\sigma$ -brane). Points are measured on the simulated system and compared with the exact curves.

the form of this dependence using conformal field theory. We have performed regression of the form

$$\langle \mathcal{O}_i \rangle(r) = a + \frac{b}{r^{\Delta_i}} \quad (1.54)$$

and performed normalization of  $\sigma$  and  $\epsilon$  induced by the normalization of two-point functions. Then we read off the normalized coefficient  $b$  that can be compared with the exact value encoded in the boundary state that we will determine using string field theory methods at the end of this thesis.

In the case of  $\sigma$  variable near the  $+$  or  $-$  boundary, we get multiplicative constant 1.02. It is not far away from the correct value  $2^{1/8} \approx 1.09$ . Near the free boundary the  $\sigma$  one-point function is vanishing. In the case of the energy density  $\epsilon$  correct values are 0.5 in the case of the fixed boundary condition and  $-0.5$  in the case of the free boundary. Numerically, we have found values 0.41 and -0.51, respectively. The agreement is still not bad if we realize the finite number of sites present on the simulated lattice that spoils the criticality, which is present only in the thermodynamic limit. Better agreement can be obtained performing longer simulation on a bigger system, but that is not the central topic of this thesis.

## 2. Conformal field theory

### 2.1 Quantum field theory description

Consider a general  $d$ -dimensional toroidal lattice in thermodynamic limit with a lattice spacing  $a$  and some interaction between its sites. Main quantity from the previous chapter was the partition function

$$Z = \text{Tr } e^{-\beta \mathcal{H}}, \quad (2.1)$$

where  $\mathcal{H}$  was the classical Hamiltonian. If we consider the theory on the scale, where the lattice spacing is negligible  $x \gg a$ , we can think of the lattice of spins as continuous function of the spin density and study such a statistical field by methods of quantum field theory (QFT). The role of the partition function in QFT is played by the generating functional

$$Z = \int [d\phi] e^{-S[\phi]}, \quad (2.2)$$

where  $S$  is the action of the theory and  $\phi$  denotes a set of fundamental local fields. The two approaches are identical at the critical temperature due to collective behavior of spins. In this regime, properties do not depend on the details at the microscopical scales. For further details see [5, 40].

One can find a correspondence between the transfer matrix  $\hat{T}$  and quantum Hamiltonian  $H$ . For the two-dimensional Ising model, element of the transfer matrix was a part of the partition function corresponding to the area between two slices of the lattice with fixed values of the spins. It can be viewed as an operator acting on the space of all possible configurations starting with the initial configuration and transferring it to the new configuration on the next slice. Partition function on the torus can be obtained as a trace of the appropriate power of the transfer matrix. The same procedure is performed in QFT when constructing a Hilbert space. A state corresponds to a configuration on the equal-time slice and time translation is performed by exponential of the Hamiltonian. We recover the correspondence

$$\hat{T} = e^{-\Delta y H}, \quad (2.3)$$

where  $H$  is the Hamiltonian performing translation along the torus and  $\Delta y$  is the length of the torus. Diagonalization of the transfer matrix  $\hat{T}$  is equivalent to finding the energy eigenstates in the continuum limit of the theory. At the critical point these eigenstates will be in one-to-one correspondence with the local operators in the theory.

To illustrate, how to construct the quantum Hamiltonian  $H$ , we will sketch the procedure for the Ising model. We will see that the Ising model in the continuum limit can be described by free Majorana fermion [41].

Let us consider a lattice of  $N \times N$  spins with Hamiltonian (1.1) but zero external magnetic field  $B = 0$  and with possibly different interaction constants in vertical and horizontal directions denoted as  $J$  and  $J'$ . Firstly, we will construct the transfer matrix acting on the  $2^N$ -dimensional Hilbert space of all possible configurations on the horizontal slice of the lattice. Elements of the transfer

matrix can be constructed similarly as in the case of the Ising model in one dimension. If we denote  $\tilde{\sigma}_i(a) = 1 \otimes \dots \otimes 1 \otimes \sigma_i \otimes 1 \otimes \dots \otimes 1$ , for all Pauli matrices  $\sigma_i$  and  $x$  labeling its position in the product, we can write the transfer matrix as

$$\hat{T} = \prod_{x=1}^N \left[ e^{\mathcal{J}\tilde{\sigma}_3(x)\tilde{\sigma}_3(x+1)} e^{\mathcal{J}'\tilde{\sigma}_1(x)} \right], \quad (2.4)$$

where we have denoted  $\mathcal{J} = \beta J$  and  $\mathcal{J}' = \beta J'$ .

To find the Hamiltonian we wish to take the limit  $\Delta y \rightarrow 0$ . Then we can read off the Hamiltonian from the relation  $\hat{T} \approx 1 - \Delta y H$ . We must be careful in performing the limit since interaction constants must be renormalized appropriately to maintain properties of the original theory. If one proceeds correctly, the solution for the Hamiltonian is

$$H = - \sum_{x=1}^N [\tilde{\sigma}_1(x) + \tilde{\sigma}_3(x)\tilde{\sigma}_3(x+1)]. \quad (2.5)$$

This Hamiltonian can be easily diagonalized using Wigner-Jordan transformation. We can introduce a fermionic operator

$$c(x) = \prod_{y=-N}^N e^{i\pi\tilde{\sigma}^+(y)\tilde{\sigma}^-(y)} \tilde{\sigma}^-(x), \quad (2.6)$$

where we have moreover introduced

$$\tilde{\sigma}^\pm(x) = \frac{1}{2}[\tilde{\sigma}_1(x) \pm i\tilde{\sigma}_2(x)]. \quad (2.7)$$

It is simple matter of fact that they satisfy fermionic anti-commutation relations  $\{c(x), c^\dagger(x')\} = \delta_{xx'}$ . Using the fermionic operators, the Ising model Hamiltonian can be written in the form

$$H = -2 \sum_x c^\dagger(x)c(x) - \lambda \sum_x [c^\dagger(x) - c(x)][c^\dagger(x+1) - c(x+1)] \quad (2.8)$$

as can be easily checked by substitution. We have obtained quadratic function of fermionic operators. This expression can be diagonalized. Introducing new fermionic operators  $c \rightarrow \psi$  that diagonalize the Hamiltonian

$$H = \sum_{k,x} \Lambda(x)_k \psi_k^\dagger(x) \psi_k(x), \quad (2.9)$$

we get a theory of *Majorana fermion*  $\psi$  satisfying relations

$$\psi_i^\dagger(x) = \psi_i(x), \quad \{\psi_i(x), \psi_j(x')\} = \delta_{ij}\delta_{xx'}, \quad \psi_i^2(x) = \frac{1}{2}. \quad (2.10)$$

We have thus argued that the Ising model in two dimensions is equivalent to the Majorana fermion.

Classifying all universality classes and solving corresponding theories reduces to study of fixed points in QFTs. If we adopt some other natural assumptions, we will be able to make a huge progress in this direction using methods of conformal field theory.

One can easily adopt standard methods of QFT, such as perturbative expansions, for the Ising model [4, 5]. In this thesis, we are interested especially in non-perturbative results and we will avoid this discussion here.



Another comment will be on the universality class of the Ising model. We can consider a QFT of bosonic field  $X$  with effective potential

$$U(X) = \frac{m^2}{2}X^2 + \frac{g}{4!}X^4. \quad (2.11)$$

This theory has  $Z_2$  symmetry and we could expect it to belong to the same universality class as the Ising model. The potential has one unique minimum for  $m^2 > 0$  at the origin and two minima for  $m^2 < 0$  as shown in the figure 2.1. The critical point corresponds to the case when  $m^2 = 0$  (the two minima joint and the only one centered at the origin remains) and we can identify correspondence  $m^2 \approx (T - T_c)$ . A critical theory thus corresponds to a 'massless theory' [4, 5]. This theory can be solved using mean field theory and Landau-Ginsburg model gives correct critical exponents above the upper critical dimension  $d = 4$ . In this case, the theory belongs to the same universality class as the Ising model.

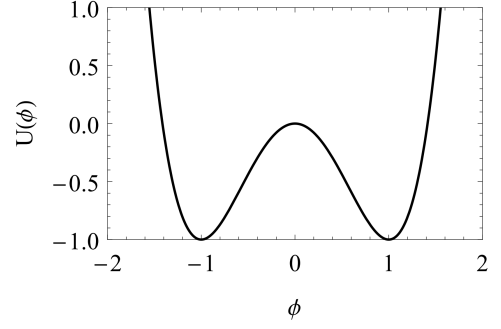


Figure 2.1: Effective potential of free boson describing the universality class of the Ising model.

## 2.2 Conformal invariance

As described in the previous two sections, one can effectively describe a lattice theory at the critical point by means of QFT. Moreover, at the critical point (i.e. fixed point of the RG) the scale invariance appears. But we can do better. If the model satisfy some other natural conditions, we can obtain whole conformal invariance that will be described in the following parts of this chapter. Before restricting to the case of two-dimensional *conformal field theory* (CFT) let us emphasize a CFT in general dimension  $d$ . This chapter will be a review of the basic facts that can be found in most of the textbooks on CFT [8, 42, 43] or string theory [9, 44, 45]. We will extract some essentialities from these books and sometimes extend the discussion a bit. Proper explanation of the CFT methods can be found in these texts.

Consider a generic  $d$  dimensional space with a metric  $g_{\mu\nu}$  and local coordinates  $x^\mu$ . Coordinate transformation  $x^\mu \rightarrow x'^\mu(x)$  is called conformal if the corresponding metric only locally rescales under the transformation

$$g'_{\mu\nu} = \Lambda(x)g_{\mu\nu}. \quad (2.12)$$

Recalling the definition of the angles, one can easily check that conformal transformations do not change them. Conformal transformations can be thus viewed as a subgroup of the group of all diffeomorphisms providing local rescaling, rotation, and translation.

Let us assume an infinitesimal transformation  $x^\mu \rightarrow x'^\mu = x^\mu + \epsilon^\mu(x)$ . Under the infinitesimal transformation the metric transforms as  $g'_{\mu\nu} = g_{\mu\nu} + \partial_\mu \epsilon_\nu(x) + \partial_\nu \epsilon_\mu(x)$ . Substituting into the (2.12), one finds condition

$$\partial_\mu \epsilon_\nu(x) + \partial_\nu \epsilon_\mu(x) = \rho(x)g_{\mu\nu}, \quad (2.13)$$

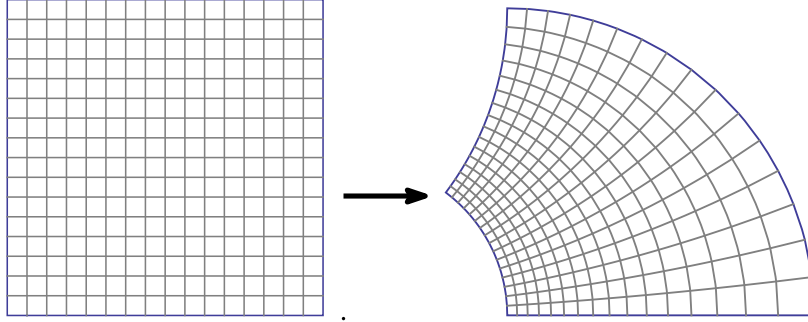


Figure 2.2: An example of conformal transformation mapping coordinate net to the new one. One can see that angles have not been changed and the net is only locally rescaled and rotated.

for some function  $\rho$ . Taking the trace

$$2\partial \cdot \epsilon = d\rho(x) \quad (2.14)$$

and substituting back to the (2.13), we get a constraint on the infinitesimal conformal transformations

$$\partial_\mu \epsilon_\nu(x) + \partial_\nu \epsilon_\mu(x) = \frac{2}{d}(\partial \cdot \epsilon)g_{\mu\nu}. \quad (2.15)$$

In higher dimensions  $d > 2$ , the only possible transformations that are conformal are translations, dilation, rotations, and so-called special conformal transformations, which follows from the constraint above. All the transformations are reviewed in the table 5.1. One can check that infinitesimal versions of these transformations satisfy above constraint (2.15). It can be also shown that these transformations generate whole conformal group, but since we are interested in two dimensional theories, we will skip the discussion here. These estimations can be found in early mathematical work of Lie and others.

Translation	$x^\mu \rightarrow x^\mu + a^\mu$
Dilation	$x^\mu \rightarrow \lambda x^\mu$
Rotation	$x^\mu \rightarrow M^\mu_\nu x^\nu, \quad M_{\mu\nu} = -M_{\nu\mu}$
Spec. conf. trans.	$x^\mu \rightarrow \frac{x^\mu - b^\mu x^2}{1 - b^\mu x_\mu + b^2 x^2}$

Table 2.1: Four fundamental conformal transformations that generate whole conformal group for  $d > 2$  dimensions.

Now, we will state Polyakov's conjecture [7, 46]. A field theory with local interactions described by the action  $S$  with translational, rotational, and scale invariance is also conformally invariant. Having a continuum limit of the lattice model with homogenous and isotropic local interactions, like the Ising model, we are precisely in this situation. Finding all the universality classes of the local, translationally, and rotationally invariant theories is equivalent to classifying all CFTs.

For each local theory, we can define the stress-energy tensor  $T_{\mu\nu}$  as response of the action on the coordinate transformation

$$\delta S = \frac{1}{(2\pi)^{d-1}} \int d^d x T_{\mu\nu}(x) \partial^\mu \epsilon^\nu(x). \quad (2.16)$$

If the action is invariant under the conformal transformations, we get restrictions on the stress-energy tensor. Clearly, translation  $\epsilon^\mu = a^\mu$  obeys (2.15) and integrating (2.16) by parts one finds a conservation law for the stress-energy tensor

$$\partial_\mu T^{\mu\nu} = 0. \quad (2.17)$$

Similarly, invariance under the rotation  $\epsilon^\mu = M^{\mu\nu} x_\nu$ , for  $M^{\mu\nu}$  antisymmetric tensor, constraints  $T^{\mu\nu}$  to be symmetric

$$T^{\mu\nu} = T^{\nu\mu}. \quad (2.18)$$

Finally, from the dilatation transformation invariance  $\epsilon^\mu = \lambda x^\mu$ , the stress-energy tensor  $T^{\mu\nu}$  must be traceless

$$T^\nu_\nu = 0. \quad (2.19)$$

To finish our proof of the conformal invariance, consider (2.16) and integrate it by parts with the use of the above identities for the stress-energy tensor

$$\begin{aligned} \delta S &= \frac{1}{(2\pi)^{D-1}} \int d^D x T_{\mu\nu}(x) \partial^\mu \epsilon^\nu(x) \\ &= \frac{1}{2} \frac{1}{(2\pi)^{D-1}} \int d^D x (T_{\mu\nu}(x) + T_{\nu\mu}(x)) \partial^\mu \epsilon^\nu(x) \\ &= \frac{1}{2} \frac{1}{(2\pi)^{D-1}} \int d^D x g^{\mu\nu} T_{\mu\nu}(x) \partial \cdot \epsilon = 0 \end{aligned} \quad (2.20)$$

and our proof of the conformal invariance is finished. All the local, translationally, rotationally, and scale invariant theories in the continuum limit are also conformally invariant.

In the following, let us restrict on 2D models. Some of the statements hold similarly in general dimension, but general discussion goes beyond the scope of this treatment.

As we mentioned earlier, conformal group becomes infinite dimensional in two dimensions [47]. Substituting  $d = 2$  into the (2.15) and fixing coordinates to ensure  $g_{\mu\nu} = \delta_{\mu\nu}$ , one explicitly ends with

$$\partial_0 \epsilon_0 = \partial_1 \epsilon_1, \quad (2.21)$$

for  $(\mu, \nu) = (0, 0)$  component, and

$$\partial_0 \epsilon_1 = -\partial_1 \epsilon_0, \quad (2.22)$$

for  $(\mu, \nu) = (0, 1)$ . These are precisely Cauchy-Riemann equations. If we naturally introduce a complex notation  $\epsilon(z) = \epsilon_0(z) + i\epsilon_1(z)$  and  $\bar{\epsilon}(\bar{z}) = \epsilon_0(\bar{z}) - i\epsilon_1(\bar{z})$  for complex coordinates  $z = \sigma_0 + i\sigma_1$  and  $\bar{z} = \sigma_0 - i\sigma_1$ , every holomorphic function  $\epsilon(z)$  satisfy the above Cauchy-Riemann conditions and thus define a conformal transformation. In two dimensions we are given an infinite set of conformal transformations since infinitely many independent holomorphic functions exist.

It is natural to regard  $z$  and  $\bar{z}$  as independent variables since they correspond to two independent algebras as we will see later. At the end of the day the physical situation will be restored equating  $\bar{z} = z^*$ .

In the conformal group in two dimensions there exists a subgroup called *special conformal group*. General conformal transformation in two dimensions need not to be everywhere well-defined and invertible. Every conformal transformation that is well behaved can be written in the form

$$f(z) = \frac{az + b}{cz + d}, \quad (2.23)$$

where  $ad - bc = 1$ . It can be easily shown that it is indeed closed under the composition of transformations and it is invertible. These transformations form a subgroup isomorphic with  $SL(2, \mathbb{C})$  and  $SO(3, 1)$ . We learn that special conformal group has 6 parameters with the same generators as in the table 5.1. It can be easily shown that transformations (2.23) are the only globally defined invertible holomorphic mappings.

## 2.3 Primary operators

In this section, we will define so-called *primary operators* introduced in [47] and show that invariance with respect to the global conformal transformations constraints the form of the correlation functions. Primary operators will play main role in the later analysis.

Consider CFT with a set of all operators  $\{\mathcal{O}_\alpha\}$  and assume the existence of subset  $\{V_\alpha\} \subset \{\mathcal{O}_\alpha\}$  of operators, transforming under the conformal transformation  $z \rightarrow w = f(z)$ ,  $\bar{z} \rightarrow \bar{w} = \bar{f}(\bar{z})$  as

$$V_\alpha(z, \bar{z}) \rightarrow V'_\alpha(w, \bar{w}) = \left(\frac{\partial f}{\partial z}\right)^{-h_\alpha} \left(\frac{\partial \bar{f}}{\partial \bar{z}}\right)^{-\bar{h}_\alpha} V_\alpha(z, \bar{z}), \quad (2.24)$$

where  $h_\alpha$  and  $\bar{h}_\alpha$  are conformal weights for a primary field  $V_\alpha$ . Primary field will be a special case of the scaling fields with similar properties under the special conformal transformations.

Due to the invariance of the action  $S[\phi]$  and measure  $[d\phi]$ , general correlator of  $n$  primary fields

$$\langle V_1(z_1, \bar{z}_1) \dots V_n(z_n, \bar{z}_n) \rangle = \frac{1}{Z} \int [d\phi] V_1(z_1, \bar{z}_1) \dots V_n(z_n, \bar{z}_n) \exp(-S[\phi]) \quad (2.25)$$

transforms according to (2.24) as

$$\langle V'_1(w_1, \bar{w}_1) \dots V'_n(w_n, \bar{w}_n) \rangle = \prod_{\alpha=1}^n \left(\frac{\partial f}{\partial z}\right)^{-h_\alpha} \left(\frac{\partial \bar{f}}{\partial \bar{z}}\right)^{-\bar{h}_\alpha} \langle V_1(z_1, \bar{z}_1) \dots V_n(z_n, \bar{z}_n) \rangle, \quad (2.26)$$

where we have defined the partition function  $Z = \langle \mathbb{1} \rangle$ .

Conformal invariance constraints the form of the correlation functions. In the case of 2- and 3-point functions the form of the correlator is completely fixed. In the case of the higher correlation functions, conformal invariance does not suffice to fix its form and other constraints will have to be adopted. If there

are four insertions at points  $z_1, z_2, z_3$  and  $z_4$  in the correlator, we can construct so-called *crossing* (or harmonic) *ratios*  $\eta$  that are invariant under the conformal transformations

$$\eta = \frac{(z_1 - z_2)(z_3 - z_4)}{(z_1 - z_3)(z_2 - z_4)}. \quad (2.27)$$

Similarly, we can define  $\bar{\eta}$  for the antiholomorphic part. We have then ambiguity in adding some function of these ratios when fixing the form of the correlator.

We will show, how the form of 2-point and 3-point functions is fixed. From the translational and rotational invariance, correlators can only depend on the relative positions  $z_{ij} = (z_i - z_j)$  and  $\bar{z}_{ij} = (\bar{z}_i - \bar{z}_j)$ . For a 2-point function, there is only one such a term  $z_{12} = (z_1 - z_2)$  (with corresponding anti-holomorphic counterpart) and prescribed transformation under the dilatations  $x^\mu \rightarrow \lambda x^\mu$  forces the correlator to be of the form

$$\langle V_1(z_1, \bar{z}_1) V_2(z_2, \bar{z}_2) \rangle = \frac{C_{12}}{z_{12}^{h_1+h_2} \bar{z}_{12}^{\bar{h}_1+\bar{h}_2}}, \quad (2.28)$$

where we have denote  $C_{12}$  a constant given by particular normalization of the fields  $V_1$  and  $V_2$ . Moreover, special conformal transformation gives us constraint  $h_1 = h_2$  and  $\bar{h}_1 = \bar{h}_2$  for  $C_{12} \neq 0$ . 2-point function of primary fields with different conformal weights vanishes. Since any linear combination of primary fields with conformal weights  $(h, \bar{h})$  is again a primary field with weights  $(h, \bar{h})$ , we can always find a basis of primary operators such that  $C_{ij} = \delta_{ij}$ .

Similar procedure holds also for 3-point function. After substitution of the formulas for the dilatation and special conformal transformation one finds

$$\begin{aligned} \langle V_1(z_1, \bar{z}_1) V_2(z_2, \bar{z}_2) V_3(z_3, \bar{z}_3) \rangle &= \frac{C_{123}}{z_{12}^{h_1+h_2-h_3} z_{23}^{h_2+h_3-h_1} z_{13}^{h_3+h_1-h_2}} \\ &\times \frac{1}{\bar{z}_{12}^{\bar{h}_1+\bar{h}_2-\bar{h}_3} \bar{z}_{23}^{\bar{h}_2+\bar{h}_3-\bar{h}_1} \bar{z}_{13}^{\bar{h}_3+\bar{h}_1-\bar{h}_2}}. \end{aligned} \quad (2.29)$$

Indetermined constants  $C_{123}$  are called *structure constant* of the theory.

We can see that two-point functions of primary operators has the same form as the correlators in the lattice theory at the critical temperature. We will see that primary operators will play a role of local variables in the lattice theory. If we compare (2.28) with correlators of the Ising model, we can see that the spin operator must have conformal dimension  $(h_\sigma, h_\sigma) = \left(\frac{1}{16}, \frac{1}{16}\right)$  and the operator of the energy density must have dimensions  $(h_\epsilon, h_\epsilon) = \left(\frac{1}{2}, \frac{1}{2}\right)$ . Clearly, it must be spinless and the scaling behavior must be in correspondence with critical exponents  $\eta$  and  $\Delta_\epsilon$ . Only if the operators scales with this weights, we obtain correct behavior of the 2-point function.

As discussed above, conformal invariance does not fix precise form of the higher correlators. We will introduce concept of *operator product expansion* (OPE) that will prove useful when computing higher correlation functions. Using OPEs, one can locally exchange two nearby operators  $V_\alpha$  and  $V_\beta$  by string of operators inserted at one of the two point<sup>1</sup>

$$\mathcal{O}_\alpha(z, \bar{z}) \mathcal{O}_\beta(w, \bar{w}) = \sum_\gamma C_{\alpha\beta}^\gamma (z - w, \bar{z} - \bar{w}) \mathcal{O}_\gamma(w, \bar{w}). \quad (2.30)$$

---

<sup>1</sup>All operator equations must be viewed to hold within correlation functions. To clarify relation between operator equations and path integral formulation see nice review in the appendix of [9].

We will be mostly interested in the singular part of this expansion and the remaining regular part will be usually neglected while  $\sim$  will be used except for the equality. This singular part will lead to the commutation relations for operators in radial quantization and it will tell us, what are the transformation properties of the fields.

## 2.4 Stress-energy tensor

*Stress-energy tensor* (also called energy-momentum tensor) defined in (2.16) plays central role in CFT since it generates conformal transformations. Transforming  $T_{\mu\nu}$  into the complex plane language

$$\begin{aligned} T_{xx} &= T_{zz} + T_{z\bar{z}} + T_{\bar{z}z} + T_{\bar{z}\bar{z}} \\ T_{xy} &= i(T_{zz} - T_{z\bar{z}} + T_{\bar{z}z} - T_{\bar{z}\bar{z}}) \\ T_{yx} &= i(T_{zz} + T_{z\bar{z}} - T_{\bar{z}z} - T_{\bar{z}\bar{z}}) \\ T_{yy} &= -T_{zz} + T_{z\bar{z}} + T_{\bar{z}z} - T_{\bar{z}\bar{z}}, \end{aligned} \quad (2.31)$$

performing the inverse transformation and using constraints (3.7), (3.8), and (3.9), we get

$$T_{z\bar{z}} = T_{\bar{z}z} = 0, \quad \bar{\partial}T(z, \bar{z}) = 0, \quad \partial\bar{T}(z, \bar{z}) = 0, \quad (2.32)$$

where we have set  $T = T_{zz}$  and  $\bar{T} = T_{\bar{z}\bar{z}}$ . We can see that  $T(z)$  and  $\bar{T}(\bar{z})$  are holomorphic resp. anti-holomorphic functions. This fact will lead to decoupling of the holomorphic and antiholomorphic part of the theory that could be treated separately.

Invariance of the action under the conformal transformations will lead us to the conformal Ward identities. Stress-energy tensor gives us conserved currents for conformal transformations. Consider a general conformal transformations  $z \rightarrow z + \epsilon(z)$  and  $\bar{z} \rightarrow \bar{z} + \bar{\epsilon}(\bar{z})$ . Corresponding currents are  $J^{\bar{z}} = T_{zz}(z)\epsilon(z) = T(z)\epsilon(z)$  for the first transformation and  $\bar{J}^z = \bar{T}(\bar{z})\bar{\epsilon}(\bar{z})$  for the second one as can be easily deduced from the definition of the stress-energy tensor. Let  $\tilde{\mathcal{O}} = \mathcal{O}_1(z_1, \bar{z}_1) \dots \mathcal{O}_n(z_n, \bar{z}_n)$  be a string of operators and let  $z \rightarrow z + \epsilon(z)$  be a transformation with compact support that is conformal in the neighbor of each point, where the operator is inserted. We will denote the collection of all neighbors  $D$  and the situation is sketched in the figure 2.3.

Using the identity

$$\int [d\phi] \tilde{\mathcal{O}} \delta S e^{-S[\phi]} = \int [d\phi] \delta \tilde{\mathcal{O}} e^{-S[\phi]}, \quad (2.33)$$

we will derive conformal *Ward identities*. Substituting for  $\delta S$  from the definition of the stress-energy tensor (2.16) and recognizing correlator

$$\delta \langle \tilde{\mathcal{O}} \rangle = \sum_{\alpha=1}^n \langle \mathcal{O}_1(z_1, \bar{z}_1) \delta \mathcal{O}_\alpha(z_\alpha, \bar{z}_\alpha) \mathcal{O}_n(z_n, \bar{z}_n) \rangle \quad (2.34)$$

on the right-hand side, one finds from the relation (2.3)

$$\delta \langle \tilde{\mathcal{O}} \rangle = \frac{1}{2\pi} \int_{\mathbb{R}^2/D} d^2\sigma \langle (\partial_\mu \epsilon_\nu) T^{\mu\nu} \tilde{\mathcal{O}} \rangle = -\frac{1}{2\pi} \int_{\mathbb{R}^2/D} d^2\sigma \langle \partial_\mu J^\mu \tilde{\mathcal{O}} \rangle, \quad (2.35)$$

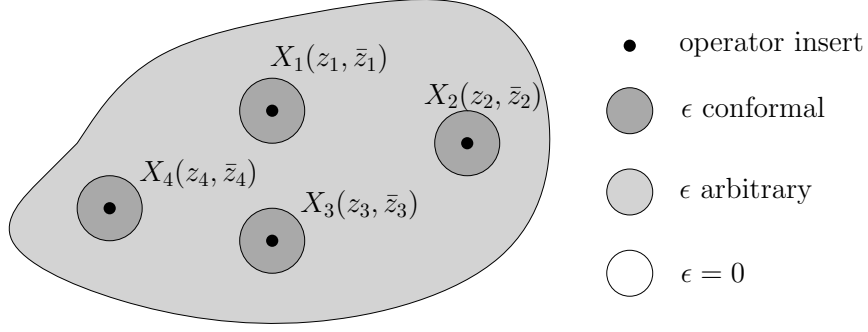


Figure 2.3: Visualized situation used in derivation of the Ward identities.

where we have used the fact that  $\delta S$  vanishes in  $D$  and  $T^{\mu\nu}$  is conserved. In two dimensions, we can benefit from the Stokes theorem that reads

$$\int_{\mathbb{R}^2/D} \partial_\mu J^\mu = \oint_{\partial D} (J_0 d\sigma^1 - J_1 d\sigma^0) = -i \oint_{\partial D} (J_z dz - J_{\bar{z}} d\bar{z}) \quad (2.36)$$

since  $\epsilon$  has compact support and thus infinity is a regular point. With the use of this identity, we get the conformal Ward identities

$$\frac{i}{2\pi} \oint_{\partial D} dz \langle J_z(z, \bar{z}) \tilde{\mathcal{O}} \rangle - \frac{i}{2\pi} \oint_{\partial D} d\bar{z} \langle J_{\bar{z}}(z, \bar{z}) \tilde{\mathcal{O}} \rangle = \delta \langle \tilde{\mathcal{O}} \rangle. \quad (2.37)$$

Specially for the transformation  $z \rightarrow z + \epsilon(z)$  in the neighbor of  $z_\alpha$  and zero elsewhere else, we get relation

$$\delta \mathcal{O}_\alpha(z_\alpha) = -\text{res}_{z_\alpha} [J_z(z) \mathcal{O}_\alpha(z_\alpha)] = -\text{res}_{z_\alpha} [\epsilon(z) T(z) \mathcal{O}_\alpha(z_\alpha)] \quad (2.38)$$

and analogically for the transformation  $\bar{z} \rightarrow \bar{z} + \bar{\epsilon}(\bar{z})$ . The consequence of this result is that whenever we know the OPE of  $T$  and  $\bar{T}$  with the operator  $\mathcal{O}_\alpha$ , we can reconstruct arbitrary conformal transformation of this operator.

If we focus on the infinitesimal translation  $\delta z = \epsilon$ , then all the operators transform as  $\mathcal{O}_\alpha(z - \epsilon) = \mathcal{O}_\alpha(z) - \epsilon \partial \mathcal{O}_\alpha(z)$  and the Ward identity gives us the least singular term of the OPE

$$T(z) \mathcal{O}_\alpha(w, \bar{w}) \sim \dots + \frac{\partial \mathcal{O}_\alpha(w, \bar{w})}{z - w}. \quad (2.39)$$

The other singular terms are not so easily computable since not all operators transform simply under the other conformal transformations. Consider rotations and scaling for a while. Later we will construct a basis of local operators with good transformation properties under these transformations. The transformation will be determined by two real numbers  $(h_\alpha, \bar{h}_\alpha)$  defined as

$$\delta \mathcal{O}_\alpha = -\epsilon(h_\alpha \mathcal{O}_\alpha + z \partial \mathcal{O}_\alpha) - \bar{\epsilon}(\bar{h}_\alpha \mathcal{O}_\alpha + \bar{z} \bar{\partial} \mathcal{O}_\alpha), \quad (2.40)$$

for transformations  $\delta z = \epsilon z$  and  $\delta \bar{z} = \bar{\epsilon} \bar{z}$ . We will call  $\Delta_\alpha = h_\alpha + \bar{h}_\alpha$  the *scaling dimension* and  $s_\alpha = h_\alpha - \bar{h}_\alpha$  the *spin* of the field  $\mathcal{O}_\alpha$ , since these transformation encodes scaling and rotational properties. We can identify  $L = -i(\sigma_0 \partial_1 - \sigma^1 \partial_0) = z \partial - \bar{z} \bar{\partial}$  and  $D = \sigma^\alpha \partial_\alpha = z \partial + \bar{z} \bar{\partial}$  as scaling and dilation operators respectively.

From the Ward identity (2.38), we see that operators with transformation (2.40) have following OPE

$$T(z)\mathcal{O}(w, \bar{w}) \sim \dots + \frac{h\mathcal{O}(w, \bar{w})}{(z-w)^2} + \frac{\partial\mathcal{O}(w, \bar{w})}{z-w} \quad (2.41)$$

with the stress-energy tensor.

There is a special set of operators for which the process stops here and no more singular term is needed. These are precisely the primary operators introduced earlier. One can check it performing infinitesimal conformal transformation  $z \rightarrow z + \epsilon(z)$  and using the definition of primary fields (2.24)

$$\begin{aligned} V_\alpha &\rightarrow (1 + \partial\epsilon)^{-h_\alpha} V_\alpha(z - \epsilon) = (1 - h_\alpha \partial\epsilon V_\alpha)(V(z) - \epsilon \partial V_\alpha) \\ &= V(z) - h_\alpha \partial\epsilon V_\alpha - \epsilon \partial V_\alpha, \end{aligned} \quad (2.42)$$

where we have restricted only on the holomorphic sector and neglected terms containing higher powers of  $\epsilon$ . In the antiholomorphic sector the situation is the same. This relation is valid for all conformal transformations and from the Ward identities (2.38), one immediately sees that there are no other singular terms in the OPE with the stress-energy tensor for primary fields.

In the following part of this section, we will define the central charge of the theory that will be a key parameter in later discussion. Some properties of the stress-energy tensor will be discussed.

Scaling dimension of the stress-energy tensor is  $\Delta_T = 2$  since the energy can be obtained performing an integration over the space. Moreover, it is symmetric 2-tensor and thus it has spin  $s = 2$ . From these two facts one concludes that the stress-energy tensor has weights  $(2, 0)$ , whereas  $\bar{T}$  has weights  $(0, 2)$ . Let us derive general OPE for the two components of the stress-energy tensor. Restricting to the holomorphic part, all terms in the OPE has form  $\mathcal{O}_n/(z-w)^n$ , where weight of the operator  $\mathcal{O}_n$  must be  $4 - n$  to scale correctly. If we consider only unitary models, we will prove in the next section that only fields with positive conformal weights are allowed and the most singular term must be  $(z-w)^{-4}$  multiplied by a constant. The term  $(z-w)^{-3}$  cannot be present because it would spoil the equality  $T(z)T(w) = T(w)T(z)$  that must hold within any correlator as can be easily shown. The most general OPE for the stress-energy tensor of unitary theories is

$$T(z)T(w) \sim \frac{c/2}{(z-w)^4} + \frac{2T(w)}{(z-w)^2} + \frac{\partial T(w)}{(z-w)} \quad (2.43)$$

and similarly for  $\bar{T}$  with corresponding constant  $\bar{c}$ . Constants  $(c, \bar{c})$  are called *central charges* and play crucial role in the whole theory.

Knowing the above OPE, it is not difficult to find a transformation prescription for the stress-energy tensor. Substituting the expansion of a general holomorphic function

$$\epsilon(z) = \epsilon(w) + \epsilon'(w)(z-w) + \frac{1}{2}\epsilon''(w)(z-w)^2 + \frac{1}{3}\epsilon'''(w)(z-w)^3 + \dots \quad (2.44)$$

into the Ward identity for the stress-energy tensor, we get for the infinitesimal conformal transformations

$$\delta T(w) = -\text{res}_w [\epsilon(z)T(z)T(w)]$$



$$\begin{aligned}
&= -\text{res}_w \left[ \epsilon(z) \left( \frac{c/2}{(z-w)^4} + \frac{2T(w)}{(z-w)^2} + \frac{\partial T(w)}{(z-w)} + \dots \right) \right] \\
&= -\epsilon(w) \partial T(w) - 2\epsilon'(w)T(w) - \frac{c}{12} \epsilon'''(w).
\end{aligned} \tag{2.45}$$

Exponentiating this infinitesimal transformation leads to the following transformation prescription for the finite transformations  $z \rightarrow w(z)$

$$T'(w) = \left( \frac{dw}{dz} \right) \left[ T(z) - \frac{c}{12} \{w; z\} \right], \tag{2.46}$$

where we have introduced the *Schwarzian derivative*

$$\{w; z\} = \frac{w'''}{w'} - \frac{3}{2} \left( \frac{w''}{w'} \right)^2. \tag{2.47}$$

We can easily convince ourselves that infinitesimal version of this transformation is indeed (2.45) and it has correct properties under the composition of two transformations. Detailed discussion is provided for example in [43]. In the case of global conformal transformations given by (2.23) Schwarzian derivative vanishes and the transformation of the stress-energy tensor is primary-like.

Since the central charge is a key parameter in our analysis, let us spend some time to get intuition for this quantity. Extra term in the transformation (2.46) is independent of  $T$  and plays a role of the Casimir energy of the system related to the introduction of macroscopic length scale. Let us illustrate it by a simple example of the theory defined on the cylinder parametrized by  $w = \sigma_0 + i\sigma_1$  for  $\sigma_1 \in [0, 2\pi)$  and  $\sigma_0 \in [-\infty, \infty)$ . This cylinder can be conformally mapped to the whole complex plane by  $z = \exp w$ . Schwarzian derivative for this transformation can be easily computed and  $T$  transforms as

$$T_{\text{cylinder}}(w) = z^2 T_{\text{plane}}(z) + \frac{c}{24}. \tag{2.48}$$

If the ground state energy on the complex plane vanishes  $\langle T_{\text{plane}} \rangle = 0$  then on the cylinder, where the Hamiltonian is

$$H = \int d\sigma T_{\sigma_0\sigma_0} = - \int d\sigma (T_{ww} + \bar{T}_{\bar{w}\bar{w}}), \tag{2.49}$$

the ground state energy is no more zero

$$E = -2\pi \frac{c + \bar{c}}{24}. \tag{2.50}$$

This is the Casimir energy of the theory on the cylinder induced by the introduction of the compact dimension.

Another effect, where  $c$  is important, is the *Weyl Anomaly*. We have shown that trace of the stress-energy tensor  $T$  vanishes at the classical level. This will no longer be true in the quantum case with curved backgrounds. As discussed in [43], it is proportional to the central charge

$$\langle T^\alpha_\alpha \rangle = -\frac{c}{12} R, \tag{2.51}$$

where  $R$  is the Ricci scalar. Extended discussion of the central charge, introduced in [47], can be found for example in [45] or [42]. The Weyl invariance of the theory requires  $c = 0$ . This condition plays central role in string theory, where the Weyl invariance emerges as a gauge symmetry, and restricts the theory dramatically.

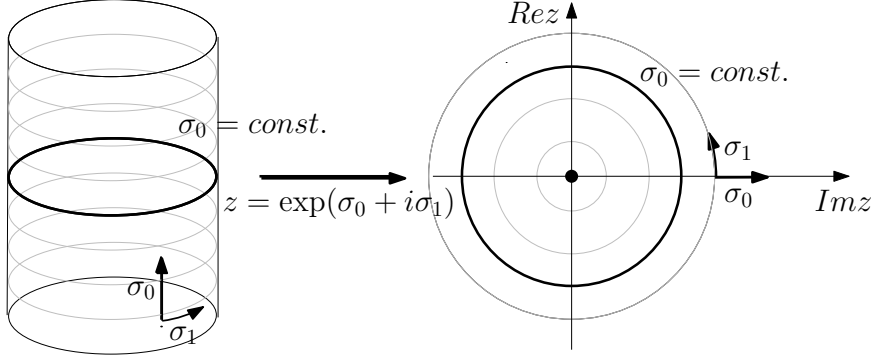


Figure 2.4: Conformal mapping of the theory defined on the cylinder to the complex plane. Equal-time slicings map to the concentric circles.

## 2.5 Operator formalism

In this section, we will empathize representations of the conformal group. Let us assume a theory on an infinite cylinder parametrized by coordinates  $w = \sigma_0 + i\sigma_1$  with compactification  $\sigma_1 \sim \sigma_1 + 2\pi$ . In this picture, we can think of the theory as a theory of a closed string evolving in time  $\sigma_0$ . A Hilbert space corresponds to the slices of constant  $\sigma_0$ . Performing conformal map  $z = \exp w$ , one arrives at whole complex plane, where slicings map to concentric circles as shown in the figure 2.4. Time translation  $\sigma_0 \rightarrow \sigma_0 + a$  in this picture corresponds to rescaling  $z \rightarrow e^a z$ . We wish to construct CFT Hilbert space in this scheme. This scheme of quantizing is called *radial quantization* and it has been proposed in [47] and later developed in [48, 49].

If we switch to the complex plane description, the Hamiltonian of the system becomes dilatation operator

$$D = z\partial + \bar{z}\bar{\partial} \quad (2.52)$$

since it provides stretching of constant-time circles.

Similarly as the time-ordering appears in the standard definition of correlation functions, radial ordering must be introduced in the radial quantizing scheme

$$R(\mathcal{O}_1(z)\mathcal{O}_2(w)) = \begin{cases} \mathcal{O}_1(z)\mathcal{O}_2(w) & \text{for } |z| > |w| \\ \mathcal{O}_2(w)\mathcal{O}_1(z) & \text{for } |z| < |w|. \end{cases} \quad (2.53)$$

Let us see, how the conformal generators emerge in the radial quantization. In the operator formalism, symmetry generators can be constructed by integrating a Noether current over a fixed-time slice. In the case of conformal symmetry, the currents are  $J = T\epsilon$  and  $\bar{J} = \bar{T}\bar{\epsilon}$ . Performing the constants time contour integration for  $\epsilon = z^n$  or  $\epsilon = \bar{z}^n$  respectively, where  $n \in \mathbb{Z}$ , one finds prescription for conformal generators

$$L_n = \frac{1}{2\pi i} \oint dz z^{n+1} T(z), \quad \bar{L}_n = \frac{1}{2\pi i} \oint d\bar{z} \bar{z}^{n+1} \bar{T}(\bar{z}), \quad (2.54)$$

where the integration is encircling the origin. Conformal generators are modes of the stress-energy tensor since the previous relations can be inverted and we find

$$T(z) = \sum z^{-n-2} L_n \quad \bar{T}(\bar{z}) = \sum \bar{z}^{-n-2} \bar{L}_n. \quad (2.55)$$

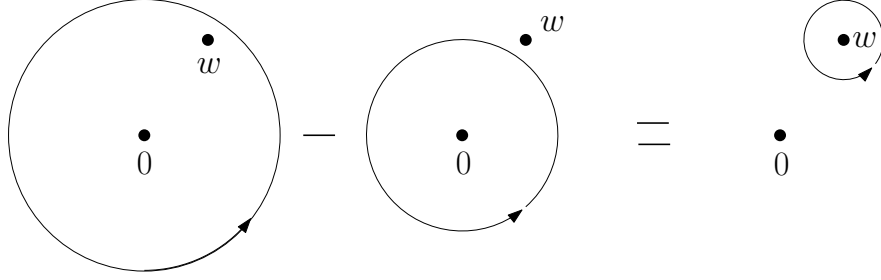


Figure 2.5: Contour deformation performed when deriving the relation for commutators of two operators.

To find a Lie algebra of these so-called *Virasoro generators*  $L_n$  and  $\bar{L}_n$  one needs to find their commutation relations. Generally, consider  $a$  and  $b$  to be holomorphic fields and  $A$  and  $B$  corresponding operators obtained as equal-radius contour integrals. Commutator of the operators  $A$  and  $B$  corresponds to the switch of the two integrations, namely

$$[A, B] = \oint_{\mathcal{C}_1} dz \oint_{\mathcal{C}_2} dw a(z)b(w) - \oint_{\mathcal{C}_1} dz \oint_{\mathcal{C}_2} dw b(z)a(w), \quad (2.56)$$

where the radius of  $\mathcal{C}_1$  is bigger than the radius of  $\mathcal{C}_2$ . Using contour deformation from the figure 2.5 and definition of the radial ordering for the deformed contour, we get explicit expression for desired commutator

$$[A, B] = \oint_0 dw \oint_w dz a(z)b(w). \quad (2.57)$$

With the use of the  $TT$  OPE (2.43), we get specially for the Virasoro generators

$$\begin{aligned} [L_n, L_m] &= \oint_0 dw \oint_w dz T(z)T(w) \\ &= \frac{1}{(2\pi i)^2} \oint_0 dw w^{m+1} \oint_w dz z^{n+1} \left[ \frac{c/2}{(z-w)^4} + \frac{2T(w)}{(z-w)^2} + \frac{\partial T(w)}{(z-w)} \right] \\ &= \frac{1}{2\pi i} \oint_0 dw w^{m+1} \left[ \frac{c}{12}(n^2+1)nw^{n-2} + 2(n+1)w^n T(w) + w^{n+1} \partial T(w) \right] \\ &= (n-m)L_{m+n} + \frac{c}{12}n(n-1)\delta_{m+n,0}. \end{aligned} \quad (2.58)$$

Similar computation can be performed for  $\bar{T}$ .  $L_m$ s with the above commutation relations form *Virasoro algebra*. This algebra has been introduced in [50] and later used to in CFT [47]. At classical level the term proportional to  $c$  is not present, but it emerged as a consequence of conformal anomaly.

Using the Virasoro generators one can find explicit expression for the quantum Hamiltonian. Since  $L_0 + \bar{L}_0$  corresponds to the transformation  $\delta z = z$ ,  $\delta \bar{z} = \bar{z}$ , it stretches concentric circles corresponding to given time and thus provides time translation in the radial picture. The dilatation operator can be written using Virasoro generators as

$$D = L_0 + \bar{L}_0. \quad (2.59)$$

Mapping the stress-energy tensor back to the cylinder, we get the energy operator

$$H = L_0 + \bar{L}_0 - 2\pi \frac{c + \bar{c}}{24}. \quad (2.60)$$

In CFT, we have one-to-one correspondence between operators and states. Assume asymptotic state on the cylinder  $\tau \rightarrow -\infty$ . This state maps into the origin in the radial quantization and we are left with a single point. Specifying a state is now equivalent to specifying local disturbance at the origin. This can be done by operator insertion. Classifying all the possible states is equivalent to classifying all the operators.

Now, we will construct highest weight representations of the Virasoro algebra. Suppose  $|h, \bar{h}\rangle$  is an eigenstate of  $L_0$  and  $\bar{L}_0$  with corresponding eigenvalues  $h$  and  $\bar{h}$ . These are the energy eigenstates on the cylinder with the energy  $E = 2\pi \left( h + \bar{h} - \frac{c + \bar{c}}{24} \right)$ , which can be seen from (2.60). From the commutation relations (2.58), we find that

$$L_0 L_n |h, \bar{h}\rangle = (h - n) |h, \bar{h}\rangle \quad (2.61)$$

and even  $L_n |h, \bar{h}\rangle$  is the energy eigenstate. We can generate whole spectrum acting by  $L$ s on the initial state. To get a spectrum bounded below, which is needed for the theory to be unitary as we will see later, there must exist a state annihilated by all  $L_n$ s with positive  $n$ . Such state is a *primary state* and has the lowest possible energy in given column of states. These highest weight representations are also called *Verma modules*. Fields obtained from a primary field by action of some combination of  $L_{-n}$ s, for  $n > 0$ , are called *descendant fields* and first few states of given Verma module are given in the table 2.2, where we have decomposed the fields into the left and right sectors  $|h, \bar{h}\rangle = |h\rangle \otimes |\bar{h}\rangle$  and we have written only the chiral representation explicitly. The decomposition can be done since left and right Virasoro algebras are independent. The other chiral representations can be obtained by  $h \rightarrow \bar{h}$ ,  $L \rightarrow \bar{L}$ . Total Virasoro representation is a tensor product of the two chiral representations.

Conformal weight	State
$h$	$ h\rangle$
$h + 1$	$L_{-1} h\rangle$
$h + 2$	$L_{-1}^2 h\rangle, L_{-2} h\rangle$
$h + 3$	$L_{-1}^3 h\rangle, L_{-2}L_{-1} h\rangle, L_{-3} h\rangle$
$h + 4$	$L_{-1}^4 h\rangle, L_{-2}L_{-1}^2 h\rangle, L_{-3}L_{-1} h\rangle, L_{-2}^2 h\rangle, L_{-4} h\rangle$

Table 2.2: First few states in the chiral representation of Virasoro algebra with corresponding conformal weights (levels).

In the table 2.2, all independent descendants on the first few levels are mentioned since all the other possibilities can be obtained commuting Virasoro generators to the right. One can associate a *character*

$$\chi_{(c,h)} = \text{Tr } q^{L_0 - c/24} = \sum_{n=0}^{\infty} \dim(h+n) q^{n+h-\frac{c}{24}}, \quad (2.62)$$

to a given Verma module with central charge  $c$  and conformal weight  $h$ , where  $q = e^{2\pi i \tau}$  and  $\dim(h+n)$  measures the number of the linearly independent states

at level  $n$ . In terms of these characters, modular partition functions can be written since it is precisely the trace of  $q^{L_0 + \frac{c}{24}}$  over the whole Hilbert space. The characters for the antiholomorphic Verma module are defined analogously.

Characters tells us, how many states are there at each level. It is simple to find general form for the characters of a Verma module. The number of states on given level is the partition number  $p(n)$  as can be easily deduced from the structure of Verma modules. Generating function for the partition numbers is

$$\frac{1}{\phi(q)} = \prod_{n=1}^{\infty} \frac{1}{1 - q^n} = \sum_{n=0}^{\infty} p(n) q^n \quad (2.63)$$

as can be easily checked expanding the term  $1/(1 - q^n)$  and multiplying all the terms. Defining so-called *Dedekind function*

$$\eta(q) = q^{1/24} \phi(q), \quad (2.64)$$

one can rewrite a generic Virasoro character conventionally as

$$\chi_{(c,h)} = \frac{q^{h+(1-c)/24}}{\eta(q)}. \quad (2.65)$$

We have seen the form of correlators for primary fields. Primary fields correspond to the highest weight states, but there are also many descendants. We wish to compute correlators of these descendants. Although we will use a technique of conservation laws to compute correlators in string field theory, we will comment on different method now. The method is based on the action of differential operator  $\mathcal{L}_{-n}$  corresponding to the descendant  $L_{-n}V_\alpha$  on the correlator of  $V_\alpha$  alone.

Using contour deformation and OPE of the stress-energy tensor  $T$  with primary field  $V_\alpha$ , one can compute a correlator of a descendant with other operators  $V = V_1(w_1, \bar{w}_1) \dots V_n(w_n, \bar{w}_n)$  as

$$\begin{aligned} \langle L_{-n} V_0(w) V \rangle &= \frac{1}{2\pi i} \oint_w dz (z - w)^{1-n} \langle T(z) V_0(w) V \rangle \\ &= -\frac{1}{2\pi i} \sum_\alpha \oint_{w_\alpha} dz (z - w)^{1-n} \left[ \frac{1}{z - w_\alpha} \partial_{w_\alpha} \langle V_0(w) V \rangle \right. \\ &\quad \left. + \frac{h_\alpha}{(z - w_\alpha)^2} \langle V_0(w) V \rangle \right] = \mathcal{L}_{-n} \langle V_0 V \rangle, \end{aligned} \quad (2.66)$$

where we have introduced a differential operator

$$\mathcal{L}_{-n} = \sum_i \left[ \frac{(n-1)h_i}{(w_i - w)^n} - \frac{1}{(w_i - w)^{n-1}} \partial_{w_i} \right] \quad (2.67)$$

that brings us from the correlator of primary fields to the correlator of their descendants. Generalization to correlators with different number of different Virasoro generators acting on different operator insertions is straightforward. One only needs to act by appropriate operators on the formula for the correlator of corresponding primary operators.

Now, we will comment on the operator algebra introduced earlier. Using OPE one can reduce the number of operators inserted in the correlator. Two

operators are exchanged by infinite sum of single insertions. It can be interpreted as multiplication on the space of all operators in the theory. In the following, we will see that, except of the structure constants introduced earlier, all coefficients of the OPEs are fixed by conformal invariance.

Consider a theory with primary operators  $V_\alpha$  and their descendants. Scaling invariance then fixes the form of the operator algebra

$$V_1(z, \bar{z})V_2(0, 0) = \sum_{\alpha} \sum_{I, J} C_{12}^{\alpha I J} z^{h_\alpha - h_1 - h_2 + |I|} \bar{z}^{\bar{h}_\alpha - \bar{h}_1 - \bar{h}_2 + |J|} (L_{-I} \bar{L}_{-J} V_\alpha(0, 0)), \quad (2.68)$$

where the sum runs over all primaries and their descendants given by multi-indices  $I$  and  $J$ , for  $I = (k_1, k_2, \dots)$  and  $L_{-I} = \dots L_{-2}^{k_2} L_{-1}^{k_1}$ . We have also denoted  $|I| = \sum_i k_i$  and similarly  $|J| = \sum_i l_i$  in the antiholomorphic sector.

One can now compute an overlap of this expression applied on the vacuum  $|0\rangle$  with other primary field  $V_\beta$ . Only term proportional to  $C_{12}^{\alpha 00}$  remains and the amplitude can be also rewritten using known form of the 3-point function. One arrives at

$$\langle V_\beta | V_1(z, \bar{z}) | V_2 \rangle = \frac{C_{\beta 12}}{z^{h_1 + h_2 - h_\beta} \bar{z}^{\bar{h}_1 + \bar{h}_2 - \bar{h}_\beta}} \quad (2.69)$$

and we can identify the first coefficient of the OPE with corresponding structure constant  $C_{\alpha 12} = C_{12}^{\alpha 00}$ . All the other coefficients are determined by conformal invariance and structure constants are the only needed ingredients to compute arbitrary correlator.

Since correlation functions of descendants are obtained from the correlators of corresponding primaries, we expect the other coefficients to have form

$$C_{12}^{\alpha I J} = C_{\alpha 12} \beta_{\alpha 12}^I \bar{\beta}_{\alpha 12}^J. \quad (2.70)$$

Due to the relation  $C_{\alpha 12} = C_{12}^{\alpha 00}$  we set  $\beta_{\alpha 12}^0 = 1$  and all the other coefficients are fixed by requirement that both sides of the expression (2.68) behave identically under the conformal transformation.

Consider a spinless primary  $|h, h\rangle$  and let us restrict ourselves only on the holomorphic part. We will use notation

$$\phi(z) = \sum_I C_{\alpha 12} z^{|I|} \beta_{\alpha 12}^I L_{-I}. \quad (2.71)$$

In the operator algebra, states of the form

$$|z, h_\alpha\rangle = \phi(z) |h_\alpha\rangle = \sum_{N=0}^{\infty} z^{|I|} |N, h_\alpha\rangle \quad (2.72)$$

multiplied by corresponding structure constant emerge. We have also denoted  $|N, h_\alpha\rangle$  a state on the level  $N$  in corresponding Verma module.

Acting by (2.68) on the vacuum  $|0\rangle$  and using the notation described above, one finds

$$V_1(z, \bar{z}) |h_2, \bar{h}_2\rangle = \sum_{\alpha} C_{\alpha 12} z^{h_\alpha - 2h} \bar{z}^{\bar{h}_\alpha - 2\bar{h}} \phi(z) \bar{\phi}(\bar{z}) |h_\alpha, \bar{h}_\alpha\rangle. \quad (2.73)$$

If we apply  $L_n$ , for  $n > 0$ , on this equation we get on the left-hand side

$$L_n V_1(z, \bar{z}) |h_2, \bar{h}_2\rangle = (z^{n+1} \partial_z + (n+1)h) V_1(z, \bar{z}) |h_2, \bar{h}_2\rangle, \quad (2.74)$$

where we have commuted  $L_n$  that annihilates a primary state to the right. On the other side, we find

$$\begin{aligned} & \sum_{\alpha} C_{\alpha 12} z^{h_{\alpha}-2h} \bar{z}^{\bar{h}_{\alpha}-2\bar{h}} L_n |z, h_{\alpha}\rangle |z, \bar{h}_{\alpha}\rangle \\ &= \sum_{\alpha} C_{\alpha 12} z^{h_{\alpha}-2h} \bar{z}^{\bar{h}_{\alpha}-2\bar{h}} ((h_{\alpha} + h(n-1))z^n + z^{n+1}\partial_z) |z, h_{\alpha}\rangle |z, \bar{h}_{\alpha}\rangle. \end{aligned} \quad (2.75)$$

Comparing coefficients on each side, one finds recursion relation that leads to the solution for the states  $|N, h_{\alpha}\rangle$  and so for the coefficients  $\beta_{\alpha 12}^{IJ}$ . Using this relation for  $N = 0$  the only nontrivial constraint is given by  $n = 1$  and one finds

$$L_1 |1, h_{\alpha}\rangle = h_{\alpha} |h_{\alpha}\rangle = \beta_{\alpha 12}^1 L_1 L_{-1} |h_{\alpha}\rangle = \beta_{\alpha 12}^1 [L_1, L_{-1}] |h_{\alpha}\rangle = 2h_{\alpha} \beta_{\alpha 12}^1 |h_{\alpha}\rangle. \quad (2.76)$$

We can now identify the coefficient  $\beta_{\alpha 12}^1 = 1/2$ . Similar procedure holds for higher levels, but the computation becomes more tedious. We have thus shown that structure constants are the only needed input for the operator algebra to be defined. All the other coefficients are then determined by conformal invariance.

Assume the existence of the vacuum state  $|0\rangle$  on which we will construct the Hilbert space. This state is defined to be as much symmetrical as possible. We define it to be annihilated by all  $L_n$ s, where  $n \geq 0$ . The vacuum cannot be annihilated by all the Virasoro generators because of consistency with the central charge term. If it were not the case then

$$0 = L_{-n} |0\rangle = L_n L_{-n} |0\rangle = \left( L_{-n} L_n + \frac{c}{12} (n^3 - n) \right) |0\rangle = \frac{c}{12} (n^3 - n) |0\rangle \neq 0. \quad (2.77)$$

The contradiction do not appear in the case  $L_{-n} |0\rangle \neq 0$ , for  $n \geq 2$ .

Being equipped by the vacuum state  $|0\rangle$  corresponding to the insertion of the identity operator at the origin, we can get arbitrary primary state with  $L_0, \bar{L}_0$  eigenvalues  $(h, \bar{h})$  by insertion of a primary field (also called *vertex operator* in this context) with conformal weights  $(h, \bar{h})$ . Clearly,

$$\begin{aligned} L_n |V_{\alpha}\rangle &= \oint \frac{dz}{2\pi i} z^{n+1} T(z) V_{\alpha}(0) |0\rangle \\ &= \oint \frac{dz}{2\pi i} z^{n+1} \left( \frac{h V_{\alpha}}{z^2} + \frac{\partial V_{\alpha}}{z} + \dots \right) |0\rangle = 0, \end{aligned} \quad (2.78)$$

for  $n > 0$  and  $V_{\alpha}$  primary operator, due to regularity of the expression which is being integrated. Oppositely, if a state is annihilated by all the Virasoro generators with  $n > 0$  and there exists a vertex operator, the singular part of the OPE with the stress-energy tensor must stop with  $z^{-2}$  term and it must be primary field. Moreover, we see from the above calculation that  $L_0 |V_{\alpha}\rangle = h_{\alpha} |V_{\alpha}\rangle$  and  $L_{-1} |V_{\alpha}\rangle = |\partial V_{\alpha}\rangle$ .

Finally, we will show that unitarity condition leads us to positivity of  $L_0$  eigenvalues. We need to define a dual states to  $|h, \bar{h}\rangle$ . They will correspond to the fields inserted on the other side of the Riemann sphere  $z \rightarrow \infty$ . Intuitional definition is obtained by mapping a primary operator  $V_{\alpha}$  to the infinity using  $w \rightarrow -1/w$ . We define BPZ-dual state to be

$$\langle V_{\alpha} | = \text{BPZ}(|V_{\alpha}\rangle) = \lim_{z \rightarrow 0} \langle 0 | V_{\alpha} \left( -\frac{1}{z}, -\frac{1}{\bar{z}} \right) \frac{1}{z^{2h_{\alpha}}} \frac{1}{\bar{z}^{2\bar{h}_{\alpha}}} \quad (2.79)$$

The overlap of states  $|V_1\rangle$  and  $|V_2\rangle$  is then regularized correlator of fields inserted at the origin and at the infinity. We will denote BPZ-conjugation of the vacuum  $\langle 0|$ . We wish to find BPZ-conjugation of operator modes appearing in a mode expansion of general operator

$$\mathcal{O}_\alpha = \sum_{m,n \in \mathbb{Z}} \frac{\mathcal{O}_{m,n}^\alpha}{z^{-m-h_\alpha} \bar{z}^{-n-\bar{h}_\alpha}} \quad (2.80)$$

that generalizes the expansion (2.55) of the stress-energy tensor. Performing the mapping as in the case of primary operators, one finds

$$\text{BPZ}(\mathcal{O}_{m,n}^\alpha) = (-1)^{n+m+\Delta_\alpha} \mathcal{O}_{-m,-n}^\alpha. \quad (2.81)$$

This algebra will be important later when performing computations in string field theory. Detailed discussion can be found in the books listed at the beginning of this chapter. In the rest of this chapter, we will focus on some examples that help us in clarifying the above abstract considerations.

## 2.6 Examples of CFTs

### 2.6.1 Free boson

In this subsection, we will study the free scalar field that will prove useful in discussions of bosonic string theory and double Ising model. The action of the theory

$$S = \frac{1}{4\pi} \int d^2\sigma \partial_\alpha X \partial^\alpha X \quad (2.82)$$

is clearly conformally invariant since field  $X$  transforms under rescaling  $\sigma^\alpha \rightarrow \lambda \sigma^\alpha$  as  $X(\sigma^\alpha) \rightarrow X(\lambda^{-1} \sigma^\alpha)$ . Note that any inclusion of polynomial term, such as the mass term, would spoil the conformal invariance.

Standard procedure leads to the stress-energy tensor of the theory

$$T_{\alpha\beta} = -\partial_\alpha X \partial_\beta X + \frac{1}{2} \delta_{\alpha\beta} (\partial X)^2, \quad (2.83)$$

where the expression on the left must be understood to be normal ordered product. Taking the trace, one can check it vanishes. Switching to the complex coordinates, we get

$$T = -\partial X \partial X, \quad \bar{T} = -\bar{\partial} X \bar{\partial} X. \quad (2.84)$$

Varying the action (2.82), we find equation of motion

$$\partial \bar{\partial} X = 0, \quad (2.85)$$

which tells us that  $\partial X$  is holomorphic field and  $\bar{\partial} X$  is antiholomorphic field. Due to the equation of motion  $\partial \bar{\partial} X = 0$ , we can split  $X$  into the holomorphic (left) and antiholomorphic (right) piece  $X(z, \bar{z}) = X_L(z) + \bar{X}_R(\bar{z})$ .

Let us proceed by computation of propagator. Consider the path integral of total functional derivative

$$0 = \int [DX] \frac{\delta}{\delta X(\sigma)} \left[ e^{-S(X(\sigma'))} X(\sigma') \right] \quad (2.86)$$

$$= \int [DX] e^{-S(X)} \left[ \frac{1}{2\pi} \partial^2 X(\sigma) X(\sigma') + \delta(\sigma - \sigma') \right]. \quad (2.87)$$



We find differential equation for the propagator

$$\langle \partial^2 X(\sigma) X(\sigma') \rangle = -2\pi \delta(\sigma - \sigma') \quad (2.88)$$

with well known solution

$$\langle X(\sigma) X(\sigma') \rangle = -\frac{1}{2} \ln(\sigma - \sigma')^2. \quad (2.89)$$

The same derivation can be performed with arbitrary other insertions and we obtain OPE

$$X(z) X(w) = -\frac{1}{2} \ln(z - w). \quad (2.90)$$

It is clear that this OPE does not correspond to a primary operator, but performing a derivative, one finds

$$\partial X(z) \partial X(w) = -\frac{1}{2} \frac{1}{(z - w)^2}, \quad (2.91)$$

i.e. OPE of primary operators with conformal weights  $(1, 0)$ . Similar expression would appear in the antiholomorphic case. To prove that  $\partial X$  is a primary field we must find its transformation properties. They are encoded in the OPE with the stress-energy tensor

$$\begin{aligned} T(z) \partial X(w) &= - : \partial X(z) \partial X(z) : \partial X(w) \sim 2 \frac{1}{2} \frac{\partial X(z)}{(z - w)^2} \\ &\sim \frac{\partial X(w)}{(z - w)^2} + \frac{\partial^2 X(w)}{z - w}, \end{aligned} \quad (2.92)$$

where the number 2 comes from two contractions in the Wick formula and we have used OPE (2.91) with expansion of holomorphic field  $\partial X$  around  $w$ . This is precisely the OPE for primary fields. Similarly, one can find OPE with  $\bar{T}$  to be trivial. We have thus proved that  $\partial X$  is a primary field with conformal weights  $(1, 0)$  and similarly  $\bar{\partial} X$  is a primary field with weights  $(0, 1)$ .

There can be found other primaries for the free boson, namely  $:e^{ikX}:$ . We wish to prove that these field are indeed primary and find their conformal weights. Expanding the normal ordered exponential and using the Wick's formula, one finds

$$\partial X(z) : e^{ikX(w)} : \sim -\frac{ik}{2} \frac{e^{ikX(w)}}{z - w}. \quad (2.93)$$

With this knowledge it is easy to derive OPE with  $T$

$$\begin{aligned} T : e^{ikX(w)} : &:= - : \partial X(z) \partial X(z) : : e^{ikX(w)} : \\ &\sim \frac{k^2}{4} \frac{e^{ikX(w)}}{(z - w)^2} + \frac{\partial e^{ikX(w)}}{z - w}, \end{aligned} \quad (2.94)$$

where the first term comes from two contractions, while the second one comes from a single contraction. Similar derivation holds for OPE with  $\bar{T}$  and we have thus proved that  $:e^{ikX}:$  is a primary operator with conformal weights  $(k^2/4, k^2/4)$ . In the following, we will omit normal ordering colons for abbreviation.

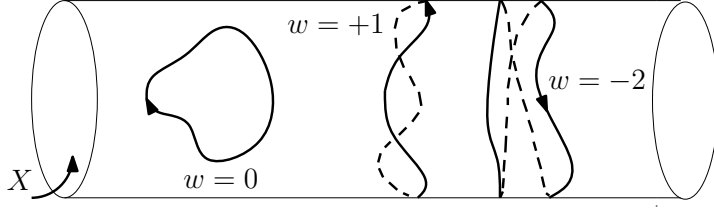


Figure 2.6: Closed strings in a compactified dimension  $X$  with different winding numbers  $w$ .

Using relation (2.89), the Wick theorem, and expansion of  $e^{ikX(z)}$  around the point  $w$  one finds OPE

$$\begin{aligned} e^{ik_1 X(z_1, \bar{z}_1)} e^{ik_2 X(z_2, \bar{z}_2)} &= |z_{12}|^{k_1 k_2} (1 + iz_{12} k_1 \partial X + i\bar{z}_{12} k_1 \bar{\partial} X \\ &- |z_{12}|^2 k_1^2 \partial X \bar{\partial} X + \dots) e^{i(k_1 + k_2) X(z_2, \bar{z}_2)} \end{aligned} \quad (2.95)$$

that will be needed when studying correspondence between the doubled Ising model and the free boson living on the orbifold with radius  $\sqrt{2}$ .

Finally, the central charge can be determined from the OPE of the stress-energy tensors

$$T(z)T(w) \sim \frac{1/2}{(z-w)^4} + \frac{2T(w)}{(z-w)^2} + \frac{\partial T(w)}{z-w} \quad (2.96)$$

and we find that  $c = 1$ . Similarly, one can also find that  $\bar{c} = 1$ .

Consider an example of the compactified boson  $X(\sigma+L, \tau) \sim X(\sigma, \tau) + 2\pi m R$ , where  $m$  is called *winding number* and counts the number of times a string is wound on the compactified dimension as shown in the figure 2.6. Since  $\partial X(z)$  is holomorphic and  $\bar{\partial} X(\bar{z})$  is antiholomorphic, we can expand it into the Laurent series

$$\partial X(z) = -i \frac{1}{\sqrt{2}} \sum_{m=-\infty}^{\infty} \frac{\alpha_m}{z^{m+1}}, \quad \bar{\partial} X(\bar{z}) = -i \frac{1}{\sqrt{2}} \sum_{m=-\infty}^{\infty} \frac{\tilde{\alpha}_m}{\bar{z}^{m+1}}. \quad (2.97)$$

Quantizing the momentum one finds

$$\frac{n}{R} = p = \frac{1}{2\pi} \oint (dz \partial X - d\bar{z} \bar{\partial} X) = \frac{1}{\sqrt{2}} (\alpha_0 + \tilde{\alpha}_0) \quad (2.98)$$

and from the winding around the compact dimension

$$Rw = \frac{1}{2\pi} \oint (dz \partial X + d\bar{z} \bar{\partial} X) = \frac{1}{\sqrt{2}} (\alpha_0 - \tilde{\alpha}_0). \quad (2.99)$$

From the above two relations we can define left and right momenta

$$k_L = \sqrt{2} \alpha_0 = \frac{n}{R} + wR \quad k_R = \sqrt{2} \tilde{\alpha}_0 = \frac{n}{R} - wR. \quad (2.100)$$

One can split the field  $X$  into the holomorphic and antiholomorphic parts  $X(z, \bar{z}) = X_L(z) + X_R(\bar{z})$  and any vertex operator corresponding to state  $|k_L, k_R\rangle$  can be written in the form

$$V_{k_L, k_R}(z, \bar{z}) = e^{ik_L X_L(z) + ik_R X_R(\bar{z})}, \quad (2.101)$$

$\Delta$	Primary field
0	$\mathbb{1}$
$\frac{1}{2R^2}$	$\cos \frac{X}{R}$
$\frac{R^2}{2}$	$\cos R\tilde{X}$
$\frac{1}{R^2}$	$\cos \frac{2X}{R}$
$\frac{1}{2R^2} + \frac{R^2}{2}$	$\cos \frac{X+R^2\tilde{X}}{R}, \cos \frac{X-R^2\tilde{X}}{R}$
$R^2$	$\cos 2R\tilde{X}$

Table 2.3: Spectrum of primary operators in non-twisted sector of the free boson on the orbifold  $S/Z_2$  with radius  $R$ .

where  $k_L$  and  $k_R$  are appropriately quantized. We will also denote  $\tilde{X}(z, \bar{z}) = X_L(z) - X_R(\bar{z})$ . Since the stress-energy tensor can be written in terms of  $\alpha$ -oscillators, we can find correspondence

$$L_m = \frac{1}{2} \sum_{n=-\infty}^{\infty} \alpha_{m-n} \alpha_n \quad (2.102)$$

and descendant fields are expressible as  $\alpha$ -descendants.

The last example that we will consider in this subsection is the boson living on the orbifold  $S^1/Z_2$ . In this theory only vertex operators that preserve orbifold symmetry  $X \sim -X$  will remain. On the other hand, new sector of so-called *twisted states* satisfying  $X(\sigma_0, \sigma_1 + 2\pi R) = -X(\sigma_0, \sigma_1)$  appears.

Consider states that remain in the theory after projecting out the states that are not invariant under the  $Z_2$  symmetry. Clearly, odd  $\alpha$ -descendants will be projected out. We need to find primary operators that maintain the invariance. Half of the primaries have to be crossed out and few remaining primary operators are listed in the table 2.3

We can see that spectrum does not change if we provide a switch  $X \rightarrow \tilde{X}$  and  $\tilde{X} \rightarrow X$  together with the change of the radius of the compactified dimension  $R \rightarrow \frac{1}{R}$ . This correspondence is called T-duality and it has far reaching consequences.

As mentioned above, there is also twisted sector in the spectrum of operators. The twisted sector correspond to the antiperiodic boundary conditions and  $X$  must have half-integral mode expansion. The antiperiodicity forbids any momentum and the center of mass must be localized at fixed points. Corresponding vacua will be denoted as  $|T_1\rangle$  and  $|T_2\rangle$  and their weights are  $(\frac{1}{16}, \frac{1}{16})$ . We can find them similarly as in the antiperiodic sector of the free fermion in the next subsection. Detailed argument can be found in [9]. In the twisted sector only even excitations are present since the other are projected out by  $Z_2$  projection.

## 2.6.2 Free fermion

In this subsection, we will rest a bit on the free fermion  $\psi, \bar{\psi}$  on the cylinder with the action

$$S = \frac{1}{8\pi} \int (\psi \bar{\partial} \psi + \bar{\psi} \partial \bar{\psi}). \quad (2.103)$$

Similarly as in the case of the free boson, one finds OPEs

$$\psi(z)\psi(w) \sim -\frac{1}{z-w}, \quad \bar{\psi}(\bar{z})\bar{\psi}(\bar{w}) = -\frac{1}{\bar{z}-\bar{w}}. \quad (2.104)$$

The stress-energy tensor is

$$T(z) = \frac{1}{2} : \psi(z)\partial\psi(z) :, \quad \bar{T}(\bar{z}) = \frac{1}{2} : \bar{\psi}(\bar{z})\bar{\partial}\bar{\psi}(\bar{z}) : \quad (2.105)$$

and computing  $TT$  OPE, one finds that  $(c, \bar{c}) = (\frac{1}{2}, \frac{1}{2})$ . From the  $T\psi$  OPE one can verify that  $\psi$  and  $\bar{\psi}$  are indeed primary fields and they have conformal weights  $(\frac{1}{2}, 0)$  and  $(0, \frac{1}{2})$  respectively.

Now, we are ready to construct all states in the free fermion theory. Expanding field  $\psi$ , one finds

$$i\psi(z) = \sum_n \psi_n z^{-n-1/2}, \quad (2.106)$$

where modes  $\psi_n$  satisfy anticommutation relations

$$\{\psi_n, \psi_m\} = - \oint \frac{dw}{2\pi i} w^{m-1/2} \oint \frac{dz}{2\pi i} z^{n-1/2} \frac{-1}{z-w} = \delta_{n+m,0}.$$

There are two sectors in the fermionic theory related to the boundary conditions chosen for  $2\pi$  rotation around the origin. Fields with periodic and anti-periodic boundary conditions satisfy one of the conditions  $\psi(e^{2\pi i}z) = \pm\psi(z)$ . We immediately see that the periodic field has modes labeled by half-integers whereas the anti-periodic fields has integer modes. The first sector is called Neveu-Schwarz (NS) and the other one is Ramond (R).

It is convenient to introduce an operator  $(-1)^F$ , where  $F$  is the *fermionic number*, defined as

$$(-1)^F \psi(z) = -\psi(z)(-1)^F. \quad (2.107)$$

In the case of Ramond sector, the presence of the zero mode, satisfying

$$\{\psi_0, \psi_0\} = 1, \quad \{\psi_0, (-1)^F\} = 0, \quad (2.108)$$

has to be taken into account. Applying  $\psi_0$  on the  $L_0$  eigenstate remains to be  $L_0$  eigenstate and thus we have a ground state degeneracy in this sector. Corresponding primary fields are called *order* and *disorder fields*  $\sigma$  and  $\mu$  and they are defined as eigenstates of  $(-1)^F$  with eigenvalue  $+1$  or  $-1$  respectively. It is not difficult to prove that both  $\sigma$  and  $\mu$  has conformal weights  $(\frac{1}{16}, \frac{1}{16})$ . Similar degeneration appeared in the twisted sector of the boson living on the orbifold.

### 2.6.3 bc-ghost system

During quantization of the bosonic strings in covariant gauge, so-called fermionic ghost fields  $b$  and  $c$  appear. The action for this system is

$$S = \frac{g}{2} \int d^2\sigma b_{\mu\nu} \partial^\mu c^\nu, \quad (2.109)$$

where ghosts are fermions and  $b_{\mu\nu}$  is traceless and symmetric. In the complex notation, equations of motion read

$$\bar{\partial}b = 0, \quad \bar{\partial}\bar{b} = 0, \quad \bar{\partial}c = 0, \quad \partial\bar{c} = 0, \quad \partial c = -\bar{\partial}\bar{c}. \quad (2.110)$$

Standard procedure will lead to the stress-energy tensor

$$T = 2(\partial c)b + c\partial b \quad (2.111)$$

and its antiholomorphic counterpart. Using path integral method, one obtains OPE

$$b(z)c(w) = \frac{1}{z-w}. \quad (2.112)$$

From the above OPE, one can prove that  $b$  and  $c$  are primary fields with conformal weights  $(2, 0)$  and  $h = (-1, 0)$  respectively, computing OPE with the stress-energy tensor  $T$ . From the  $TT$  expansion, one also finds that the central charge of the theory is -26.

We can decompose the ghost fields  $b$  and  $c$  into the modes in accordance with (2.80). Arbitrary state in radial quantization can be then obtained from the action of these modes on the vacuum, where we require  $b_n|0\rangle = 0$  for  $m > -2$  and  $c_n|0\rangle = 0$  for  $m > 1$  to get regular expressions. From the relation (2.112) one finds anticommutation relation for  $b$  and  $c$  ghosts

$$\{b_m, c_n\} = \delta_{m,-n}. \quad (2.113)$$

## 2.7 The Ising model as a minimal model

Huge progress can be done in the case of CFTs with central charge less than one. In this case, all unitary models (i.e. models containing no state with negative norm) have been found. As discussed previously, unitarity implies that the theory contains only highest weight representations and the energy eigenvalues (i.e. scaling dimensions) are positive. This requirement is physical since negative scaling dimension would correspond to growing correlations with distance. The Ising model is thus unitary and since it can be formulated in terms of free fermion that has central charge  $(\frac{1}{2}, \frac{1}{2})$ , the Ising model will have the same central charge and fall into the minimal models category.

To get unitary model, conformal charge cannot be negative since

$$\langle h|L_n L_{-n}|h\rangle = \left[2nh + \frac{1}{12}cn(n^2 - 1)\right] \langle h|h\rangle \quad (2.114)$$

becomes negative, for  $n$  sufficiently large, if  $c < 0$ .

If we denote  $|i\rangle$  the basis states in the Verma module under consideration, we can define a *Gram matrix*

$$M_{ij} = \langle i|j\rangle. \quad (2.115)$$

This Gram matrix has certainly block-diagonal structure with blocks corresponding to different levels. Using this matrix, one can reproduce a norm of general state  $|a\rangle = \sum_i a_i|i\rangle$  from the formula  $\langle a|a\rangle = a^\dagger M a$ . Matrix  $M$  can be diagonalized by a unitary matrix  $U$ . Denoting  $\Lambda_i$  its eigenvalues and  $b = Ua$ , we get

$$\langle a|a\rangle = \sum_i \Lambda_i |b_i|^2. \quad (2.116)$$

From this equation we see that unitarity is equivalent to the positivity of all eigenvalues of  $M$ .

If we study these Gram matrices, we can find restrictions on the possible values of  $c$  and  $h$ . First restriction comes from the positivity of determinants of the diagonal blocks  $M^{(l)}$  of Gram matrix, where  $l$  labels the level of corresponding block. General formula for this determinant have been found by Kac

$$\det M^{(l)} = \alpha_l \prod_{1 \leq r, s; rs \leq l} [h - h_{r,s}(c)]^{p(l-rs)}, \quad (2.117)$$

where  $\alpha_l$  is positive constant,  $p(t-rs)$  is the number of partitions of the integer  $l-rs$  and

$$c(m) = 1 - \frac{6}{m(m+1)}, \quad h_{r,s}(m) = \frac{[(m+1)r - ms]^2 - 1}{4m(m+1)}. \quad (2.118)$$

The form of the Kac determinant has been guessed in [51] and proven later [52].

It has been proven that there exists only a discrete set of CFTs with  $c < 1$  that are unitary [53]. They lie on the vanishing curve of the Kac determinant for some  $l$  and the theories can be parametrized by integers  $m$ ,  $r$ , and  $s$ , where  $1 \leq r < m$  and  $1 \leq s \leq r$  in the above expression. Theories containing only these representations associated with particular  $m$  will be called minimal models and we will label them  $\mathcal{M}(m+1, m)$ .

Now, we are ready to indicate the Ising model. It has been done in [47] for the first time. Since central charge of its chiral representation is  $\frac{1}{2}$ , which is apparent from the correspondence with free fermion, we find that  $m = 3$  in the above equation. There are three possible conformal weights of primary states for  $m = 3$ , namely  $0, \frac{1}{16}$ , and  $\frac{1}{2}$ . The field with 0 conformal weight clearly corresponds to the identity insertion. We wish to assign operators to the spin variable  $\sigma$  and the energy density  $\epsilon$  of the Ising model. This can be easily deduced recalling critical exponents from the table (1.1) and the form of the 2-point function in CFT. From the form of correlators of Ising spins, the fields has to be spinless. It means that holomorphic field has to be combined with its antiholomorphic counterpart with the same conformal weight. The field with conformal weights  $(\frac{1}{16}, \frac{1}{16})$  will decay as

$$\sim \frac{1}{z^{1/16+1/16} \bar{z}^{1/16+1/16}} = \frac{1}{|z|^{1/4}} \quad (2.119)$$

and we get correct correlator for the spin operator  $\sigma$ . The same procedure leads to the determination that the energy density  $\epsilon$  corresponds to the primary field with conformal weights  $(\frac{1}{2}, \frac{1}{2})$ .

One may ask, whether there are any other primary operators than  $\mathbb{1}$ ,  $\sigma$ , and  $\epsilon$  in the Ising model. The answer is no. These operators closes under the operator algebra and consistently describe the Ising model. Moreover, we will argue that modular invariance condition will force the Ising model CFT to be composed of precisely these three representations (no representation emerges with higher multiplicity).

Since all the primary operators in minimal models correspond to zeros of the Kac determinant, there are null states in their Verma modules. It has far reaching consequences. First of all, representations are not irreducible. If  $|\chi\rangle$  is a null state then it is orthogonal to all the other states

$$\langle h | L_{k_n} \dots L_{k_1} | \chi \rangle = 0. \quad (2.120)$$

If we wish to get irreducible representation, the null states have to be projected out. The structure of the null states is quite complicated and we invite reader to read corresponding chapter in [43] or in the original work [51]. Here, we give only few first terms of characters for operators in the Ising model.

$\mathbb{1}$	$1 + q^2 + q^3 + 2q^4 + 2q^5 + 3q^6 + \dots$
$\epsilon$	$1 + q + q^2 + q^3 + 2q^4 + 2q^5 + 3q^6 + \dots$
$\sigma$	$1 + q + q^2 + 2q^3 + 2q^4 + 3q^5 + 4q^6 + \dots$

Table 2.4: Characters of the three irreducible representations appearing in the Ising model CFT.

The existence of null states gives restriction to the operator algebra. The operator  $\mathbb{1}$  has trivial OPE with other operators and we will be interested only in  $\sigma \times \sigma$ ,  $\sigma \times \epsilon$ , and  $\epsilon \times \epsilon$  combinations [47]. There are null states in the Verma module of  $\epsilon$  and  $\sigma$  at level 2

$$\begin{aligned} |\chi_1\rangle &= \left[ L_{-2} - \frac{4}{3}L_{-1}^2 \right] |\sigma\rangle, \\ |\chi_2\rangle &= \left[ L_{-2} - \frac{3}{4}L_{-1}^2 \right] |\epsilon\rangle. \end{aligned} \quad (2.121)$$

Since this combination is null, the action of corresponding differential operators

$$\begin{aligned} \mathcal{L}_\sigma &= \left[ \mathcal{L}_{-2} - \frac{4}{3}\mathcal{L}_{-1}^2 \right], \\ \mathcal{L}_\epsilon &= \left[ \mathcal{L}_{-2} - \frac{3}{4}\mathcal{L}_{-1}^2 \right] \end{aligned} \quad (2.122)$$

on the correlation functions of primary fields vanishes

$$\begin{aligned} \mathcal{L}_\sigma \langle \sigma(z) V_1(z_1) V_2(z_2) \rangle &= 0, \\ \mathcal{L}_\epsilon \langle \epsilon(z) V_1(z_1) V_2(z_2) \rangle &= 0, \end{aligned} \quad (2.123)$$

for all operators  $V_1$  and  $V_2$ . This relation gives us constrain on the conformal weights of the other two operators and in turn on the operator algebra. After some numerical manipulations we find that only nonvanishing cases gives rise to the fusion rules

$$\begin{aligned} \sigma \times \sigma &= \mathbb{1} + \epsilon, \\ \epsilon \times \epsilon &= \mathbb{1}, \\ \epsilon \times \sigma &= \sigma \end{aligned} \quad (2.124)$$

and assuming the trivial relation  $\mathbb{1} \times \mathbb{1} = \mathbb{1}$ , we get operator algebra for the Ising model. The relation for fusion rules can be generalized for other models and details can be found for example in [43]. The above relation means that taking two fields from the Verma modules on the left-hand side and performing their OPE one finds states from the Verma modules appearing on the right-hand side. Specially in the case of the Ising model

$$\epsilon(z)\epsilon(0) = \frac{1}{z} \left( 1 + 2z^2 L_{-2} + z^3 L_{-3} + \frac{3}{7}z^4 L_{-4} + \frac{2}{7}z^4 L_{-2}L_{-2} + \dots \right) \mathbb{1}$$

$$\begin{aligned}
\sigma(z)\sigma(0) &= \frac{1}{z^{1/8}} \left( 1 + \frac{1}{4}z^2L_{-2} + \frac{1}{8}z^3L_{-3} + \frac{15}{224}z^4L_{-4} + \frac{3}{224}z^4L_{-2}L_{-2} + \dots \right) \mathbb{1} \\
&+ \frac{1}{2}z^{3/8} \left( 1 + \frac{1}{2}zL_{-1} + \frac{1}{4}z^2L_{-2} + \frac{5}{32}z^3L_{-3} + \frac{19}{256}z^4L_{-4} \right. \\
&\left. + \frac{15}{256}z^4L_{-3}L_{-1} + \dots \right) \epsilon(0) \\
\epsilon(z)\sigma(0) &= \frac{1}{2} \frac{1}{z^{1/2}} \left( 1 - 3zL_{-1} - \frac{5}{8}z^2L_{-2} + \frac{3}{56}z^3L_{-3} - \frac{29}{56}z^3L_{-2}L_{-1} \right. \\
&\left. + \frac{75}{2048}z^4L_{-4} - \frac{87}{256}z^4L_{-3}L_{-1} + \dots \right) \sigma(0).
\end{aligned} \tag{2.125}$$

and similarly for the antiholomorphic part.

In the above OPEs, structure constants  $C_{\mathbb{1}\epsilon\epsilon}$ ,  $C_{\mathbb{1}\sigma\sigma}$ , and  $C_{\sigma\sigma\epsilon}$  have been inserted. The first two are trivially 1 due to the normalization of 2-point function. Finding  $C_{\sigma\sigma\epsilon}$  needs a bit of computation. It can be derived using correspondence of the doubled Ising model with the free boson. We will proceed differently later when introducing sewing constraints. The other numerical coefficients in (2.125) have been obtained as in the case (2.76).

It is worth mentioning that correspondence of the Ising model with free Majorana fermion appears again here. Comparing conformal weights, we can find correspondence of the energy density operator

$$\epsilon(z, \bar{z}) \propto \psi(z)\bar{\psi}(\bar{z}) \tag{2.126}$$

and similarly for the operator  $\sigma$  corresponding to the order operators in the NS sector.

## 2.8 Double Ising and bosonization

Note that  $\frac{1}{2} + \frac{1}{2} = 1$ . We can thus expect that doubling the Ising model (see section about the double Ising model), we obtain some theory of the free boson. In this section, we will comment on this correspondence a bit. Double Ising model can be mapped on the theory of the free boson living on the  $S^1/Z_2$  orbifold with radius  $\sqrt{2}$  [43].

Primary states of the free boson on the orbifold  $S^1/Z_2$  have been already summarized. The precise correspondence of fields can be proven computing partition functions for these models and arguing that they are indeed the same. The computation can be found for example in [8]. Here, we will find the correspondence for the first few levels to get the intuition for it.

There is only one primary operator with conformal weight  $h=1$  in both the Ising model and the free boson theory. The operators  $\epsilon \otimes \epsilon$  and  $\partial X \bar{\partial} X$  have to be proportional. Since we know OPE of the Ising operator  $\epsilon \otimes \epsilon \times \epsilon \otimes \epsilon \sim \mathbb{1} \otimes \mathbb{1}$  and OPE of the free boson operator  $\partial X \bar{\partial} X \times \partial X \bar{\partial} X \sim \frac{1}{4} \mathbb{1} \otimes \mathbb{1}$ , we conclude that  $\epsilon \otimes \epsilon = \pm 2 \partial X \bar{\partial} X$ .

For other computations on the free boson side, we will need OPE (2.95). Using this OPE together with  $\sigma \otimes \sigma \times \sigma \otimes \sigma \sim (\mathbb{1} + \frac{1}{2}\epsilon) \otimes (\mathbb{1} + \frac{1}{2}\epsilon)$ , one finds that  $\sigma \otimes \sigma = \pm \sqrt{2} \cos(\frac{X}{\sqrt{2}})$ . If we take the value conventionally to be positive, we get correspondence

$$\sigma \otimes \sigma = \sqrt{2} \cos\left(\frac{X}{\sqrt{2}}\right)$$



Level	Fields
0	$ 0\rangle \otimes  0\rangle$
1/16	$ \sigma\rangle \otimes  0\rangle,  0\rangle \otimes  \sigma\rangle$
1/8	$ \sigma\rangle \otimes  \sigma\rangle$
1/2	$ \epsilon\rangle \otimes  0\rangle,  0\rangle \otimes  \epsilon\rangle$
9/16	$ \epsilon\rangle \otimes  \sigma\rangle,  \sigma\rangle \otimes  \epsilon\rangle$
1	$ \epsilon\rangle \otimes  \epsilon\rangle$
9/8	$(L_{-1}^{(1)} - L_{-1}^{(2)}) \sigma\rangle \otimes  \sigma\rangle$
25/16	$(L_{-1}^{(1)} - 8L_{-1}^{(2)}) \epsilon\rangle \otimes  \sigma\rangle, (8L_{-1}^{(1)} - L_{-1}^{(2)}) \sigma\rangle \otimes  \epsilon\rangle$
2	$(L_{-2}^{(1)} - L_{-2}^{(2)}) 0\rangle \otimes  0\rangle, (L_{-1}^{(1)} - L_{-1}^{(2)}) \epsilon\rangle \otimes  \epsilon\rangle$

Table 2.5: Primary fields in the double Ising model  $\text{CFT}_I \otimes \text{CFT}_I$  with conformal weights equal or less than two.

that fixes the sign in the above mentioned correspondence

$$\epsilon \otimes \epsilon = -2\partial X \bar{\partial} X$$

using the  $\sigma \otimes \sigma$  OPE.

Now, we would like to find correspondence at the level  $\frac{1}{2}$ . General primary field on this level can be written as  $a(\mathbb{1} \otimes \epsilon) + b(\epsilon \otimes \mathbb{1})$ . Comparing their OPE with the OPE for  $\cos \sqrt{2}X$  and  $\cos \sqrt{2}\tilde{X}$ , one finds

$$\begin{aligned} \cos \sqrt{2}X &= \pm \frac{1}{2}(\epsilon \otimes \mathbb{1} - \mathbb{1} \otimes \epsilon) \\ \cos \sqrt{2}\tilde{X} &= \pm \frac{1}{2}(\epsilon \otimes \mathbb{1} + \mathbb{1} \otimes \epsilon). \end{aligned} \tag{2.127}$$

To fix the sign we would have to find OPEs of primaries in the twisted sector and knowledge of the correspondence of  $\sigma \otimes \sigma$ .

There are other primaries at level  $\frac{1}{16}$ , namely  $\mathbb{1} \otimes \sigma$  and  $\epsilon \otimes \sigma$ . These primaries correspond to the two twisted states  $|T_1\rangle$  and  $|T_2\rangle$ . The fields  $\sigma \otimes \epsilon$  and  $\epsilon \otimes \sigma$  on the level  $\frac{9}{16}$  correspond to the  $\alpha$ -descendants of these twisted fields  $\alpha_{-1/2}\bar{\alpha}_{-1/2}|T_1\rangle$  and  $\alpha_{-1/2}\bar{\alpha}_{-1/2}|T_2\rangle$ .

Primary fields considered so far are not all the primaries in the theory since new operators emerge as linear combinations of descendants in separate sectors. Few first primary states are listed above 2.5. They correspond to the other primary fields in the infinite column of the free boson primaries.



# 3. Boundary CFT

## 3.1 Boundary conditions and Ishibashi states

This chapter introduces aspects of *boundary conformal field theory* (BCFT), i.e. conformal field theory with consistent conformally invariant boundary [10, 54, 55]. We will focus our attention to the case of CFT with a boundary on the real axis of the complex plane. Once we understand BCFT on the upper half plane (UHP), we can calculate correlation functions on the surfaces with different geometry of the boundary performing conformal map that deforms the real axis.

All the conformal transformations can be divided into two categories. The first category contains transformations preserving UHP and the second category provides deformations of the boundary. The transformation preserving boundary will give us restriction on the correlation functions on the UHP. From the global conformal transformations (2.23) the UHP is preserved only by the transformations satisfying  $f(\bar{z}) = \bar{f}(z)$  on the real axis. This relation constrains the parameters in (2.23) to be real and the special conformal group reduces to  $SL(2, \mathbb{R})$ .

Now, we will follow the same procedure that led us to the conformal Ward identities but now for conformal transformations preserving real axis [56]. Consider a finite set of fields  $\tilde{\mathcal{O}} = \mathcal{O}_1(z_1, \bar{z}_1) \dots \mathcal{O}_n(z_n, \bar{z}_n)$  inserted at different points on the UHP and let  $z \rightarrow z + \epsilon(z, \bar{z})$  be a transformation preserving real axis with compact support that is holomorphic in the region  $K$  with all the insertions inside as in the figure 3.1. We will again use the identity (2.33) and integration by parts with the assumption of conformally invariant boundary  $\delta S|_D = 0$  and we find

$$\delta \langle \tilde{\mathcal{O}} \rangle = \frac{1}{2\pi} \int_{\partial(K/D)} n_\nu \langle \epsilon_\mu T^{\mu\nu} \tilde{\mathcal{O}} \rangle - \frac{1}{2\pi} \int_{K/D} \epsilon_\mu \partial_\nu \langle T^{\mu\nu} \tilde{\mathcal{O}} \rangle, \quad (3.1)$$

where  $n_\nu$  a unit vector normal to the boundary and we use notation from the previous chapter.

From the second term on the left hand side, we see that stress-energy tensor is conserved away from the insertion points. This term gives us the same prescription for operator transformations as in the bulk. The first term gives us new constraint on the stress-energy tensor,  $T^{xy}(x, 0) = 0$ . We can give physical interpretation to this constrain that there is no energy flow across the boundary. This condition is necessary and sufficient to ensure conformal invariance on the UHP. In complex coordinates this condition translates into the relation

$$T(x, x^*) = \bar{T}(x, x^*). \quad (3.2)$$

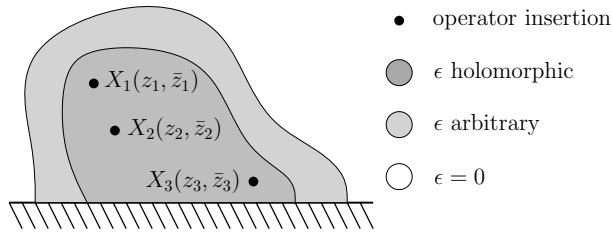


Figure 3.1: Situation used in derivation of the Ward identities on the UHP.

This relation constraints a boundary condition but not uniquely. We wish to classify all the consistent boundary conditions and thus all BCFTs for given CFT.

In the bulk theory, we were given two independent components of the stress-energy tensor  $T$  and  $\bar{T}$ . It is no more true if we introduce a boundary. Since  $T(x) = \bar{T}(x)$  on the real axis and both  $T(z, z^*)$  and  $\bar{T}(z^*, z)$  are analytic, the equation  $T(z, z^*) = \bar{T}(z^*, z)$  must hold everywhere due to analytic continuation. We can think of  $\bar{T}$  to be analytic continuation of  $T$  to the other half of the plane. This technique is often referred to as the *doubling trick* [57] since we can think of  $\bar{T}$  to be  $T$  in the mirror image of the original insertion point and correspondingly we consider antiholomorphic parts of bulk primaries to be inserted in the mirror image point.

Now, we will give a Hilbert space formulation of the theory with a boundary in radial quantization scheme. There are two possible ways in doing so. The first one that will lead us to the notion of boundary state is based on the quantization around a point in the bulk. Boundary state describing a boundary condition will be out state in this scheme. The other possibility is the expansion around a point on the boundary and it will lead us to the notion of boundary operators that will be discussed in the next section.

In the bulk, there are still two copies of Virasoro generators  $L_n, \bar{L}_n$ . Consider for a while following set-up. The theory is formulated on the unit disk centered at the origin with a given boundary condition on its boundary. In radial quantization, we are given a set of states and we wish to find such out state that gives us 1-point function of field  $\mathcal{O}$  inserted at the origin as an overlap

$$\langle\langle B | \mathcal{O} \rangle = \langle \mathcal{O} \rangle_B \quad (3.3)$$

with a boundary state  $|B\rangle$  describing particular boundary. There are many constraints to be satisfied by the boundary state. First of all, it must ensure consistency constrain  $T(x) = \bar{T}(x)$  after mapping to the UHP. Mapping UHP to the unit disk by

$$f(z) = \frac{i - z}{i + z}, \quad (3.4)$$

the constraint translates into the relation

$$e^{2i\theta} T(z, z^*) = e^{-2i\theta} \bar{T}(z, z^*), \quad (3.5)$$

for  $z = e^{i\theta}$ . Recalling definition of the Virasoro generators  $L_n$  with a contour running on the circular boundary, the relation translates into the mode condition  $L_n = \bar{L}_{-n}$  on the boundary. Solution to this condition

$$(L_n - \bar{L}_{-n})|I\rangle = 0 \quad (3.6)$$

has been found by Ishibashi [58] and the states satisfying this condition are called the *Ishibashi states*. We will now comment on this construction.

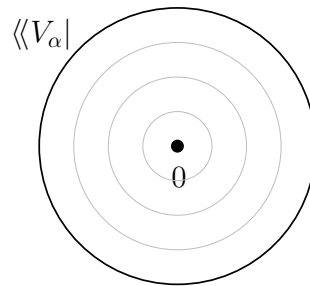


Figure 3.2: Boundary state in radial quantization around bulk point on the unit disk.

For each diagonal primary, i.e. primary state  $|V_\alpha\rangle$  with equal left/right conformal weights  $h = \bar{h}$ , there is corresponding Ishibashi state, which is given unambiguously up to the normalization as we will see from construction. The Ishibashi state can be constructed level by level solving the above condition (3.6) for each  $n$ . For the first two levels, solving corresponding equations, one finds

$$|V_\alpha\rangle\rangle = \left(1 + \frac{1}{2h_\alpha}L_{-1}\bar{L}_{-1} + \dots\right)|V_\alpha\rangle, \quad (3.7)$$

for  $h_\alpha \neq 0$ . Similarly for the higher levels. If null states are present at some level, the null directions have to be projected out.

If  $\{|n, V_\alpha\rangle\}_n$  is orthonormal basis of states in the chiral irreducible representation of Virasoro algebra (i.e. BPZ-product is  $\langle V^\alpha|V_\beta\rangle = \delta^\alpha_\beta$ ), the Ishibashi state can be constructed as

$$|V_\alpha\rangle\rangle = \sum_n |n, V_\alpha\rangle \otimes \overline{|n, V_\alpha\rangle}. \quad (3.8)$$

Condition (3.6) is indeed satisfied if one checks that it holds if multiplied with any of the basis states of given irreducible representation  $|n, V_\alpha\rangle \otimes \overline{|m, V_\alpha\rangle}$

If we are given a basis constructed by the action of Virasoro generators on the highest weight state  $L_{-I}|V_\alpha\rangle$  in the holomorphic sector, where null states are projected out (i.e. we are given irreducible representation), the solution for the Ishibashi states can be easily written. Using the inverse of

$$M_{IJ}(h_\alpha) = \langle V^\alpha|L_I L_{-J}|V_\alpha\rangle, \quad (3.9)$$

one can obtain orthonormal basis in the holomorphic sector and the Ishibashi state is

$$|V_\alpha\rangle\rangle = \sum_{I,J} M^{IJ}(h_\alpha) L_{-I} \bar{L}_{-J} |V_\alpha\rangle, \quad (3.10)$$

where  $M^{IJ}(h_\alpha)$  is the inverse matrix  $M^{IJ}M_{JK} = \delta^K_I$ .

## 3.2 Boundary fields

If we wish to construct the Hilbert space around a point  $x_0$  on the real axis, we are given only one set of Virasoro generators since

$$L_n = \frac{1}{2\pi i} \oint_0 dz z^{n+1} T(z, z^*) = -\frac{1}{2\pi i} \oint_0 dz z^{*n+1} \bar{T}(z^*, z) = \bar{L}_n, \quad (3.11)$$

where we have reversed direction of the contour integration. The situation is similar to the bulk case and every highest weight state can be interpreted as a primary operator living on the boundary. We will call them *boundary primaries* or boundary vertex operators. Action of  $L_n$ s gives rise to descendant fields but only single copy of Virasoro generators is present here. Highest weight property is again equivalent to the energy being bounded below.

For a while, think of a BCFT on the strip with width  $R$ . This picture will be quite intuitive when speaking about open string worldsheet. On each side of the strip, there can be imposed different boundary condition. Hilbert space  $\mathcal{H}_{ab}$  is dependent on these two conditions that will be labeled as  $a$  and  $b$ . If we transform the strip by  $z(w) = \exp\left(\frac{i\pi}{R}w\right)$  into the UHP, we have different

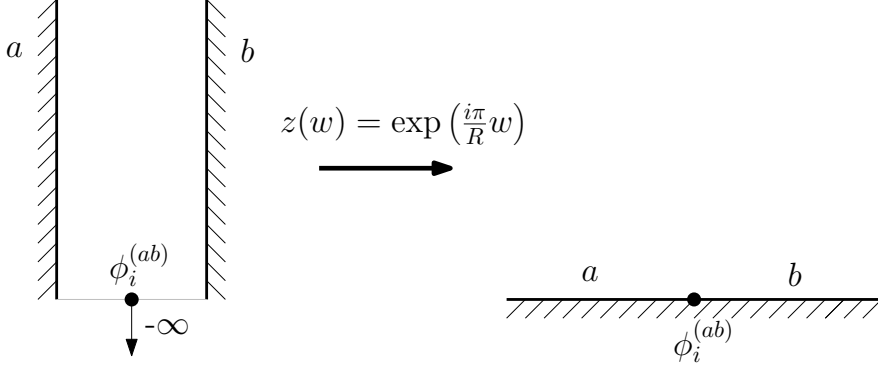


Figure 3.3: BCFT defined on the strip with boundary conditions  $a$  and  $b$  mapped to the UHP with the insertion of the boundary changing operator. This situation will correspond to the open string worldsheet.

boundary conditions on the negative and positive real axis. Singularity at the origin can be obtained by insertion of the *boundary changing operator*. The notion of operators living on the boundary has been introduced by Cardy [59, 60] and they correspond to vertex operators of open strings with boundary conditions  $a$  and  $b$ .

Let us review what fields appear in general BCFT. Firstly, bulk fields  $\mathcal{O}_\alpha$  are still present in the theory. Moreover, so-called boundary operators can be inserted on the boundary. A boundary operator that could be inserted between boundary conditions  $a$  and  $b$  will be denoted as  $\phi_i^{(ab)}$ , where  $i$  labels different possible operators. Even if the two boundary conditions are the same, we can insert an operator  $\phi_i^{(aa)}$  on the boundary. Such operator does not change the boundary condition and we can think of it as a degree of freedom of boundary  $a$ .

Analogously as the bulk fields, boundary fields can be inserted into the correlation functions. Conformal invariance fixes the form of the boundary 1-point, 2-point, and 3-point functions. In the first case

$$\langle \phi_i^{(ab)} \rangle_{\text{UHP}}^{ab} = 0 \quad \langle \mathbb{1} \rangle_a = g^a \quad (3.12)$$

and in the other two cases

$$\langle \phi_i^{(ab)}(x) \phi_j^{(ba)}(y) \rangle_{\text{UHP}}^{ab} = \delta_{ij} \alpha_i^{(ab)} \frac{1}{(x-y)^{h_i}} \quad (3.13)$$

and

$$\langle \phi_i^{(ab)}(u) \phi_j^{(bc)}(v) \phi_k^{(ca)}(w) \rangle_{\text{UHP}}^{ac} = \frac{\alpha_i^{(ab)} C_{jk}^{(bca)i}}{x_{12}^{h_1+h_2-h_3} x_{23}^{h_2+h_3-h_1} x_{13}^{h_3+h_1-h_2}}. \quad (3.14)$$

The coefficient in the boundary 2-point function can no more be fixed to the unity by normalization since it is already fixed by normalization of the bulk fields as we will see later. We have introduced boundary structure constants  $C_{jk}^{(bca)i}$  and the  $g$ -function of the boundary  $g^a$ . Logarithm of  $g^a$  is often called boundary entropy since it measures boundary contribution to the entropy.

One can also combine bulk operators with boundary operators within the correlation functions. Bulk-boundary correlation function can be thus introduced

and its form is also fixed by conformal invariance. The bulk-boundary correlator is then of the form

$$\langle V_\alpha(x+iy)\phi_i^{(aa)}(0) \rangle_{\text{UHP}}^{aa} = \frac{\alpha_i^{(aa)} B_{\alpha i}^{(aa)}}{(2y)^{\Delta_\alpha - h_i} (x^2 + y^2)^{h_i}}, \quad (3.15)$$

where  $B_{\alpha i}^{(aa)}$  is a bulk-boundary structure constant.

### 3.3 Sewing constraints

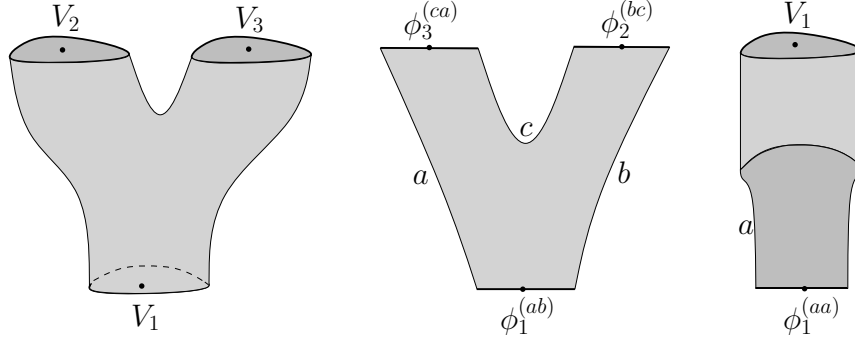


Figure 3.4: basic constituents of BCFT amplitudes: bulk 3-point function, boundary 3-point function and bulk-boundary correlator in string theory picture.

To solve particular CFT, i.e. to be able to compute all the possible correlators in the bulk, one needs to know conformal charges  $(c, \bar{c})$ , the spectrum of primary operators with weights  $(h_\alpha, \bar{h}_\alpha)$ , and the structure constants  $C_{ijk}$  of the theory. Without the loss of generality, one can assume that 2-point functions are vanishing for different basis primaries, which can always be done as discussed previously. Conformal symmetry then fixes 2- and 3-point functions and the OPE coefficients of descendant fields. Using OPE one can reduce higher-point correlators to an infinite sum of 3-point functions and correlators of descendant fields can be found using differential operators introduced earlier. This procedure is often referred to as sewing since it corresponds to the construction of general closed string amplitude by sewing three string amplitudes in the closed string theory picture.

If the boundary is introduced, one needs boundary and bulk-boundary OPE to be able to compute arbitrary amplitude. Boundary OPE will have the same form as in the bulk case, but we can also introduce bulk-boundary OPE that exchanges a bulk operator near the boundary by series of boundary operators

$$V_\alpha(z) \sim \sum_i (2 \operatorname{Im} z)^{h_i - \Delta_\alpha} B_{\alpha i}^a \phi_i^{(aa)}(\operatorname{Re} z) \quad (3.16)$$

in accordance with the bulk-boundary correlator (3.15).

In the presence of boundary, one can include boundary operators and we need to know the spectrum of boundary primaries, their 2-point and 3-point functions, and also bulk-boundary structure constants  $B_{\alpha i}^a$ . If one knows all of these together with the previous quantities in the bulk, one can reconstruct arbitrary correlator similarly as in the bulk case. Boundary fields correspond to open string states

in the geometrical picture of sewing string amplitudes. Basic constituents can be seen in the figure 3.4.

There are generally more ways to reconstruct higher-point correlator and the theory to be consistent must be independent of the choice of its decomposition. This gives us a set of consistency (sewing) conditions. We will list six sufficient sewing conditions that ensure consistency of the theory. If the six sewing conditions are satisfied, the theory is consistent on arbitrary surface with arbitrary genus and arbitrary configuration of boundaries. All the correlators can be then unambiguously cut into the collection of the three simple constituents. Detailed proof of the statement that only the six constraints ensure consistency has been performed by Lewellen in [61], who extended estimations of Sonoda [62] from CFT to BCFT.

### 3.3.1 Crossing symmetry

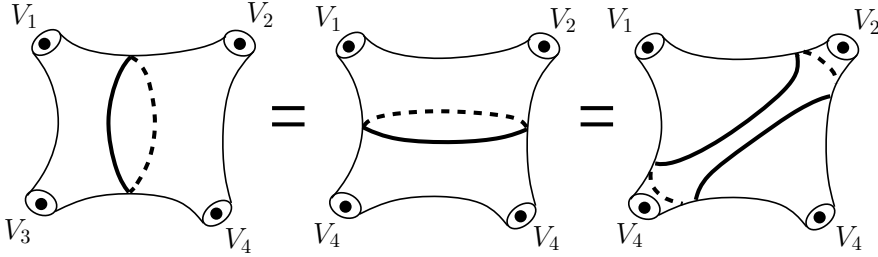


Figure 3.5: Crossing symmetry of 4-point amplitude with 3 possible cuttings.

Now, we will go through the sewing constraints and make some comments. First two constraints shown in the pictures 3.5 and 3.6 arise even in the theory without a boundary and they are known as crossing-symmetry and modular invariance [47]. These relations constraint OPE coefficients for bulk fields and the spectrum of primary fields.

Let us consider crossing symmetry first of all. Conformal symmetry fixes the form of the 4-point function

$$\langle V_1(z_1, \bar{z}_1) V_2(z_2, \bar{z}_1) V_3(z_3, \bar{z}_1) V_4(z_4, \bar{z}_1) \rangle = \prod_{i < j} (z_i - z_j)^{r - h_i - h_j} (\bar{z}_i - \bar{z}_j)^{\bar{r} - \bar{h}_i - \bar{h}_j} Y(\eta, \bar{\eta}), \quad (3.17)$$

where  $r = \frac{1}{3} \sum_{i=1}^4 h_i$  and  $\eta, \bar{\eta}$  are crossing ratios introduced earlier.  $Y(\eta, \bar{\eta})$  can be arbitrary function of these ratios due to their conformal invariance. Performing conformal transformation, we can set  $z_4 = 0$ ,  $z_1 = \infty$ , and  $z_2 = 1$  and then we get  $z_3 = \eta$ . This can always be done using some special conformal transformation since it is determined by the transformation of three points in the complex plane. Performing the map we get

$$\begin{aligned} Y(\eta, \bar{\eta}) &= \lim_{z_1, \bar{z}_1 \rightarrow 0} z_1^{-2h_1} \bar{z}_1^{-2\bar{h}_1} \langle V_1(-1/z_1, -1/\bar{z}_1) V_2(1, 1) V_3(\eta, \bar{\eta}) V_4(0, 0) \rangle \\ &= \langle h_1, \bar{h}_1 | X_2(1, 1) X(\eta, \bar{\eta}) | h_h, \bar{h}_4 \rangle. \end{aligned} \quad (3.18)$$

We can use OPE to replace the last two operators by a sum of single operators

$$V_3(\eta, \bar{\eta}) V_4(0, 0) = \sum_{\alpha} C_{34}^{\alpha} \eta^{h_{\alpha} - h_3 - h_4} \bar{\eta}^{\bar{h}_{\alpha} - \bar{h}_3 - \bar{h}_4} \Psi_{\alpha}, \quad (3.19)$$



where we have denoted

$$\Psi_\alpha = \sum_{I,J} \beta_{\alpha 34}^I \bar{\beta}_{\alpha 34}^J (L_{-I} \bar{L}_{-J} V_\alpha)(0,0). \quad (3.20)$$

Whole correlator can be rewritten as

$$Y(\eta, \bar{\eta}) = \sum_{\alpha} C_{\alpha 34} C_{\alpha p 12} F_{12,34}^\alpha(\eta) \bar{F}_{12,34}^\alpha(\bar{\eta}), \quad (3.21)$$

where we have split the holomorphic and antiholomorphic parts of the remaining expression and defined conformal blocks

$$F_{12,34}^\alpha(\eta) = \eta^{h_\alpha - h_3 - h_4} \sum_I \beta_{\alpha 34}^I \eta^{|I|} \frac{\langle h_1 | V_2(1) L_{-I} | h_\alpha \rangle}{\langle h_1 | V_2(1) | h_\alpha \rangle}. \quad (3.22)$$

In the procedure above, we have chosen to sew the last two insertions. There are three possible ways how to perform sewing and repeating the same procedure, we find that

$$\begin{aligned} Y(\eta, \bar{\eta}) &= \sum_{\alpha} C_{12\alpha} C_{34\alpha} F_{12,34}^\alpha(\eta) \bar{F}_{12,34}^\alpha(\bar{\eta}) \\ &= \sum_{\alpha} C_{14\alpha} C_{23\alpha} F_{14,23}^\alpha(1-\eta) \bar{F}_{14,23}^\alpha(1-\bar{\eta}) \\ &= \sum_{\alpha} C_{13\alpha} C_{24\alpha} F_{13,24}^\alpha(1/\eta) \bar{F}_{13,24}^\alpha(1/\bar{\eta}) \end{aligned} \quad (3.23)$$

should equal to have consistent theory. Conformal block  $F_{12,34}^\alpha(\eta)$  gives contribution to the amplitude from the primary field  $V_\alpha$  and all its holomorphic descendants and analogously  $\bar{F}_{12,34}^\alpha(\bar{\eta})$  for the antiholomorphic components.

If there is only finite number of conformal blocks  $F$  in the expression above, each sum in (3.23) contains the same number of terms and conformal blocks are linear combinations of one another. They are related by duality matrices [63]

$$F_{ij,kl}^\alpha = \sum_{\beta} M \begin{bmatrix} i & l \\ j & k \end{bmatrix}_{\alpha\beta} F_{il,jk}^\beta(1-\eta) \quad (3.24)$$

It can be shown that in the case of minimal models, this condition together with the crossing symmetry gives us a constraint on the structure constants

$$C_{12\alpha} C_{34\alpha} M \begin{bmatrix} 1 & 4 \\ 2 & 3 \end{bmatrix}_{\alpha\beta} = C_{14\beta} C_{23\beta} M \begin{bmatrix} 1 & 2 \\ 4 & 3 \end{bmatrix}_{\beta\alpha}. \quad (3.25)$$

This set of equations gives us overdetermined system for the structure constants and solving this condition leads to their determination.

### 3.3.2 Modular invariance

If the theory is defined on the torus, there is ambiguity in the computation of partition function. Although the sewing constraint from the figure 3.6 take into account one insertion on the torus, we will consider only partition function (i.e. the case with  $\mathbb{1}$  insertion) here. Considering general case leads to many difficulties and gives only little information beyond the constraints obtained from

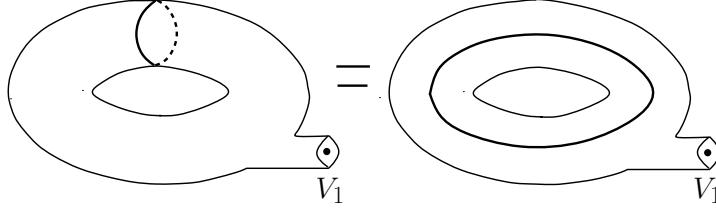


Figure 3.6: Modular invariance and 2 possible ways of computing 1-point function on the torus.

the partition function alone. Modular invariance put a constraint on the spectrum of operators in the theory [57].

A torus is given by two independent vectors (or complex numbers  $\omega_1$  and  $\omega_2$ ) called *periods* that give identification of points with relative position given by integer combination of these vectors. CFT does not depend on the scaling, nor on the absolute orientation of the lattice. Relevant parameter will be a *modular parameter*  $\tau = \frac{\omega_2}{\omega_1}$  that erase the dependence described above. The partition function of the theory can be written in the form

$$Z(\tau) = \text{Tr} \left( q^{L_0 - \frac{c}{24}} \bar{q}^{\bar{L}_0 - \frac{\bar{c}}{24}} \right), \quad (3.26)$$

where  $q = \exp 2\pi i \tau$  and the central term in the Hamiltonian emerges due to mapping from the plane. Since the partition function should not depend on the change of labeling  $w_1$  and  $w_2$  and correspondingly the direction that we interpret as time and space in the Hilbert space formulation force partition function to be modular invariant

$$Z(\tau) = Z(1/\tau). \quad (3.27)$$

This is the modular invariance from the figure 3.6 with identity insertion.

In terms of characters of  $\alpha$  representation  $\chi_{(c,\alpha)}(\tau) = e^{-i\pi c/12} \text{Tr}_\alpha e^{2\pi i \tau L_0}$ , one can rewrite the partition function for diagonal theories (only primary fields with the same homomorphic and antiholomorphic conformal weights are present) as

$$Z = \sum_{\alpha} N_{c,\alpha} \chi_{(c,\alpha)}(\tau) \bar{\chi}_{(c,\alpha)}(\bar{\tau}), \quad (3.28)$$

where  $N_{c,\alpha}$  is the multiplicity of the occurrence of the representation  $\alpha$ .

Now, we would like to know, how characters transform under the modular transformation. Performing direct computation, one can find that in the case of minimal models characters transform as [43]

$$\chi_{r,s}(1/\tau) = \sum_{(\rho\sigma)} S_{rs,\rho\sigma} \chi_{\rho,\sigma}(\tau) \quad (3.29)$$

under the modular transformation  $\tau \rightarrow 1/\tau$ , where we have introduced the modular S-matrix

$$S_{rs,\rho\sigma} = 2\sqrt{\frac{1}{pp'}} (-1)^{1+s\rho+r\sigma} \sin\left(\pi \frac{p}{p'}\right) \sin\left(\pi \frac{p'}{p}\right) \quad (3.30)$$

and the sum runs over all primaries in the theory labeled by  $\rho$  and  $\sigma$ . Quantities  $p$  and  $p' = p + 1$  label different minimal models  $\mathcal{M}(p', p)$ .

Modular invariance gives restriction on the spectrum of primary operators since numbers  $N_{c,\alpha}$  are constrained. It can be shown that in the case of the Ising model, only  $\mathbb{1}$ ,  $\sigma$ , and  $\epsilon$  with multiplicity one are allowed by modular invariance. No other coefficients  $N_{c,\alpha}$  give consistent theory. Now, we have completed the proof of correspondence between the critical Ising model and the  $\mathcal{M}(4, 3)$  minimal model.

### 3.3.3 Cardy's condition

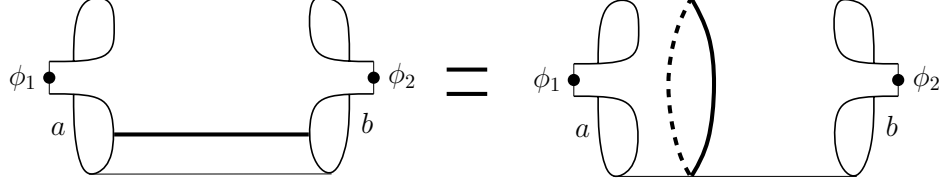


Figure 3.7: Cardy's condition taking into account two different ways of computation the 2-point boundary function on the cylinder or partition function in the case of identity field insertion.

Now, we are moving to BCFT. The next sewing relation (sometimes called Cardy's condition) constraints possible boundary conditions and spectrum of boundary operators [60]. As mentioned above, conformally invariant boundary condition corresponds to a linear combination of the Ishibashi states, but not all combinations give us consistent boundary. Only particular combinations satisfy Cardy's condition. Here we restrict our attention to the cylinder with no insertions and interpret the amplitude as the partition function. General solution with the two operator insertions as in the figure 3.7 is not known and likely gives no additional information.

Partition function on the cylinder with boundary conditions  $a$  and  $b$  can be written in two ways. One can interpret it as an amplitude between the initial state  $||a\rangle\rangle$  and the final state  $||b\rangle\rangle$

$$Z_{ab} = \langle\langle a || e^{-i\frac{\pi}{\tau}(L_0 + \bar{L}_0 - \frac{c}{12})} || b \rangle\rangle \quad (3.31)$$

or it can be interpreted as a trace over the spectrum of boundary states with boundary conditions  $a$  and  $b$

$$Z_{ab} = \text{Tr}_{ab} e^{2\pi i\tau(L_0 - \frac{c}{12})} = \sum_i N_{ab}^i \chi_i(q), \quad (3.32)$$

where  $N_{ab}^i$  is the multiplicity of the occurrence of corresponding representation and  $q$  is a function of  $\tau$ . In the string theory point of view, the first case corresponds to the evolution of the closed string from the original state  $||a\rangle\rangle$  to the final state  $||b\rangle\rangle$  whereas the second case corresponds to the open string living between  $a$ -brane and  $b$ -brane and evolving along the circle.

This condition will lead us to the boundary states that will be looked for in the form of linear combination of Ishibashi states  $|i\rangle\rangle$ . If Ishibashi states are normalized, we can rewrite the above relation (3.31) as

$$Z_{ab} = \sum_{i,j} \langle\langle \alpha || i \rangle\rangle \langle\langle i || e^{-i\frac{\pi}{\tau}(L_0 + \bar{L}_0 - \frac{c}{12})} || j \rangle\rangle \langle\langle j || \beta \rangle\rangle = \sum_j \langle\langle \alpha || j \rangle\rangle \langle\langle j || \beta \rangle\rangle \chi_j(q), \quad (3.33)$$

where we assume that the theory is diagonal.

On the other hand, one can use the modular invariance to transform (3.32) and obtain the same expansion in terms of Virasoro characters

$$Z_{ab} = \sum_{ij} N_{ab}^i S_i^j \chi_j(q), \quad (3.34)$$

where we have denoted the modular S-matrix  $S_i^j$  for abbreviation. Equating the two expressions for the partition function, one find expression for the boundary state. In the case of unitary models, it can be shown that  $S_0^j$  is positive. From the above equation, one finds explicit expression for the boundary states

$$|a\rangle\rangle = \sum_j \frac{S_a^j}{\sqrt{S_0^j}} |j\rangle\rangle. \quad (3.35)$$

We have reconstructed boundary states as linear combinations of Ishibashi states with coefficients determined by the modular S-matrix.

From the constraint

$$\sum_k S_k^j N_{ab}^k = \langle\langle a||j\rangle\rangle \langle\langle j||b\rangle\rangle = \frac{S_a^j S_b^j}{S_0^j}, \quad (3.36)$$

one can also determine the boundary spectrum. Using considerations about modular S-matrix, one can derive so-called Verline formula that states that the right-hand side is equal to

$$\frac{S_a^j S_b^j}{S_0^j} = \sum_k S_k^j \mathcal{N}_{ab}^k, \quad (3.37)$$

where  $\mathcal{N}_{ab}^k$  are the fusion coefficients in the operator algebra [43]. The spectrum of boundary fields inserted between boundaries  $a$  and  $b$  can be thus determined from the fusion rules  $a \times b$ .

### 3.3.4 Boundary crossing symmetry

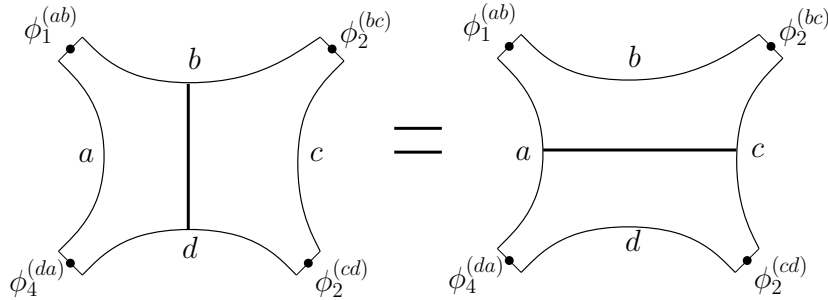


Figure 3.8: Sewing constraint relating two possible ways of cutting boundary 4-point function

There are three sewing constraints left [61]. Consider four boundary insertions at first. Situation is almost the same as in the bulk. Conformal symmetry fixes the form of the 4-point function on the real axis

$$\langle\phi_1^{(ab)}(x_1)\phi_2^{(bc)}(x_2)\phi_3^{(cd)}(x_3)\phi_4^{(da)}(x_4)\rangle = \prod_{i<j} (x_j - x_i)^{r-h_i-h_j} Y(\eta), \quad (3.38)$$

where  $x_4 > x_3 > x_2 > x_1$ , but now only one sector is present. Sewing constraint gives us condition

$$Y(\eta) = \sum_p C_{12p}^{(abc)} C_{34p}^{(cda)} \alpha_p^{(ac)} F_{12,34}^p(\eta) = \sum_p C_{41p}^{(dab)} C_{23p}^{(bcd)} \alpha_p^{(db)} F_{14,23}^p(1-\eta), \quad (3.39)$$

where we are now restricted to the real axis. Due to the ordering on the boundary, there are only two possible ways of sewing amplitudes.

In the case of rational theories, we obtain similar relation for boundary structure constants as in the case on bulk operators

$$\sum_p C_{12p}^{(abc)} C_{34p}^{(cda)} \alpha_p^{(ac)} M \begin{bmatrix} 1 & 4 \\ 2 & 3 \end{bmatrix}_{pq} = C_{41q}^{(dab)} C_{23q}^{(bcd)} \alpha_q^{(db)}. \quad (3.40)$$

Solving this constraint leads to the determination of the boundary structure constants.

### 3.3.5 Open-open-closed amplitude

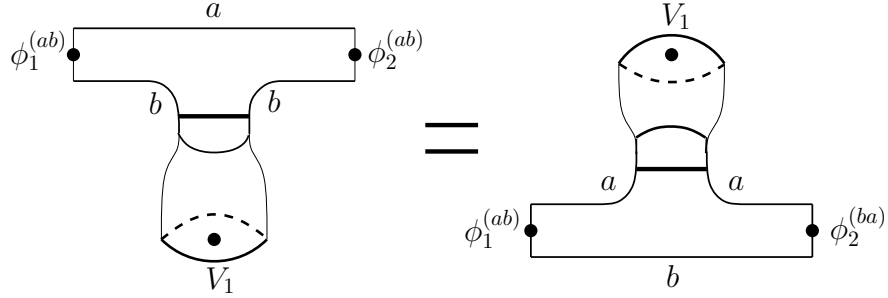


Figure 3.9: Sewing condition relating two possibilities of the cutting of correlators containing one bulk and two boundary insertions.

The next sewing condition incorporates two boundary operators  $\phi_1^{(ab)}$ ,  $\phi_2^{(ba)}$ , and one bulk operator  $V_1$  on the UHP.

There are two possible ways how to decompose the above correlator depending on the situation whether  $x_1 < \text{Re } z < x_2$  or  $x_1 < x_2 < \text{Re } z$ , where  $x_1$  and  $x_2$  are insertion points of the boundary operators whereas  $z$  is the point, where the bulk field is inserted. In the first case, we can use the bulk-boundary expansion of the bulk field near the boundary  $b$  and in the second case expansion near the other boundary  $a$ . Performing these two expansions and proceeding in the same way as in the previous discussion, one finds another sewing constraint that relates boundary and bulk-boundary structure constants.

### 3.3.6 Open-closed-closed amplitude

The last sewing constraint that is needed to be satisfied is consistency in the decomposition of the correlator containing one boundary field and two bulk fields on the UHP. There are two options how to decompose the amplitude. Firstly, if we restrict to the case with no boundary insertion (identity insertion), we can use the bulk OPE to get single insertion or two bulk-boundary OPEs to obtain two boundary fields.

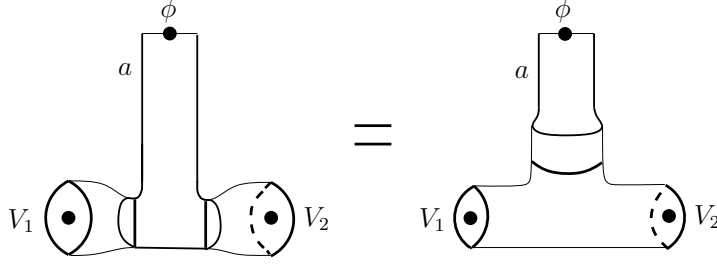


Figure 3.10: Sewing constraint relating two ways how to decompose the correlator containing one boundary field insertion and two bulk field insertions.

In general case with boundary insertion, the situation is a bit more difficult, but it is doable in the case of rational theories and leads to five-point sewings. This constraint relates bulk and bulk-boundary structure constants.

### 3.4 Solving the Ising model BCFT

In this section, we will sketch the procedure how to solve the Ising model BCFT, solving the sewing constraints. Detailed discussion of the computation can be found in the following treatment [61]. This machinery is mentioned here to illustrate its difficulty and the main results will be needed later. Using level truncation, we will need the solution of the theory in some BCFT background. With this solution, all the other boundary states will be constructed using string field theory in the next two chapters.

From the previous section we know that modular invariance forces the Ising model to contain only fields  $\mathbb{1}$ ,  $\epsilon$ , and  $\sigma$  with conformal weights  $(0, 0)$ ,  $(\frac{1}{16}, \frac{1}{16})$ , and  $(\frac{1}{2}, \frac{1}{2})$ . Without the loss of generality, we will consider primary states to be orthonormal. Fusion rules of the Ising operators read

$$\mathbb{1} \times \mathbb{1} = \mathbb{1}, \quad \epsilon \times \epsilon = \mathbb{1}, \quad \sigma \times \sigma = \mathbb{1} + \epsilon. \quad (3.41)$$

Computing conformal block functions and coefficients relating them, one finds that the only non-trivial duality matrices are

$$\begin{aligned} M \begin{bmatrix} \epsilon & \epsilon \\ \epsilon & \epsilon \end{bmatrix} &= \begin{pmatrix} 1 & 0 \\ 0 & 1 \end{pmatrix} & M \begin{bmatrix} \epsilon & \epsilon \\ \sigma & \sigma \end{bmatrix} &= \begin{pmatrix} 2 & 0 \\ 0 & 2 \end{pmatrix} \\ M \begin{bmatrix} \epsilon & \sigma \\ \epsilon & \sigma \end{bmatrix} &= \begin{pmatrix} \frac{1}{2} & 0 \\ 0 & \frac{1}{2} \end{pmatrix} & M \begin{bmatrix} \epsilon & \sigma \\ \sigma & \epsilon \end{bmatrix} &= \begin{pmatrix} -1 & 0 \\ 0 & -1 \end{pmatrix} \\ M \begin{bmatrix} \sigma & \sigma \\ \sigma & \sigma \end{bmatrix} &= \begin{pmatrix} \frac{1}{\sqrt{2}} & \frac{1}{2\sqrt{2}} \\ \sqrt{2} & -\frac{1}{\sqrt{2}} \end{pmatrix}. \end{aligned} \quad (3.42)$$

With the knowledge of these matrices, one can find bulk structure constants solving the crossing symmetry constraint

$$C_{\epsilon\epsilon\mathbb{1}} = C_{\sigma\sigma\mathbb{1}} = 1, \quad C_{\sigma\sigma\epsilon} = \frac{1}{2}. \quad (3.43)$$

We can construct boundary states corresponding to the three bulk primaries present in the theory solving Cardy's condition. The modular S-matrix for the

Ising model can be obtained plugging into the general expression (3.30) and we find that

$$S = \begin{pmatrix} \frac{1}{2} & \frac{1}{2} & \frac{1}{\sqrt{2}} \\ \frac{1}{2} & \frac{1}{2} & -\frac{1}{\sqrt{2}} \\ \frac{1}{\sqrt{2}} & -\frac{1}{\sqrt{2}} & 0 \end{pmatrix}. \quad (3.44)$$

Knowing the modular S-matrix, one can explicitly find the solution for the Cardy's boundary states in terms of the Ishibashi states

$$\begin{aligned} |\mathbb{1}\rangle\rangle &= \frac{1}{\sqrt{2}}|\mathbb{1}\rangle\rangle + \frac{1}{\sqrt{2}}|\epsilon\rangle\rangle + \frac{1}{\sqrt{2}}|\sigma\rangle\rangle \\ |\epsilon\rangle\rangle &= \frac{1}{\sqrt{2}}|\mathbb{1}\rangle\rangle + \frac{1}{\sqrt{2}}|\epsilon\rangle\rangle - \frac{1}{\sqrt{2}}|\sigma\rangle\rangle \\ |\sigma\rangle\rangle &= |\mathbb{1}\rangle\rangle - |\epsilon\rangle\rangle. \end{aligned} \quad (3.45)$$

The first two states, differing only by relative sign in front of the Ishibashi state  $|\sigma\rangle\rangle$ , can be interpreted as fixed boundary conditions in the lattice model. This is also evident from the graphs of 1-point functions obtained in the first chapter using numerical simulations and the regression parameters obtained from this dependence. The last boundary state can be associated with the free boundary conditions. Using CFT we have been able to determine consistent boundary conditions and compute explicitly behavior of the theory near the boundary

Now, we would like to determine boundary and bulk-boundary structure constants. We will restrict ourselves only to the case with the same boundary condition on the whole real axis. Recalling the Verline formula, we find that only boundary primary field  $\mathbb{1}$  with conformal weight 0 can be inserted on the  $|\mathbb{1}\rangle\rangle$  and  $|\epsilon\rangle\rangle$  boundary. On the  $|\sigma\rangle\rangle$  boundary, one more field  $\epsilon$  with conformal weight  $\frac{1}{2}$  emerges.

From the prescription for the boundary states, one finds normalization constants  $g^B = \langle \mathbb{1} \rangle_B$  as an overlap with  $\langle 0|$

$$g^{\mathbb{1}} = g^{\epsilon} = \frac{1}{\sqrt{2}}, \quad g^{\sigma} = 1. \quad (3.46)$$

Product of any operator with the identity gives the original operator and clearly

$$C_{i\mathbb{1}i}^a = C_{\mathbb{1}ii}^a = 1 \quad (3.47)$$

for all boundary conditions. One can easily deduce that

$$C_{\epsilon\epsilon\mathbb{1}}^{\sigma} = \alpha_{\epsilon}^{\sigma} = 1. \quad (3.48)$$

Boundary crossing-symmetry does not give us much more information, but it also constraints the boundary state

$$\alpha^{\sigma} = \sqrt{2}\alpha^{\mathbb{1}} = \sqrt{2}\alpha^{\epsilon}. \quad (3.49)$$

The constraint is automatically satisfied, but generally one has to take into account that Cardy's condition is not the only constraint on the boundary state.

$C_{111} = 1$	$C_{11\epsilon} = 0$	$C_{11\sigma} = 0$
$C_{1\epsilon 1} = 0$	$C_{1\epsilon\epsilon} = 1$	$C_{1\epsilon\sigma} = 0$
$C_{1\sigma 1} = 1$	$C_{1\sigma\epsilon} = 0$	$C_{1\sigma\sigma} = 1$
$C_{\epsilon 11} = 0$	$C_{\epsilon 1\epsilon} = 1$	$C_{\epsilon 1\sigma} = 0$
$C_{\epsilon\epsilon 1} = 1$	$C_{\epsilon\epsilon\epsilon} = 0$	$C_{\epsilon\epsilon\sigma} = 0$
$C_{\epsilon\sigma 1} = 0$	$C_{\epsilon\sigma\epsilon} = 0$	$C_{\epsilon\sigma\sigma} = \frac{1}{2}$
$C_{\sigma 11} = 0$	$C_{\sigma 1\epsilon} = 0$	$C_{\sigma 1\sigma} = 1$
$C_{\sigma\epsilon 1} = 0$	$C_{\sigma\epsilon\epsilon} = 0$	$C_{\sigma\epsilon\sigma} = \frac{1}{2}$
$C_{\sigma\sigma 1} = 1$	$C_{\sigma\sigma\epsilon} = \frac{1}{2}$	$C_{\sigma\sigma\sigma} = 0$

Table 3.1: Bulk structure constants for the Ising model.

$C_{111}^1 = 1$		
$C_{111}^\epsilon = 1$		
$C_{111}^\sigma = 1$	$C_{\epsilon\epsilon\epsilon}^\sigma = 0$	
$C_{\epsilon 11}^\sigma = 0$	$C_{1\epsilon 1}^\sigma = 0$	$C_{11\epsilon}^\sigma = 0$
$C_{1\epsilon\epsilon}^\sigma = 1$	$C_{\epsilon 1\epsilon}^\sigma = 1$	$C_{\epsilon\epsilon 1}^\sigma = 1$

Table 3.2: Boundary structure constants for the Ising model.

From the considerations of the two-point function near the boundary and the last sewing constraint listed above, Cardy with Levellen have found bulk-boundary structure constants

$$\begin{aligned}
B_{\epsilon 1}^1 &= B_{\epsilon 1}^\epsilon = 1 & B_{\epsilon 1}^\sigma &= -1 \\
B_{\sigma 1}^\sigma &= 0 & B_{\sigma 1}^1 &= 2^{1/4} \\
B_{\sigma 1}^\epsilon &= -2^{1/4} & B_{\sigma\epsilon}^\sigma &= 2^{-1/4}.
\end{aligned} \tag{3.50}$$

In this section, we have listed all necessary constants needed to find in principle arbitrary correlator in the Ising model CFT. We have also found boundary states solving Cardy's condition and verified that it indeed satisfy all the other conditions. In the following, we wish to find all the boundary states using different method developed in string field theory and we will avoid solving the huge set of sewing conditions. All the structure constants are reviewed in the tables.

$B_{11}^1 = 1$	$B_{\epsilon 1}^1 = 1$	$B_{\sigma 1}^1 = 2^{1/4}$
$B_{11}^\epsilon = 1$	$B_{\epsilon 1}^\epsilon = 1$	$B_{\sigma 1}^\epsilon = -2^{1/4}$
$B_{11}^\sigma = 1$	$B_{\epsilon 1}^\sigma = -1$	$B_{\sigma 1}^\sigma = 0$
$B_{1\epsilon}^\sigma = 0$	$B_{\epsilon\epsilon}^\sigma = 0$	$B_{\sigma\epsilon}^\sigma = 2^{-1/4}$

Table 3.3: Bulk-boundary structure constants for the Ising model.



### 3.5 Folded models

In the previous chapter, we studied double Ising model consisting of two Ising spins at each point. In this section, we will find boundary states for this doubled model. The importance of this problem becomes clear if we realize that conformal boundary conditions in doubled model are equivalent to conformal defects in simple model. By a defect we mean a line of inhomogeneity, where expectation values of fields are allowed to be discontinuous. One can fold the model along the defect and find doubled model with some boundary condition imposed on the defect line [13].

The double Ising model is equivalent to the free boson on the  $S^1/Z_2$  orbifold and we will start with the revision of the free boson D-branes. When deriving equations of motion from the action, a boundary term emerges

$$\delta S = \frac{1}{4\pi} \int_W d^2\sigma (-\partial_\sigma^2 + \partial_\tau^2) X \delta X + \frac{1}{4\pi} \int_{\partial W} dl (n \cdot \nabla X) \delta X. \quad (3.51)$$

The first term leads to the equation of motion and the new term can be set to zero introducing *Neumann boundary condition*  $\partial X|_{\partial W} = 0$  or *Dirichlet boundary condition*  $\delta X|_{\partial W} = 0 = \partial_\tau X|_{\partial W}$ . In bosonic string theory, each space-time coordinate is described as a free boson on the two dimensional worldsheet. Different boundary condition can be assigned to each space-time direction. If there are  $p$  Neumann boundary conditions on both sides, we say that the string is living on the  $Dp$ -brane (i.e.  $p$  dimensional extended object on which open strings can end). In the following part of this section, we will restrict to the single boson case.

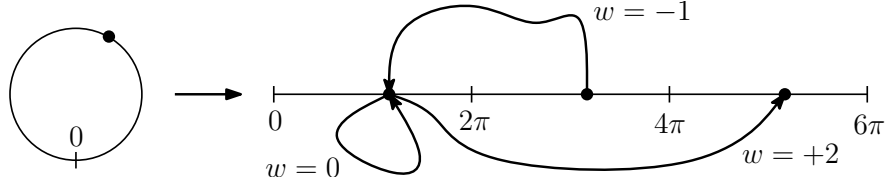


Figure 3.11: Open bosonic string living in the compactified space.

Consider a boson on the circle  $X \sim X + 2\pi R$ . Fundamental domain of this theory is interval  $[0, 2\pi R)$  and a string can be free (with Neumann boundary condition) or it can end on a D-brane located anywhere within the interval  $[0, 2\pi R)$ . Moreover, new (winding) states appear in this case. Open string beginning on a D-brane can wrap the curled dimension and it can end on the same D-brane. Such string is topologically nontrivial since it is not contractible to the point and belong to different sector than the non-wrapped strings.

Effectively the theory with compact dimension looks like a system of parallel D-branes equally spaced by  $2\pi R$ . A string can joint any two of these D-branes and corresponding vacuum in each sector can be denoted as  $|n, m\rangle$ , where  $n$  labels the D-brane, where the string begins and  $m$  labels the D-brane, where the string ends. These vacua are called *Chan – Patton* factors. We will denote the winding numbers  $w$  as in the bulk case. It is not difficult to find explicitly boundary states for the free boson, but the intuitive picture will be enough for our later discussions.

We wish to identify boundary states of the free boson on the orbifold with boundary states of the Ising model. Due to the orbifold symmetry, the funda-

$(\text{Ising})^2$ D-brane	Interpretation	$\langle \mathbb{1} \rangle_B$	$\frac{\langle \partial X \bar{\partial} X \rangle}{\langle \mathbb{1} \rangle}$	Position
$\mathbb{1} \otimes \varepsilon$	fractional D0	$\frac{1}{2}$	+1	$\pi R$
$\varepsilon \otimes \mathbb{1}$	fractional D0	$\frac{1}{2}$	+1	$\pi R$
$\mathbb{1} \otimes \mathbb{1}$	fractional D0	$\frac{1}{2}$	+1	0
$\varepsilon \otimes \varepsilon$	fractional D0	$\frac{1}{2}$	+1	0
$\mathbb{1} \otimes \sigma$	fractional D1	$\frac{1}{\sqrt{2}}$	- 1	-
$\sigma \otimes \mathbb{1}$	fractional D1	$\frac{1}{\sqrt{2}}$	- 1	-
$\varepsilon \otimes \sigma$	fractional D1	$\frac{1}{\sqrt{2}}$	- 1	-
$\sigma \otimes \varepsilon$	fractional D1	$\frac{1}{\sqrt{2}}$	- 1	-
$\sigma \otimes \sigma$	centered bulk D0	1	+1	$\frac{\pi R}{2}$
continuum set	generic bulk D0	1	+1	$\phi R$
continuum set	generic bulk D1	$\sqrt{2}$	- 1	-

Table 3.4: Correspondence between D-branes in the double Ising model and in the free boson theory. The energy  $\langle \mathbb{1} \rangle_B$ , coefficient characterizing type of the boundary condition  $\langle \partial X \bar{\partial} X \rangle / \langle \mathbb{1} \rangle$ , and the position of the corresponding D-brane is mentioned.

mental domain is restricted to the  $[0, \pi R)$  and all the string states have to be symmetrical under the reflection. The first possibility to get correct picture is to consider system of two D-branes on the interval  $(-\pi R, \pi R)$  that map to each other under the  $Z_2$  reflection and a string living on these D-branes. The other possibility is the existence of *fractional* D-brane being placed at one of the two singular points and being build in the twisted sector. There are 4 Neumann and 4 Dirichlet fractional D-branes in the twisted sector. This D-brane will have half of the energy then the pair of D-branes. All the free boson D-branes with their Ising model counterparts are listed in the table 3.4.

The interpretation in each picture is done comparing coefficients of the boundary states with the knowledge of the correspondence between bulk states. The energy of the D-brane can be computed from the  $\langle \mathbb{1} \rangle_a$ , where  $a$  labels different D-branes. Moreover, the coefficient  $\frac{\langle \partial X \bar{\partial} X \rangle_a}{\langle \mathbb{1} \rangle_a}$  characterizes the nature of the boundary condition. Following from the propagator on the disk, we get +1 in the case of Dirichlet boundary condition and -1 in the case of Neumann boundary condition. These two coefficients give us interpretation from the second column of the table. From the  $\langle \cos(\frac{X}{\sqrt{2}}) \rangle$  coefficient, one finds position of D-branes. In the case of D1-branes, this coefficient cannot be interpreted as D-brane position. We can see that some boundaries carry the same coefficients. These differs in the twisted sector and can be distinguished by the introduction of some twisted charges. We can see that we have indeed 4 Dirichlet fractional D-branes and 4 Neumann fractional D-branes.

In the doubled Ising model, tensor products of boundary states from the single Ising model remain to be boundary states, but including all the new primaries,

new boundary states emerge. There are two sets of them with energy 1 and  $\sqrt{2}$  corresponding to general D0-brane and  $D1$ -brane. All the states from this continuous spectrum can be obtained by marginal deformations of the theory. The two sets of boundary states are related by T-duality.

The last thing, we would like to do is demystification of the correspondence between boundary spectra.  $\mathbb{1} \otimes \mathbb{1}$  boundary condition together with all the first four D-branes from the table 3.4 corresponds to the fractional D0-brane at  $X = 0$ . The only boundary operators in the Ising model picture are descendants of the identity. On the orbifold side, the identity and some winding primary states are present since  $\partial X$  and half of the winding states are removed by the orbifold projection. The surviving boundary primary states up to the level 2 are

$h$	(Ising) <sup>2</sup>	Orbifold
0	$\mathbb{1}$	$\mathbb{1}$
2	$T \otimes \mathbb{1} - \mathbb{1} \otimes T$	$\cos \sqrt{2} \tilde{X}$

(3.52)

$\mathbb{1} \otimes \sigma$  boundary condition together with the other three corresponding boundary conditions in the doubled Ising corresponds to the fractional D1-brane. We have additional  $\mathbb{1} \otimes \epsilon$  boundary primary in this case. On the D1-brane, momentum modes instead of winding modes are present. The orbifold projection once again removes  $\partial X$  and half of the momentum modes

$h$	(Ising) <sup>2</sup>	Orbifold
0	$\mathbb{1}$	$\mathbb{1}$
$\frac{1}{2}$	$\mathbb{1} \otimes \epsilon$	$\cos \frac{X}{\sqrt{2}}$
2	$T \otimes \mathbb{1} - \mathbb{1} \otimes T$	$\cos \sqrt{2} X$

(3.53)

The situation with  $\sigma \otimes \sigma$  boundary condition, which corresponds to D0-brane at  $X = \frac{\pi R}{2}$ , is the most complicated. The boundary primaries on the Ising side are constructed over all four combinations of  $\mathbb{1}$  and  $\epsilon$  in each subsector. In the free boson picture, the boundary condition corresponds to two D-branes on the domain  $(-\pi, \pi)$  with positions  $\frac{\pi R}{2}$  and  $-\frac{\pi R}{2}$ . To describe the free boson, we will use Chan-Paton-like description. The  $Z_2$  symmetry acts on the  $2 \times 2$  matrices as

$$Z \begin{pmatrix} a & b \\ c & d \end{pmatrix} = \begin{pmatrix} d & c \\ b & a \end{pmatrix}. \quad (3.54)$$

In the non-twisted sector, there are following boundary primary fields: the identity,  $\partial X$ , and winding modes with integer winding number, all multiplied by the Chan-Paton factors. Unlike the previous cases, we have a nontrivial twisted sector (that appears as the off-diagonal components of the matrices) that describes states going from the D0-brane to its mirror image. The primaries in the twisted sector are winding modes with half integer winding times the Chan-Paton factors. Up to the mixing between the states at the same level, the match between the primary states is

$h$	$(\text{Ising})^2$	Orbifold	
$0$	$\mathbb{1} \otimes \mathbb{1}$	$\begin{pmatrix} 1 & 0 \\ 0 & 1 \end{pmatrix}$	
$\frac{1}{2}$	$\mathbb{1} \otimes \epsilon$	$\begin{pmatrix} 0 & 1 \\ 1 & 0 \end{pmatrix} \cos \frac{\tilde{X}}{\sqrt{2}}$	
$\frac{1}{2}$	$\epsilon \otimes \mathbb{1}$	$\begin{pmatrix} 0 & 1 \\ -1 & 0 \end{pmatrix} \sin \frac{\tilde{X}}{\sqrt{2}}$	(3.55)
$1$	$\epsilon \otimes \epsilon$	$\begin{pmatrix} 1 & 0 \\ 0 & -1 \end{pmatrix} \partial X$	
$2$	$\partial\epsilon \otimes \epsilon - \epsilon \otimes \partial\epsilon$	$\begin{pmatrix} 1 & 0 \\ 0 & 1 \end{pmatrix} \cos \sqrt{2}\tilde{X}$	
$2$	$T \otimes \mathbb{1} - \mathbb{1} \otimes T$	$\begin{pmatrix} 1 & 0 \\ 0 & -1 \end{pmatrix} \sin \sqrt{2}\tilde{X}$	

Precise correspondence can be found in similar fashion as in the case of bulk fields using OPEs. General D0 brane will have the same boundary spectrum but the position of the D-brane will be different. Using the correspondence of the boundary primaries on the  $\sigma \otimes \sigma$ -brane, we will be able to compare our truncated action with the action proposed in [64] for parallel D-branes.

# 4. String Field theory

## 4.1 Bosonic open string theory

Before explaining basics of string field theory (SFT), we will review some facts from the first quantized string theory. For more details see for example [9]. The Polyakov action for bosonic string is<sup>1</sup>

$$S = \frac{1}{4\pi} \int_W d^2\sigma g^{1/2} g^{ab} \partial_a X^\mu \partial_b X_\mu, \quad (4.1)$$

where the integration runs over string worldsheet  $W$  parametrized by  $\sigma^1 \in (0, \pi)$  and  $\sigma^0 \in (-\infty, \infty)$  and index  $\mu$  runs over all  $D$  spacetime dimensions. String theory has huge gauge freedom. This action is invariant under the Lorentz transformation in target space, diffeomorphisms on the worldsheet, and local rescaling (Weyl symmetry).

We can partially fix the gauge introducing the conformal gauge  $g_{ab} = e^{2\omega(\sigma)} \delta_{ab}$  using diffeomorphisms and Weyl transformation. All the configurations related by gauge transformations are equal and we need to ensure that only one representant of each gauge orbit is counted when performing the path integral. The integration over gauge orbits have to be divided out. Fixing gauge leads to the introduction of so-called *Fadeev-Popov determinant*. This term can be interpreted as a new term in the action. Introducing fermionic fields  $b$  and  $c$ , we get new action

$$\frac{1}{2\pi} \int d^2z \partial X^\mu \bar{\partial} X_\mu + \frac{1}{2\pi} \int d^2z (b \bar{\partial} c + \bar{b} \partial \bar{c}) \quad (4.2)$$

with ghost part as a relict of the Fadeev-Popov determinant.

We are given CFT with matter fields  $X^\mu$  and two ghost fields  $b$  and  $c$ . Since there is no boundary for the closed strings, they correspond to the bulk operators whereas open string states correspond to boundary insertions. To each field, one can assign a ghost number. We define  $c$  to have ghost number 1,  $b$  ghost number -2. Hilbert space of the theory can be obtained by the action of modes of the operators on the primary states of the theory. In the case of open bosonic string that we are interested in,

$$\mathcal{H} = \text{Span}\{\alpha_{l_1}^{\mu_1} \dots \alpha_{-l_q}^{\mu_q} b_{-k_1} \dots b_{-k_r} c_{-n_1} \dots c_{-n_s} |p\rangle\}, \quad (4.3)$$

where  $l_1 \geq l_2 \geq \dots \geq l_q$ ,  $m_1 \geq m_2 \geq \dots \geq m_r$ ,  $n_1 \geq n_2 \geq \dots \geq n_s$ ,  $l_i \geq 1$ ,  $m_i \geq 1$ ,  $n_i \geq 0$ , and  $|p\rangle$  labeling vacua with different momenta.

Not all the states above are physical. The physical states will be identified with BRST cohomology in so-called BRST quantization. After gauge fixing, residual symmetry that combines matter and ghost fields remains. This symmetry is called BRST symmetry with corresponding BRST charge

$$Q_B = \sum_{n=-\infty}^{\infty} (c_n L_{-n}^m + \bar{c}_n \bar{L}_{-n}^m) + \sum_{m,n=-\infty}^{\infty} : (c_m c_n b_{-m-n} + \bar{c}_m \bar{c}_n \bar{b}_{-m-n}) : - (c_0 + \bar{c}_0). \quad (4.4)$$

---

<sup>1</sup>We use convention for the Regge slope  $\alpha' = 1$ .

Physical states are annihilated by this BRST charge

$$Q_B|\psi\rangle_{phys} = 0. \quad (4.5)$$

In order the BRST charge to be consistently conserved, it must be nilpotent

$$Q_B^2 = 0. \quad (4.6)$$

This is the case only if the matter theory has total central charge 26 to sum up to zero with the central charge of the ghost sector. Since the free boson CFT has conformal charge 1, it implies that we need 26 bosons and corresponding 26 spacetime dimensions.

Due to the hermiticity of  $Q_B$ , all  $Q_B$ -exact states has vanishing inner product with all the physical states. Moreover,  $Q_B$  rises the ghost number of the string state and we can restrict ourselves on the states with particular ghost number that is equivalent to the restriction to the particular cohomology class. Physical states differing only by  $Q_B$ -exact term are then equivalent and if we denote  $\mathcal{H}^{(g)} \subset \mathcal{H}$  the subspace of states with ghost number  $g$ , we can make a restriction and consider only states from the cohomology class

$$\mathcal{H}_{phys} = \mathcal{H}_{closed}^{(1)} / \mathcal{H}_{exact}^{(1)}. \quad (4.7)$$

Let us state an identity that will be useful later when introducing Siegel gauge in string field theory. It can be easily shown that

$$\{b_m, Q_B\} = L_m. \quad (4.8)$$

## 4.2 Witten's cubic string field theory

The standard procedure from the previous section can, in principle, provide a framework for calculation of an arbitrary on-shell scattering amplitude. To study non-perturbative aspects of string theory, such as tachyon condensation, the off-shell formalism is needed. Cubic open string field theory (OSFT), originally introduced by Witten in 1986, provides the off-shell formulation and we will now give basics of this theory [16]. For more details see reviews [65, 66, 67].

We would like to construct an OSFT action that gives equation of motion  $Q_B\Psi = 0$  at linearized level for string field  $\Psi$ . The string field  $\Psi$  is generally off-shell extension of the string states and correspond to some state in the Hilbert space  $\mathcal{H}_{BCFT}$  of the tensor product of matter and ghost boundary conformal field theory  $BCFT = BCFT^m \otimes BCFT^{gh}$ . The matter part  $BCFT^m$  must have central charge  $(26, 26)$  to obtain consistent theory as discussed above. General state in  $\mathcal{H}_{BCFT}$  can be written as

$$|\Psi\rangle = \sum_{i,I,J} \Phi_{iIJ} L_{-I}^m L_{-J}^{gh} |i\rangle, \quad (4.9)$$

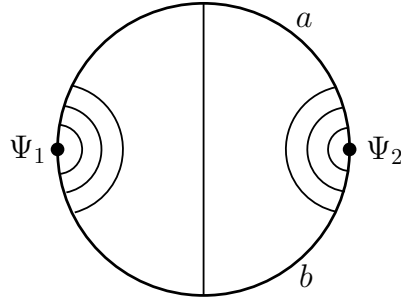


Figure 4.1: 2-vertex in SFT.

where  $i$  runs over all boundary primaries present in particular BCFT background and  $I$  and  $J$  are multi-indices running through the all descendants of particular primary.

Appropriate linearized action can be written in three different forms as

$$S_{lin} = -\frac{1}{2}\langle\Psi|Q_B|\Psi\rangle \equiv -\frac{1}{2}\langle\Psi, Q_B\Psi\rangle \equiv -\frac{1}{2}\int\Psi * Q_B\Psi, \quad (4.10)$$

where  $\langle\Psi|$  is the BPZ-conjugate of  $|\Psi\rangle$ . Witten has included interaction term into the action and inspired by Chern-Simons theories, he proposed an action

$$S = -\int\left(\frac{1}{2}\Psi * Q_B\Psi + \frac{g}{3}\Psi * \Psi * \Psi\right), \quad (4.11)$$

where the integration, star product, and derivation  $Q_B$  were formally defined axiomatically. Quantity  $g$  is the interaction constant and can be set equal to 1 simply by redefinition of the string field  $\Psi \rightarrow \Psi/g$ . Form (4.10), one finds equations of motion for the string field

$$Q_B\Psi + \Psi * \Psi = 0 \quad (4.12)$$

using the Witten's axioms to manipulate with the constituents of the action. There is huge gauge freedom that extends the addition of BRST exact term in the linearized version

$$\delta\Psi = Q_B\Lambda + \Psi * \Lambda - \Lambda * \Psi, \quad (4.13)$$

for any ghost number zero string field  $\Lambda$ .

We can see that linearized version of the above relation gives us correct equation  $Q_B\Psi = 0$ . Since there is already included the interaction of strings in the Polyakov action, one has to verify that the cubic term leads to the same predictions for  $g \rightarrow 0$  as the original theory. It has been done in the case of bosonic string theory in [75, 76].

Now, we would like to rewrite the cubic term from (4.11) that corresponds to gluing three strings together in terms of CFT correlator. We will go further since we will give CFT prescription for arbitrary  $\int\Psi * \dots * \Psi$  generalizing BPZ-product that has been associated with  $\int\Psi * \Psi$ . BPZ product glues two string worldsheets and recalling its definition for the primary fields

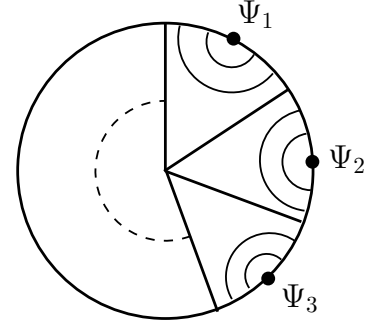


Figure 4.2: Situation corresponding to general amplitude in SFT.

$$\langle\phi_1|\phi_2\rangle = \lim_{z\rightarrow 0}\left(\frac{1}{z^2}\right)^{h_1}\langle\phi_1(-1/z)\phi_2(0)\rangle_{UHP}, \quad (4.14)$$

we can map the right-hand side correlator by a map

$$f(z) = \frac{i-z}{i+z} \quad (4.15)$$

to the unit disk and perform the limit. We get an unit disk with insertions at 1 and -1 as in the figure 4.2

$$\begin{aligned} \langle\phi_1|\phi_2\rangle &= \lim_{z\rightarrow 0}\left(\frac{1}{z^2}\right)^{h_1}(f'(-1/z))^{h_1}(f'(0))^{h_2}\langle\phi_1(f(-1/z))\phi_2(f(0))\rangle_{disk} \\ &= 4^{h_1}\langle\phi_1(-1)\phi_2(1)\rangle_{disk}, \end{aligned} \quad (4.16)$$

where we have used  $h_1 = h_2$  to get nonvanishing correlator.

Having two punctured disk obtained by gluing two string worldsheets, generalization for the higher overlaps is straightforward. For  $n$  string fields, we need to glue  $n$  worldsheets and arrive at  $n$ -punctured disk as in the figure 4.2. Functional that generalize BPZ product (4.16) can be easily constructed. We need to map  $n$  semi-disks to the wedges of the unit disk by conformal maps and compute the correlator of these wedge states with insertions glued together

$$\int \Psi_1 * \dots * \Psi_n = \langle (f_1^{(n)} \circ \Psi_1(0)) \dots (f_n^{(n)} \circ \Psi_n(0)) \rangle, \quad (4.17)$$

where corresponding conformal maps are

$$f_k^{(n)} = \left( \frac{i-z}{i+z} \right)^{\frac{2}{n}} e^{\frac{2\pi i k}{n}}. \quad (4.18)$$

Having defined star product and integration in CFT approach, it is simple computation to verify that the original Witten axioms are satisfied.

The most interesting case is the case of 3-vertex. Using the map of the above correlator to the UHP, we find UHP representation of the 3-vertex with insertions at  $-\sqrt{3}$ , 0, and  $\sqrt{3}$ . Performing the map, we get from the above functions  $f_i^{(3)}$  new one with the expansion

$$\begin{aligned} f_1(z_1) &= \sqrt{3} + \frac{8}{3}z_1 + \frac{16}{9}\sqrt{3}z_1^2 + \frac{248}{81}z_1^3 + \dots \\ f_2(z_2) &= \frac{2}{3}z_2 - \frac{10}{81}\sqrt{3}z_2^3 + \dots \\ f_3(z_3) &= -\sqrt{3} + \frac{8}{3}z_3 - \frac{16}{9}\sqrt{3}z_3^2 + \frac{248}{81}z_3^3 + \dots \end{aligned} \quad (4.19)$$

At the end of this section, we will introduce a *twist operator*  $\Omega$  [65] that reverses the parametrization of a string. We will call a field  $\Psi_+$  to be twist even if  $\Omega\Psi_+ = \Psi_+$  and twist odd if  $\Omega\Psi_- = -\Psi_-$ . It can be shown that  $\Omega|0\rangle = -|0\rangle$ ,  $\Omega L_{-n}\Omega^{-1} = (-1)^n L_{-n}$ ,  $\Omega b_{-n}\Omega^{-1} = (-1)^{n+1} b_{-n}$ , and  $\Omega c_{-n}\Omega^{-1} = (-1)^n c_{-n}$ . From this relations, we can deduce that fields on the odd levels in (4.3) are twist-odd whereas fields on the even levels are also twist-even. It is not difficult to show that

$$\langle \Psi_+, \Psi_+, \Psi_- \rangle = 0 \quad (4.20)$$

is vanishing. This identity will provide truncation of the string field to the twist-odd subspace.

### 4.3 Boundaries and Sen's conjectures

At the ends of the open strings, one can impose different boundary conditions. Choosing particular BCFT background, one finds a tachyon (a state with negative mass<sup>2</sup>) in the string spectrum. This tachyon indicates that perturbative vacuum is unstable and tends to condense to a more stable vacuum. First suggestions in this subject comes from [70, 71], but with clear picture came Ashoke Sen in 1999. He suggested that open bosonic string with free boundary conditions should be thought of as living on a space-filling D-brane and nonzero vacuum energy is associated with its tension. Tachyons in the string spectrum are instability modes of the initial D-brane. Sen came up with three conjectures [17, 18]



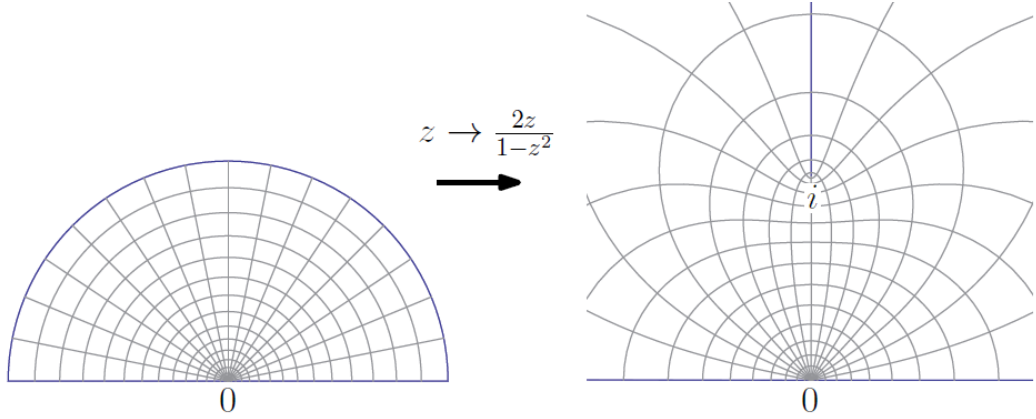


Figure 4.3: Map used in the definition of the Ellwood invariants.

1. The tachyon potential has a locally stable minimum with energy density  $\mathcal{E}$  with respect to the energy density of the unstable critical point that is equal to minus the tension of the initial D-brane
2. Lower-dimensional D-branes are solitonic solutions on the background of a D25-brane.
3. The locally stable vacuum of the system is the closed string vacuum with no open string excitations.

Since the introduction of the above conjectures, they have been tested numerically using level truncation that provides good insight into the problem. Two of the conjectures have been also proven analytically. The first conjecture was verified by Schnabl in 2005 when constructing the first analytical solution to the SFT equations of motion [24]. The solution for the tachyon vacuum was followed by the proof of the third conjecture by Schnabl and Ellwood [72]. The second conjecture still remains to be proven and lump solutions to be constructed.

## 4.4 Ellwood invariants

As mentioned in the second conjecture above, solutions to SFT equations of motion correspond to different D-brane configurations. To interpret the boundary condition, one needs to compute coefficients in front of the Ishibashi states in the boundary state. To find these coefficients, we will use gauge invariant observables originally introduced in [73, 74]. Later, Ellwood conjectured a relation to the closed string tadpole on a disk with appropriate boundary condition [22]. He computed a class of invariants for marginal deformation solutions and tachyon vacuum and argued that the relation should hold in general. Rigorous proof still remains to be done. Recently the Ellwood conjecture has been generalized and it has been shown how to use it to compute whole boundary state [23]. In this section we will describe basics of the work listed above.

Let us define the gauge invariant quantities and show their gauge invariance. Consider a ghost number 1 open string field  $|\Psi\rangle = \mathcal{O}_\Psi(0)|0\rangle$  represented by

insertion of  $\mathcal{O}_\Psi(0)$  on the unit semicircle as in the figure 4.3. To define gauge invariants  $W(\Psi, \mathcal{V}_\alpha)$ , we will need a map

$$f(z) = \frac{2z}{1-z^2} \quad (4.21)$$

that brings us from the upper half disk to the entire UHP. Then we define gauge invariants

$$W(\Psi, \mathcal{V}_\alpha) = \langle I | \mathcal{V}_\alpha(i) | \Psi \rangle = \langle \mathcal{V}_\alpha(i) f \circ \mathcal{O}_\Psi(0) \rangle_{UHP}, \quad (4.22)$$

for all  $\mathcal{V}_\alpha = c\bar{c}V_\alpha^m$  ghost number 2 closed string vertex operator with conformal weight  $(0,0)$  satisfying  $\{Q, \mathcal{V}_\alpha\} = 0$ . We have also introduced the identity string field

$$|I\rangle = U_f^\dagger |0\rangle, \quad (4.23)$$

where  $U_f$  is the generator of the transformation  $f$ , that is the identity element of the star algebra.

Now, we will proof the gauge invariance

$$W(\Psi + Q\Lambda + [\Psi, \Lambda], \mathcal{V}_\alpha) = W(\Psi, \mathcal{V}_\alpha). \quad (4.24)$$

Due to the linearity of  $W(\Psi, \mathcal{V}_\alpha)$  the above invariance is implied by

$$W(Q\Lambda, \mathcal{V}_\alpha) = 0, \quad W([\Psi, \Lambda], \mathcal{V}_\alpha) = 0. \quad (4.25)$$

The first term vanishes as a consequence of BRST invariance of the boundary condition  $\langle \{Q_B, \dots\} \rangle = 0$  since then

$$\begin{aligned} W(Q_B\Lambda, \mathcal{V}_\alpha) &= \langle \mathcal{V}_\alpha(i) f \circ \{Q_B, \mathcal{O}_\Lambda\} \rangle_{UHP} \\ &= -\langle \{Q_B, \mathcal{V}_\alpha(i)\} f \circ \mathcal{O}_\Lambda \rangle_{UHP} = 0. \end{aligned} \quad (4.26)$$

The second term also vanishes since

$$W(\Psi * \Lambda, \mathcal{V}_\alpha) = W(\Lambda * \Psi, \mathcal{V}_\alpha), \quad (4.27)$$

recalling the definition of the  $*$ -product.

Ellwood conjectured that starting on the  $BCFT_0$  background and finding a solution to the equations of motion  $\Psi$ , there exists a relation, which enables to find on-shell part of the boundary state (i.e. the part corresponding to weight  $(1,1)$  bulk primaries)

$$W(\Psi, \mathcal{V}_\alpha) - W(\Psi_{TV}, \mathcal{V}_\alpha) = -\frac{1}{4\pi i} \langle \mathcal{V}_\alpha | c_0^- | B_\Psi \rangle, \quad (4.28)$$

where  $|B_\Psi\rangle$  is the boundary state we wish to find,  $\Psi_{TV}$  is the solution for the tachyon vacuum, and  $c^- = c_0 - \bar{c}_0$ . Ellwood verified the relation for all known analytical solutions and gave a sketch of its general prove. Although it is widely believed, precise verification of the statement is still lacking.

Recently Kudrna, Maccafferri and Schnabl found a generalization of the Ellwood conjecture that enables the computation of all coefficients of the boundary state [23]. Since the boundary state is expressible as a linear combination of the Ishibashi states and every Ishibashi state corresponds to a spinless primary, one needs only to compute coefficients standing in front of the primary states. The

generalization uses following trick. We can add a  $\text{BCFT}^{aux}$  with central charge 0 to the matter sector and introduce an auxiliary primary field  $w$  in the sector with identity disk one-point function with the insertion at the origin  $\langle w(0) \rangle_{disk} = 1$ . They argued that there always exists such a theory. We can promote the original spinless primary in the matter sector  $V_\alpha$  with conformal weights  $(h_\alpha, h_\alpha)$  by tensor multiplication  $V_\alpha \otimes w$ . If the auxiliary field  $w$  has conformal weights  $(1 - h_\alpha, 1 - h_\alpha)$ , we are totally given on-shell primary operator  $c\bar{c}V_\alpha \otimes w$  with conformal weights  $(0,0)$  and the Ellwood conjecture 4.28 can be used.

The next nontrivial question that have to be addressed is the problem of lifting the solution from the original BCFT to  $\text{BCFT}' = \text{BCFT} \otimes \text{BCFT}^{aux}$ . In the cases we will be studying, the lift is following. We will be interested in the matter BCFT split into the two sectors  $\text{BCFT}_1 \otimes \text{BCFT}_2$  with central charges  $(c, c)$  and  $(26-c, 26-c)$  and we will study tachyon condensation in the first sector  $\text{BCFT}_1$ , where boundary primaries will be switched on. In the second sector, the string field will be universal with no other primaries switched on. The lift can be then performed simply replacing  $L_n^{(2)} \rightarrow L_n^{(2)} + L_n^{(aux)}$  and  $|0\rangle \rightarrow |0\rangle \otimes |0\rangle_{aux}$ . The lifted solution will be denoted as  $\tilde{\Psi}$  and the lifted bulk operator  $\tilde{\mathcal{V}}^\alpha$ . Generalized Ellwood conjecture then reads

$$\langle c\bar{c}V^\alpha | c_0^- \| B_\Psi \rangle = -4\pi i \langle E[\tilde{\mathcal{V}}^\alpha] | \tilde{\Psi} - \tilde{\Psi}_{TV} \rangle, \quad (4.29)$$

where  $\Psi_{TV}$  is the solution for the tachyon vacuum and we have adopted shorthand  $\langle E[\tilde{\mathcal{V}}^\alpha] | = \langle I | \tilde{\mathcal{V}}^\alpha(i)$ .

As discussed in the previous chapter, the boundary state can be written in terms of the Ishibashi states that are known if the spectrum of bulk primaries is known. The boundary state corresponding to the string field  $\Psi$  is

$$\| B_\Psi \rangle = \| B_\Psi \rangle_m \otimes \| B \rangle_{gh} = \sum_i n_\Psi^\alpha | V_\alpha \rangle \otimes \| B \rangle_{gh}, \quad (4.30)$$

where the sum runs over all spinless bulk primaries and we have used matter-ghost factorization of the boundary state proven in the appendix of [23]. The coefficients

$$n_\Psi^\alpha = \langle V^\alpha \| B_\Psi \rangle_m \quad (4.31)$$

remain to be determined. One can proceed by solving the difficult set of sewing constraints or use methods of the RG to construct new boundary state from the original one. SFT provides different approach due to the Ellwood conjecture. With the use of the identity  $\langle 0 | c_{-1} \bar{c}_{-1} c_0^- \| B \rangle_{gh} = -2$ , one finds for the coefficients in the boundary state

$$\begin{aligned} n_\Psi^\alpha &= \langle V^\alpha \| B_\Psi \rangle_m = -\frac{1}{2} \langle 0 | c_{-1} \bar{c}_{-1} c_0^- \| B \rangle_{gh} \langle V^\alpha \| B_\Psi \rangle_m \\ &= -\frac{1}{2} \langle c\bar{c}V^\alpha c_0^- \| B_\Psi \rangle \end{aligned} \quad (4.32)$$

and now using the generalized Ellwood conjecture, one finally finds explicit expression for the coefficients

$$n_\Psi^\alpha = 2\pi i \langle E[\tilde{\mathcal{V}}^\alpha] | \tilde{\Psi} - \tilde{\Psi}_{TV} \rangle. \quad (4.33)$$

To each solution of SFT equations of motion, there exists a boundary state describing corresponding D-brane. SFT thus provides new method how to look

for the boundary states. Instead of solving difficult sewing constraints, one only needs to solve SFT equations of motion. We assume that solutions to the equations of motion are indeed consistent and corresponding BCFTs satisfy sewing conditions.

## 4.5 Level truncation method

Level truncation is a powerful numerical method in SFT that led to the discovery of many solutions. This method will be used in the next chapter to construct solutions in the Ising model SFT and corresponding boundary states (Ising D-branes).

Level truncation has been introduced by Kosteletzky and Samuel [71] to deal with an infinite number of coefficients standing in front of the basis states of the string field. The string field truncated to the level  $L$  is the one containing only fields with scaling dimensions less or equal to  $L$  with all the other fields neglected. Examples will be seen later. We can then construct a truncated action for these truncated fields and assume that in the limit  $L \rightarrow \infty$  correct SFT results are obtained. Kosteletzky and Samuel performed the computation up to the level  $L = 4$  and managed to find a non-perturbative solution with lower energy than the energy of the original configuration.

After the introduction of D-branes and Sen's conjectures, the solution found by Kosteletzky and Samuel has been identified with the non-perturbative (closed string) vacuum with no open string excitations. In 2005, the non-perturbative vacuum appeared as the first analytic solution in SFT due to Schnabl [24]. Motivated by the Sen's conjectures, level truncation became to be a popular tool to address them.

String field can be also reduced in several ways when looking for particular solution. There is huge amount of gauge freedom in SFT and many fields can be projected out by fixing gauge in the truncated field. The Siegel gauge is typically chosen and the same is the choice in this thesis. In the Siegel gauge, only states annihilated by  $b_0$  are left. It corresponds to the situation, when all the states containing  $c_0$  are projected out.

There are two reasons to fix gauge in level truncation. First of all, it reduces number of fields at given level and thus it is numerically convenient. Moreover, it reduces number of pure-gauge solutions that can be found using level truncation. Gauge symmetry mixes fields at different levels and it is therefore broken in level truncation since the maximal level is fixed. Gauge transformation corresponds to flat directions in the potential, but it is not the case when the string field is truncated. We can find nontrivial solutions that converge to a pure gauge solution when the level increases and flatness restores.

There can be found problems in gauge fixing since gauge choices are generally not globally well defined. The validity of the Siegel gauge has been studied by Ellwood and Taylor [77]. We will assume that Siegel gauge is valid for all our solutions.

Furthermore, there are many possible ways how to truncate the string field. One can restrict the string field to the *universal subspace*  $\mathcal{H}_{univ} \subset \mathcal{H}$  composed

of the states

$$\mathcal{H}_{univ} = \text{Span}\{L_{-j_1}^m \dots L_{-j_p}^m b_{-k_1} \dots b_{-k_q} c_{-l_1} \dots c_{-l_r} |0\rangle |j_i \geq 2, k_i \geq 2, l_i \geq -1\} \quad (4.34)$$

since the other modes gives zero after the action on the perturbative vacuum  $|0\rangle$ . Note that the zero momentum tachyon  $c_1|0\rangle$  is member of  $\mathcal{H}_{univ}$ . Since BRST operator can be written in terms of  $T^m$ ,  $b$ , and  $c$  modes, we find that  $Q_B : \mathcal{H} \rightarrow \mathcal{H}$ . Moreover,  $\mathcal{H}$  clearly forms a closed subalgebra under the  $*$ -multiplication.

One can further decompose the universal subspace into the direct sum of spaces with given ghost number

$$\mathcal{H}_{univ} = \oplus_{g \in \mathbb{Z}} \mathcal{H}_{univ}^{(g)}. \quad (4.35)$$

From the previous arguments, the physical string fields have ghost number one and the string field can be consistently truncated to live in the space  $\mathcal{H}_{univ}^{(1)}$ . Since  $c_1|0\rangle = c(0)|0\rangle \in \mathcal{H}_{univ}^{(1)}$  is a ghost number one primary state, all the other states from  $\mathcal{H}_{univ}^{(1)}$  can be obtained acting with all the matter and ghost Virasoro generators on this state

$$\mathcal{H}_{univ}^{(1)} = \text{Span}\{L_{-j_1}^m \dots L_{-j_p}^m L_{-l_1}^{gh} \dots L_{-l_q}^{gh} c_1|0\rangle |j_1 \geq 2, l_i \geq 1\}. \quad (4.36)$$

The statement of the equivalence of the above set and the previous definition of  $\mathcal{H}_{univ}^{(1)}$  can be proven studying spectra of the operators in each set. The procedure is performed in [78].

Next, we can restrict our attention only to the twist even states, i.e. states containing only odd numbers of the Virasoro generators. The twist transformation corresponds to the reversion of the parametrization of the string. It can be proven that perturbative vacuum  $|0\rangle$  is twist odd together with odd modes. Note that the tachyon  $c_1|0\rangle$  remains in the spectrum. The prove that we can restrict on the even fields is based on the following arguments. Since fields on different levels in given Verma module have vanishing BPZ-product, the twist even and odd fields do not mix in the kinetic part of the action. It has been already stated that odd states cannot be present linearly in the cubic term of the action since this vertices vanish. It means that twist-even fields appear at least quadratically in the SFT action and thus can be consistently set to zero not to spoil equations of motion.

The last truncation one can perform is based on the restriction to the  $SU(1,1)$  singlets in the ghost sector. The Siegel gauge fixed equations of motion

$$L_0 \Psi + b_0 \Psi * \Psi = 0 \quad (4.37)$$

admit consistent truncation to the fields  $\Psi \in \mathcal{H}_{singl}$  satisfying

$$b_0 \Psi = \mathcal{G} \Psi = X \Psi = Y \Psi = 0, \quad (4.38)$$

where we have introduced generators of the  $SU(1,1)$  symmetry

$$\mathcal{G} = \sum_{n=1}^{\infty} (c_{-n} b_n - b_{-n} c_n), \quad X = - \sum_{n=1}^{\infty} n c_{-n} c_n, \quad Y = \sum_{n=1}^{\infty} \frac{1}{n} b_{-n} b_n. \quad (4.39)$$

The consistency can be checked applying  $SU(1,1)$  generators on  $b_0(\Psi * \Psi)$  and  $L_0 \Psi$  and showing that it vanishes if  $\Psi$  alone is a  $SU(1,1)$  singlet.

SU(1,1) singlets in the ghost sector can be conveniently described using twisted ghost CFT. Theory of the twisted ghosts is a theory with central charge -2 with Virasoro generators

$$L_k'^g = L_k^g + k j_k^{gh} + \delta_{k,0} = \sum_{n=-\infty}^{+\infty} (k-n) : b_n c_{k-n} :, \quad (4.40)$$

where  $j_k^{gh}$  are ghost current  $j^{gh} = cb$  modes. Details of the twisted ghosts CFT can be found in [79, 80]. Performing some tedious exercise with commutators, one finds commutators of the ghost number current modes

$$[j_m^{gh}, j_n^{gh}] = m \delta_{m,-n}. \quad (4.41)$$

As mentioned above the SU(1,1) singlet subspace can be now written explicitly as

$$\mathcal{H}_{singl} = \text{Span}\{L_{-k_1}'^{gh} \dots L_{-k_n}'^{gh} c_1 | 0\rangle | k_i > 1\} \otimes \mathcal{H}_{matter}. \quad (4.42)$$

Finally, putting all the truncations together (i.e. SU(1,1) subspace, twist even states, and universal fields with ghost number 1), one obtains a space

$$\text{Span}\{L_{-k_1}'^{gh} \dots L_{-k_m}'^{gh} L_{-l_1}^m \dots L_{-l_n}^m c_1 | 0\rangle | k_i > 1, l_i > 1, \sum k_i + \sum l_j \text{ is even}\}. \quad (4.43)$$

## 4.6 Conservation laws

The cubic term for primary states in the action (4.10) is readily computable if one knows corresponding structure constants. the situation is a bit more difficult in the case of descendant fields. One can proceed computing conformal maps of the inserted descendants and then apply corresponding differential operators  $\mathcal{L}_{-n}$  to get the result. The same difficulty emerges when computing Ellwood invariants, where bulk-boundary structure constants are needed to find a contribution from the primary part of the string field. In this section, we will develop a technique of conservation laws that will enable us to deal with the descendants easily.

Let us start with the derivation of the conservation laws for 3-vertex. We will represent the 3-vertex by a state  $\langle V_3 |$  in the 3-string dual Fock space defined by

$$\langle \Psi_1, \Psi_2, \Psi_3 \rangle = \langle V_3 | \Psi_1 \rangle \otimes | \Psi_2 \rangle \otimes | \Psi_3 \rangle. \quad (4.44)$$

Due to linearity of the 3-vertex, one can decompose the right-hand side into the linear combination of vertices with insertions that are Virasoro descendants of primary fields. If only primary operators are inserted, the cubic term can be easily computed from the knowledge of boundary structure constants. If there are some Virasoro generators inserted, the conservation laws allow us to replace negatively moded Virasoro generators by positively moded generators and iterating this procedure, we can eliminate all the Virasoro generators using the Virasoro commutation relation. One arrives at the simple 3-vertex with three primary operators insertions.

We will derive conservation laws for the generators of Virasoro algebra with central charge  $c$ , i.e. find coefficients  $A^k, a_n^k, b_n^k$ , and  $c_n^k$  in the expression

$$\langle V_3 | L_{-k}^{(2)} = \langle V_3 | \left( A^k c + \sum_{n \geq 0} a_n^k L_n^{(1)} + \sum_{n \geq 0} b_n^k L_n^{(2)} + \sum_{n \geq 0} c_n^k L_n^{(3)} \right), \quad (4.45)$$

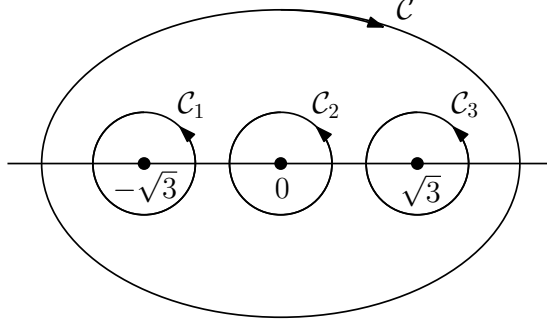


Figure 4.4: Contour deformation used in the derivation of conservation laws for 3-vertex.

where upper indices of the Virasoro generators label insertions, where the particular Virasoro generator acts [78]. Conservation laws for the other insertions can be easily obtained by cyclic permutation of these indices. Negatively moded Virasoro generators  $L_{-k}^{(2)}$  acting on the second state are traded for the sum of positively moded generators acting on all the three states.

Consider UHP representation of the 3-vertex with insertions at  $-\sqrt{3}, 0$ , and  $\sqrt{3}$ . Let  $v(z)$  be a holomorphic vector field with possible singularities at the punctures. This field transforms as  $v'(w) = \left(\frac{dz}{dw}\right)^{-1} v(z)$ . Regularity condition at the infinity constraints  $\lim_{z \rightarrow \infty} z^{-2} v(z)$  to have finite value as can be seen performing the change of variables  $z \rightarrow -1/z$ .

With the above conditions imposed on  $v(z)$ , we have following transformation under the conformal map  $w(z)$

$$T(z)v(z)dz = \left(T(w) - \frac{c}{12}S(z, w)\right)v(w)dw. \quad (4.46)$$

Since  $T(z)$  and  $v(z)$  are holomorphic almost everywhere, they can be integrated and the integration contour can be continuously deformed as long as we do not cross a puncture. Consider a contour  $\mathcal{C}$  that encircles the three punctures. Due to the regularity at the infinity, following quantity vanishes identically

$$\oint_{\mathcal{C}} v(z) \langle T(z) (f_1^{(3)} \circ \Psi_1(0)) (f_2^{(3)} \circ \Psi_2(0)) (f_3^{(3)} \circ \Psi_3(0)) \rangle dz = 0. \quad (4.47)$$

It must be so for any insertion and thus we can write simply

$$\oint_{\mathcal{C}} v(z) \langle V_3 | T(z) dz = 0. \quad (4.48)$$

Deforming the contour  $\mathcal{C}$  as in the figure 4.4 and transforming to the local coordinates using  $f_i^{(3)}$ , we obtain

$$\sum_{i=1}^3 \oint_{\mathcal{C}_i} v^i(z_i) \langle V_3 | \left( T(z_i) - \frac{c}{12} S(f_i^{(3)}(z_i), z_i) \right) dz = 0. \quad (4.49)$$

Schwarzian derivative for maps  $f_i$  is

$$S(f_i, y_i) = -\frac{10}{9} \frac{1}{(1+y_i^2)} = -\frac{10}{9} + \frac{20}{9} z_i^2 - \frac{10}{3} z_i^4 + \frac{40}{9} z_i^6 + \dots \quad (4.50)$$

and it is the same for all three maps since they differ by  $SL(2, \mathbb{R})$  transformation and is regular at the origin, where operators are inserted. The central term contributes only for singular fields  $v^{(i)}$ .

Recalling the definition of the Virasoro generators  $L_{-k}^{(i)}$ , one needs  $v^{(2)} \sim z_2^{-k+1} + O(z_2)$  around the puncture 2 and regular elsewhere to get desired relation. The fields  $v(z)$  with these properties will give us Virasoro conservation laws.

Clearly, using globally defined vector field

$$v_1(z) = -\frac{2}{9}(z^2 - 3) \quad (4.51)$$

that satisfy all the conditions described above, we get conservation laws for  $L_{-1}^{(2)}$ . After transformation to the local coordinates and performing Taylor expansion, one finds

$$\begin{aligned} v_1^{(1)}(z_1) &= -\frac{4}{3\sqrt{3}}z_1 + \frac{8}{27}z_1^2 - \frac{40}{81\sqrt{3}}z_1^3 + \frac{40}{729}z_1^4 + O(z_1^5), \\ v_1^{(2)}(z_2) &= 1 + \frac{11}{27}z_2^2 - \frac{80}{729}z_2^4 + O(z_2^5), \\ v_1^{(3)}(z_3) &= \frac{4}{3\sqrt{3}}z_3 + \frac{8}{27}z_3^2 + \frac{40}{81\sqrt{3}}z_3^3 + \frac{40}{729}z_3^4 + O(z_3^5). \end{aligned} \quad (4.52)$$

We see that leading term near the puncture at zero will give us precisely  $L_{-1}^{(2)}$ . Performing the three contour integration from (4.49) we can see that the central term do not contribute due to the regularity of  $v_1^i$  around each puncture and we can simply replace  $v_n^{(i)} z_i^n \rightarrow v_n^{(i)} L_{n-1}^{(i)}$  in the expression above and set the expression equal to zero

$$\begin{aligned} 0 &= \langle V_3 | \left( -\frac{4}{3\sqrt{3}}L_0^{(1)} + \frac{8}{27}L_1^{(1)} - \frac{40}{81\sqrt{3}}L_2^{(1)} + \frac{40}{729}L_3^{(1)} + \dots \right) \\ &+ \langle V_3 | \left( L_{-1}^{(2)} + \frac{11}{27}L_1^{(2)} - \frac{80}{729}L_3^{(2)} + \dots \right) \\ &+ \langle V_3 | \left( \frac{4}{3\sqrt{3}}L_0^{(3)} + \frac{8}{27}L_1^{(3)} + \frac{40}{81\sqrt{3}}L_2^{(3)} + \frac{40}{729}L_3^{(3)} + \dots \right). \end{aligned} \quad (4.53)$$

If  $L_{-1}$  appears at different punctures, corresponding conservation law can be found simply by cyclic permutation  $(1) \rightarrow (2)$ ,  $(2) \rightarrow (3)$ ,  $(3) \rightarrow (1)$ .

Similar procedure with the vector field

$$v_2(z) = -\frac{4}{27} \frac{z^2 - 3}{z} \quad (4.54)$$

leads to the following conservation law

$$\begin{aligned} 0 &= \langle V_3 | \left( -\frac{8}{27}L_0^{(1)} + \frac{80}{81\sqrt{3}}L_1^{(1)} - \frac{112}{243}L_2^{(1)} + \frac{304}{729\sqrt{3}}L_3^{(1)} + \dots \right) \\ &+ \langle V_3 | \left( L_{-2}^{(2)} + \frac{5}{54} + \frac{16}{27}L_0^{(2)} - \frac{19}{243}L_2^{(2)} + \dots \right) \\ &+ \langle V_3 | \left( -\frac{8}{27}L_0^{(3)} - \frac{80}{81\sqrt{3}}L_1^{(3)} - \frac{112}{243}L_2^{(3)} - \frac{304}{729\sqrt{3}}L_3^{(3)} + \dots \right), \end{aligned} \quad (4.55)$$

where the central term now contributes due to the fact that  $v_2(z)$  has a pole at the second puncture. All the other conservation laws for the 3-vertex can be derived using different vector fields.



Next category of conservation laws that will derived are the one for Ellwood invariants [23]. Total central charge of the matter-ghost theory is zero. Consider thus a theory decomposed into the two sectors  $\text{BCFT}^{(1)} \otimes \text{BCFT}^{(2)}$  with central charges  $c$  and  $-c$ . The first sector  $\text{BCFT}^{(1)}$  is the one, where we will find the solutions for D-branes. The second sector is composed of the rest matter subsector and ghost BCFT subsector. Let us denote

$$V(z, \bar{z}) = V_{(1)}^{(h, \bar{h})} V_{(2)}^{(-h, -\bar{h})}(z, \bar{z}) \quad (4.56)$$

zero-weight primary operator in the Ellwood invariants. We would like to find conservation laws for Virasoro generators in each sector. Clearly it is enough to derive them for the first sector and conservation laws in the other sector can be found simply exchanging  $c \rightarrow -c$  and  $(h, \bar{h}) \rightarrow (-h, -\bar{h})$ .

Let us define *anomalous derivation* by

$$K_n^{(1)} = L_n^{(1)} - (-1)^n L_{-n}^{(1)} = \oint \frac{dw}{2\pi i} v_n(w) T^{(1)}(w), \quad (4.57)$$

where the holomorphic vector field  $v_n(w)$  is given by

$$v_n(w) = w^{n+1} - (-1)^n w^{-n+1}. \quad (4.58)$$

In the following, we will show how this operator acts on the Ellwood state

$$\begin{aligned} \langle E[V] | K_n^{(1)} &= \langle I | V_{(1)}^{(h, \bar{h})} V_{(2)}^{(-h, -\bar{h})}(i, -i) K_n^{(1)} \\ &= \oint \frac{dw}{2\pi i} v_n(w) \langle I | V_{(1)}^{(h, \bar{h})} V_{(2)}^{(-h, -\bar{h})}(i, -i) T^{(1)}(w). \end{aligned} \quad (4.59)$$

The identity string field is defined by  $\langle I | = \langle 0 | U_f$  with conformal map defined above (4.21). We need to move the operator  $U_f$  to the right using that  $V(z, \bar{z})$  has zero conformal weight and using the knowledge how  $T$  transforms

$$\begin{aligned} &= \oint \frac{dw}{2\pi i} v_n(w) \langle I | V_{(1)}^{(h)}(i) V_{(1)}^{(\bar{h})}(-i) V_{(2)}^{(-h, -\bar{h})}(i, -i) T^{(1)}(w) \\ &= \oint \frac{dw}{2\pi i} v_n(w) \langle 0 | V_{(1)}^{(h)}(i) V_{(1)}^{(\bar{h})}(-i) \left( [f'(w)]^2 T^{(1)}(f(w)) + \frac{c}{12} S_f(w) \right) V_{(2)}^{(-h, -\bar{h})} U_f. \end{aligned} \quad (4.60)$$

Note that only singularities in the above expression are located at  $0, \pm i$ , and  $\infty$ . The expression is invariant under the transformation  $w \rightarrow -\frac{1}{w}$  as can be easily checked and the integration around the infinity gives the same contribution as the integration around the origin. Since

$$\oint_0 \dots = \oint_\infty \dots, \quad (4.61)$$

as mentioned above, we can get from the deformation sketched in 4.5 identity

$$\oint_0 \dots = -\frac{1}{2} \oint_{(i, -i)} \dots \quad (4.62)$$

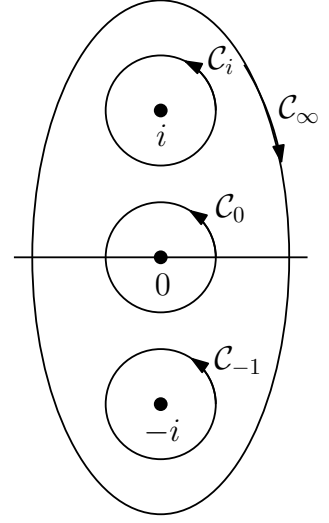


Figure 4.5: Contour deformation used in the derivation of conservation laws for the Ellwood invariants.

Now, we can evaluate the integrals using the OPE of stress-energy tensor  $T$  with primary operators

$$\begin{aligned}
&= -\frac{1}{2} \oint_{(i,-i)} \frac{dw}{2\pi i} v_n(w) [f'(w)]^2 \langle 0 | V_{(1)}^{(h)}(i) V_{(1)}^{(\bar{h})}(-i) T^{(1)}(f(w)) V_{(2)}^{(-h,-\bar{h})} U_f \\
&- \frac{c}{24} \oint_{(i,-i)} \frac{dw}{2\pi i} v_n(w) S_f(w) \langle 0 | V_{(1)}^{(h)}(i) V_{(1)}^{(\bar{h})}(-i) V_{(2)}^{(-h,-\bar{h})} \\
&= -\frac{1}{2} \oint_i \frac{dw}{2\pi i} v_n(w) [f'(w)]^2 \langle 0 | \left[ \frac{h V_{(1)}^{(h)}(i)}{(f(w) - i)^2} + \frac{\partial V_{(1)}^{(h)}(i)}{f(w) - i} \right] V_{(1)}^{(\bar{h})}(-i) V_{(2)}^{(-h,-\bar{h})} U_f \\
&- \frac{1}{2} \oint_{-i} \frac{dw}{2\pi i} v_n(w) [f'(w)]^2 \langle 0 | V_{(1)}^{(h)}(i) \left[ \frac{\bar{h} V_{(1)}^{(\bar{h})}(-i)}{(f(w) + i)^2} + \frac{\partial V_{(1)}^{(\bar{h})}(-i)}{f(w) + i} \right] V_{(2)}^{(-h,-\bar{h})} U_f \\
&- \frac{c}{24} \oint_{(i,-i)} \frac{dw}{2\pi i} v_n(w) S_f(w) \langle 0 | V_{(1)}^{(h)}(i) V_{(1)}^{(\bar{h})}(-i) V_{(2)}^{(-h,-\bar{h})}. \tag{4.63}
\end{aligned}$$

We have extracted the  $w$ -dependence from the points, where the operators are inserted and the contour deformation can be easily performed. We arrive at

$$\langle E[V] | K_n^{(1)} = n \left[ i^n \left( \frac{c}{8} - 4h \right) + (-i)^n \left( \frac{\bar{c}}{8} - 4\bar{h} \right) \right] \langle E[V] | K_n^{(1)}. \tag{4.64}$$

This conservation laws allow us to reduce Virasoro generators standing in front of the primaries in the string field and only correlators of primaries are needed to be computed.

If we study folded models, new primaries emerge at higher levels combining descendants from each sector, such as  $(L_{-1}^{(1)} - L_{-1}^{(2)})|\sigma\rangle \otimes |\sigma\rangle$  in the Ising model. Generally, combining primaries  $|h_1\rangle$  and  $|h_2\rangle$ , one finds a primary state on the first level  $|V\rangle = (h_2 L_{-1}^{(1)} - h_1 L_{-1}^{(2)})|h_1\rangle \otimes |h_2\rangle$ . We wish to look for the conservation laws for these primary operators. The only needed ingredient to derive the conservation laws is the OPE of  $L_{-1}V = \partial V$  with the stress-energy tensor

$$T(z) \partial V^{(h)}(w) \sim \frac{2hV(w)}{(z-w)^3} + \frac{(h+1)\partial V(w)}{(z-w)^2} + \frac{\partial^2 V(w)}{z-w}, \tag{4.65}$$

which can be found as a derivative of the OPE of a primary field with the stress-energy tensor. The action of  $K^{(1)}$  in the first sector is computable in similar fashion as earlier and we find

$$\begin{aligned}
\langle E[V] | K_n^{(1)} &= n \left[ i^n \left( \frac{c}{8} - 4h_1 \right) + (-1)^n \left( \frac{c}{8} - 4\bar{h}_1 \right) \right] \\
&- \frac{4}{3} h_1 i^{n+1} n (2n^2 - 5) \langle 0 | V^{h_1}(i) V^{h_2}(i) \bar{V}^{\bar{h}_1}(-i) \bar{V}^{\bar{h}_2}(-i) V^{(-h,-\bar{h})} U_f \\
&- 4i^n n \langle 0 | \partial V^{h_1}(i) V^{h_2}(i) \bar{V}^{\bar{h}_1}(-i) \bar{V}^{\bar{h}_2}(-i) V^{(-h,-\bar{h})} U_f. \tag{4.66}
\end{aligned}$$

We can see that new terms appeared. One can check that applying on the state  $\langle E[V] |$  operator  $K_n^{(1)} + K_n^{(2)}$ , the relation above indeed reduces to

$$\langle E[V] | K_n^{(1)} = n \left[ i^n \left( \frac{c}{8} - 4(h_1 + 1) \right) + (-1)^n \left( \frac{c}{8} - 4(\bar{h}_1 + 1) \right) \right]. \tag{4.67}$$

Since there are new terms, we need to find corresponding conservation laws to deal with them. The first case is obvious since a primary field is present

$$\begin{aligned}
& \langle 0 | V^{h_1}(i) V^{h_2}(i) \bar{V}^{\bar{h}_1}(-i) \bar{V}^{\bar{h}_2}(-i) V^{(-h, -\bar{h})} U_f K_n^{(1)} \\
&= n \left[ i^n \left( \frac{c}{8} - 4h_1 \right) + (-i)^n \left( \frac{\bar{c}}{8} - 4\bar{h}_1 \right) \right] \times \\
& \times \langle 0 | V^{h_1}(i) V^{h_2}(i) \bar{V}^{\bar{h}_1}(-i) \bar{V}^{\bar{h}_2}(-i) V^{(-h, -\bar{h})} U_f.
\end{aligned} \tag{4.68}$$

The second term is a bit more complicated, but the well known procedure gives us

$$\begin{aligned}
& \langle 0 | \partial V^{h_1}(i) V^{h_2}(i) \bar{V}^{\bar{h}_1}(-i) \bar{V}^{\bar{h}_2}(-i) V^{(-h, -\bar{h})} U_f \\
&= n \left[ i^n \left( \frac{c}{8} - 4(h_1 + 1) \right) + (-i)^n \left( \frac{\bar{c}}{8} - 4\bar{h}_1 \right) \right] \times \\
& \times \langle 0 | \partial V^{h_1}(i) V^{h_2}(i) \bar{V}^{\bar{h}_1}(-i) \bar{V}^{\bar{h}_2}(-i) V^{(-h, -\bar{h})} U_f \\
&- \frac{4}{3} i^{n+1} n (2n^2 - 5) \langle 0 | V^{h_1}(i) V^{h_2}(i) \bar{V}^{\bar{h}_1}(-i) \bar{V}^{\bar{h}_2}(-i) V^{(-h, -\bar{h})} U_f
\end{aligned} \tag{4.69}$$

Using these conservation laws, we can compute Ellwood invariants for primary fields obtained from the descendants on the first level in the folded models. Computing conservation laws for higher primaries would needs a bit more care.



# 5. Boundary states construction

## 5.1 The Ising model SFT

In this chapter, we wish to use the methods of SFT described in the previous chapter to construct Ising model boundary states. First of all, we have to create SFT setup. BCFT background in SFT can be decomposed into the matter and ghost part  $\text{BCFT} = \text{BCFT}^m \otimes \text{BCFT}^{gh}$ . We want to study boundary conditions (or D-branes in string theory language) in the Ising model, which is a model with central charge  $(\frac{1}{2}, \frac{1}{2})$ . Since the matter  $\text{BCFT}^m$  must have total central charge  $(26, 26)$ , one can decompose it into the two sectors  $\text{BCFT}^m = \text{BCFT}^I \otimes \text{BCFT}^R$ , where  $\text{BCFT}^I$  is the Ising model part and  $\text{BCFT}^R$  is a rest boundary conformal field theory with central charge  $(25.5, 25.5)$  to sum up with the first sector central charge to the correct value. This decomposition is done in analogy with the one proposed in [81], where lump solutions in one compactified dimension are successively looked for.

In the Ising sector  $\text{BCFT}^I$ , the theory is defined using particular background with some boundary condition described by a boundary state. In the Ising model, we will denote the  $\text{BCFT}^I$  backgrounds as  $\mathbb{1}$ -brane (corresponding to the boundary state  $|\mathbb{1}\rangle_I$ ),  $\epsilon$ -brane (corresponding to  $|\epsilon\rangle_I$ ) and  $\sigma$ -brane (corresponding to  $|\sigma\rangle_I$ ). Other D-branes can be obtained as integer linear combinations of these fundamental branes. Recall the formula for boundary states in terms of the Ishibashi states from the chapter 3

$$\begin{aligned} |\mathbb{1}\rangle_I &= \frac{1}{\sqrt{2}}|\mathbb{1}\rangle_I + \frac{1}{\sqrt{2}}|\epsilon\rangle_I + \frac{1}{\sqrt{2}}|\sigma\rangle_I \\ |\epsilon\rangle_I &= \frac{1}{\sqrt{2}}|\mathbb{1}\rangle_I + \frac{1}{\sqrt{2}}|\epsilon\rangle_I - \frac{1}{\sqrt{2}}|\sigma\rangle_I \\ |\sigma\rangle_I &= |\mathbb{1}\rangle_I - |\epsilon\rangle_I. \end{aligned} \tag{5.1}$$

Moreover, we assume the existence of a boundary state in the rest  $\text{BCFT}^R$  denoted by  $|0\rangle_R$  with  $g_0 = \langle 0|0\rangle = 1$  and we have a boundary state  $|B\rangle_{gh}$  in the ghost sector. Since we will be interested in boundary states in  $\text{CFT}^I$ , where all the primaries will be switched on, we will denote  $|V^\alpha\rangle = |V^\alpha\rangle_I \otimes |0\rangle_R$ . In the case of the Ising model,  $g$ -function is also the energy of corresponding D-brane since graviton operator is not present in the Ising sector and only overlap with  $|0\rangle$  has to be computed to find the energy of the Ising model D-brane.

We will consider  $\text{SU}(1,1)$  basis in the ghost sector in our computations and we will work in the Siegel gauge. We have to assume that Siegel gauge is restored in the limit when the truncation level approaches infinity. In the sector  $\text{BCFT}^R$  the basis of states will be universal from the section 4.5. To find solutions corresponding to D-branes in the Ising sector, one has to allow all possible degrees of freedom of the boundary, i.e. we have to consider whole boundary spectrum in given background. Spectrum of boundary operators in given background is reviewed in the table below.

Due to the fusion rules for the Ising model and considerations from the previous chapters, we can see that the string field is consistently truncated. BRST

D-brane	Energy	Boundary spectrum
$\ \mathbb{1}\rangle\rangle$	$\frac{1}{\sqrt{2}}$	$\mathbb{1}$
$\ \varepsilon\rangle\rangle$	$\frac{1}{\sqrt{2}}$	$\mathbb{1}$
$\ \sigma\rangle\rangle$	1	$\mathbb{1}, \varepsilon$

Table 5.1: Boundary spectrum of the Ising D-branes.

operator  $Q_B$  acts within the given Verma module and due to minimal models fusion rules  $*$ -multiplication of two states still remains in the truncated space of fields.

Verma modules of boundary operators in the Ising model are reducible representations of Virasoro algebra with null states. By adding multiplications of the null states we can set to zero the same number of components of the string field as is the number of null states. The states set to zero are arbitrary as long as the remaining states form a non-degenerate basis. From the form of the partition function we can see that the best irreducible basis consists of states created by only certain Virasoro operators. They are

$$L_{-2}, L_{-3}, L_{-4}, L_{-5}, L_{-11}, L_{-12}, L_{-13}, L_{-14}, L_{-18}, L_{-19}, L_{-20}, L_{-21}, \dots \quad (5.2)$$

in the Verma module of the identity, and

$$L_{-1}, L_{-4}, L_{-6}, L_{-7}, L_{-9}, L_{-10}, L_{-12}, L_{-15}, L_{-17}, L_{-20}, L_{-22}, \dots \quad (5.3)$$

in the Verma module of  $\varepsilon$ . In both cases the pattern repeats modulo 16. We have checked that this basis of descendants is non-degenerate numerically up to the level 22. Had we needed also the Verma module of  $\sigma$ , we would find that we need only  $L_{\text{odd}}$ , i.e.  $L_{-1}, L_{-3}, L_{-5}, L_{-7}, \dots$ . For further details see [1].

Using Cardy's condition we were able to construct boundary states of minimal models. But it is no more true for general CFT, where the situation becomes too difficult. Different way to proceed is using the RG. One can add a perturbation to the action of the form

$$S_\psi = \lambda \int_{\partial W} \phi(s) ds, \quad (5.4)$$

where  $\phi$  is a relevant or marginal boundary operator, and study RG flows triggered by this operator. For further details see [14], where authors study certain RG flows in the case of minimal models. Unfortunately, there is huge limitation in the methods based on the RG. The flow can only lead to the state with lower g-function  $g^a = \langle \mathbb{1} \rangle_a$ . This limitation is not present in the SFT as we will illustrate on the solution found on the  $\mathbb{1}$ -brane and  $\varepsilon$ -brane with higher boundary energy.

## 5.2 Truncated action for the Ising model

In this section, we will illustrate the level truncation method on the Ising SFT. We will construct explicitly the action for the truncated string field and find solutions to the equations of motion corresponding to the extreme value of the action. Starting from one D-brane we will find solutions that correspond to the

other two boundary conditions. The only needed ingredients are the structure constants in some BCFT background. They have been reviewed in the previous chapter.

### 5.2.1 Solutions on the $\sigma$ -brane

Let us start with the solutions on the  $\sigma$ -brane, where we will find the other two elementary boundary states. The boundary spectrum of  $\sigma$ -brane contains primary operators  $\mathbb{1}$  and  $\epsilon$  with conformal weights 0 and  $\frac{1}{2}$ . the string field truncated to the level  $L = \frac{1}{2}$  can be written as linear combination of two tachyonic modes  $c_1|0\rangle$  and  $c_1|\epsilon\rangle$  since all the other operators has higher scaling dimension

$$|\Psi\rangle = tc_1|0\rangle + ac_1|\epsilon\rangle. \quad (5.5)$$

We will study condensation on the original  $\sigma$ -brane triggered by relevant operator  $\epsilon$  to find the other two solutions.

First of all, we wish to construct the truncated action for the field (5.5). In the Siegel gauge the kinetic term reduces to  $\langle\Psi|Q_B|\Psi\rangle = \langle\Psi|c_0L_0|\Psi\rangle$ , which can be derived from (4.8). From the BPZ conjugation of the above fields

$$\text{BPZ}(|0\rangle) = \langle 0|, \quad \text{BPZ}(c_1) = c_{-1}, \quad (5.6)$$

we find in the ghost sector

$$\langle 0|c_{-1}c_0L_0c_1|0\rangle = -\langle 0|c_{-1}c_0c_1|0\rangle = -1, \quad (5.7)$$

where we have adopted normalization  $\langle c_{-1}|c_0|c_1\rangle = 1$ . In the matter sector, we get on the  $\sigma$ -brane  $\langle \mathbb{1} \rangle_\sigma = \langle 0|\sigma\rangle = 1$ . For the state  $|\epsilon\rangle$ , we find

$$\langle \epsilon|c_{-1}c_0L_0c_1|\epsilon\rangle = -\frac{1}{2}\langle \epsilon|\epsilon\rangle\langle 0|c_{-1}c_0c_1|0\rangle = -\frac{1}{2}, \quad (5.8)$$

where we have used the prescription for the boundary 2-point function of  $\epsilon$ . Putting the two expressions together we find a kinetic term in the SFT action

$$\begin{aligned} \frac{1}{2}\langle\Psi, Q_B\Psi\rangle &= \frac{1}{2}\langle tc_1 + ac_1\epsilon, c_0L_0(tc_1 + ac_1\epsilon)\rangle = \\ &= -\frac{1}{2}t^2\langle 0|c_{-1}c_0c_1|0\rangle - \frac{1}{4}a^2\langle \epsilon|c_{-1}c_0c_1|\epsilon\rangle = -\frac{1}{2}t^2 - \frac{1}{4}a^2, \end{aligned} \quad (5.9)$$

where the crossed terms vanishes due to differing conformal weights of  $\mathbb{1}$  and  $\epsilon$ .

Now, we move to the computation of the cubic term. We will use first two terms from the expansion 4.20 defining 3-vertex on the UHP. From the normalization  $\langle c_{-1}|c_0|c_1\rangle = 1$  that fixes the boundary structure constant and the knowledge of the conformal weight of  $c$ -ghost, one finds correlator

$$\langle c(z_1)c(z_2)c(z_3)\rangle = (z_1 - z_2)(z_1 - z_3)(z_2 - z_3). \quad (5.10)$$

With the use of this identity, we get in the ghost sector

$$\begin{aligned} \langle c_1, c_1, c_1\rangle &= \langle (f_1 \circ c(0))(f_2 \circ c(0))(f_3 \circ c(0))\rangle_{UHP} \\ &= \left\langle \frac{c(\sqrt{3})}{8/3} \frac{c(0)}{2/3} \frac{c(-\sqrt{3})}{8/3} \right\rangle_{UHP} = \frac{81\sqrt{3}}{64} = K^3, \end{aligned} \quad (5.11)$$

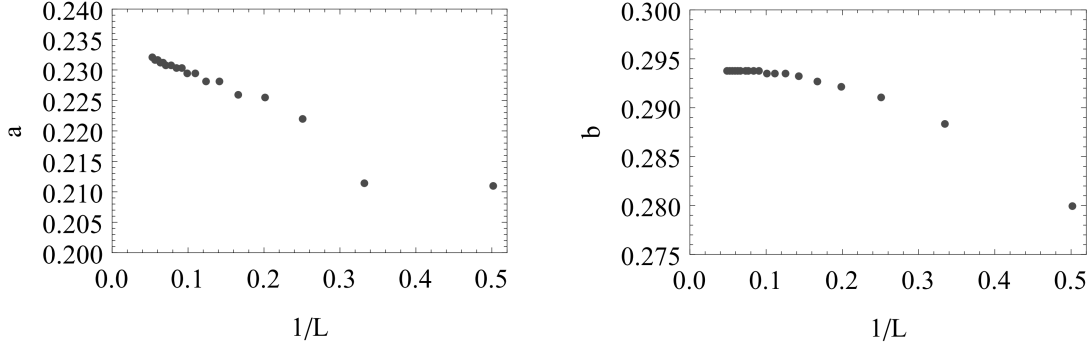


Figure 5.1: Convergence of coefficients  $t$  and  $a$  with increasing level  $L$ .

where we have conventionally denoted

$$K = \frac{3\sqrt{3}}{4}. \quad (5.12)$$

We get in the matter sector  $\langle \mathbb{1}, \mathbb{1}, \mathbb{1} \rangle = 1$ . From the Ising model fusion rules correlators including only one operator  $\epsilon$  or correlators composed of three such operators vanish. The only nonvanishing terms are those containing two  $\epsilon$  insertions and corresponding 3-vertex is

$$\langle \epsilon, \mathbb{1}, \epsilon \rangle = \sqrt{\frac{8}{3}} \sqrt{\frac{8}{3}} \langle \epsilon(-\sqrt{3}) \epsilon(\sqrt{3}) \rangle = \frac{8}{3} \frac{1}{2\sqrt{3}} = \frac{4}{3\sqrt{3}} = K^{-1} \quad (5.13)$$

and similarly for the other two options.

The interaction term is then

$$\frac{1}{3} \langle \psi, \psi, \psi \rangle = \frac{1}{3} t^3 \langle c_1, c_1, c_1 \rangle + \frac{1}{3} 3a^2 t \langle c_1 \epsilon, c_1, c_1 \epsilon \rangle = \frac{1}{3} K^3 t^3 + K^2 a^2 t, \quad (5.14)$$

where the factor 3 in the second step corresponds to three ways of the insertion of the operators. Finally, we obtain SFT action truncated to the level 0.5 for the string field (5.5)

$$\mathcal{V}(t, a) = -\frac{1}{2} t^2 - \frac{1}{4} a^2 + \frac{1}{3} K^3 t^3 + K^2 a^2 t. \quad (5.15)$$

It is simple to find solutions minimizing this action. We find two solutions that will be precised using higher level computations and will lead to the other two boundary states. The two solutions are

$$t = 0.14815, \quad a = \pm 0.24348. \quad (5.16)$$

Moreover, the tachyon vacuum can be found

$$t = 0.45618, \quad a = 0. \quad (5.17)$$

If we plug into the appropriately normalized action  $2\pi^2 \mathcal{V}(\psi) + 1$ , we find in the first case the energy 0.83029, which is quite close to the expected value  $\frac{1}{\sqrt{2}}$ . The difference is only 17%. For the tachyon vacuum one finds 0.31538.



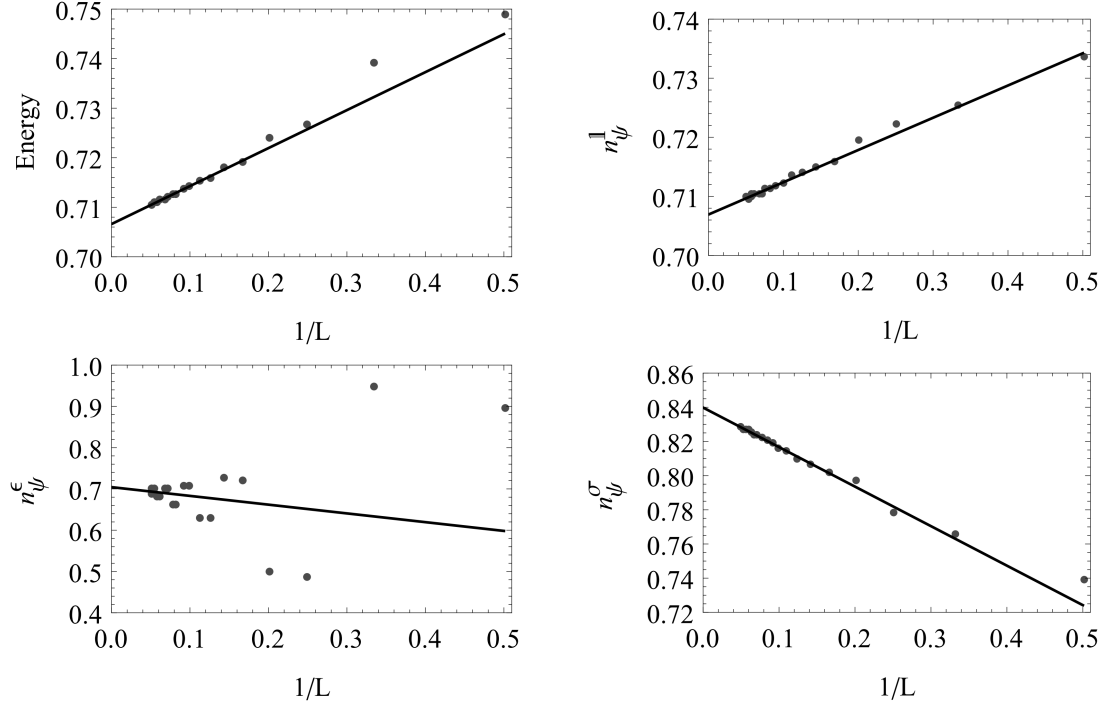


Figure 5.2: Convergence of the coefficients in the boundary state  $||1\rangle\rangle$  corresponding to the solution found on the  $\sigma$ -brane.

To illustrate the use of the conservation laws let us write explicitly the two solutions truncated to the level 2. The truncated string field has following form

$$|\Psi\rangle = tc_1|0\rangle + ac_1|\epsilon\rangle + uL_{-2}^{gh}c_1|0\rangle + vc_1L_{-2}^I|0\rangle + wc_1L_{-2}^R|0\rangle. \quad (5.18)$$

The kinetic term of descendants can be evaluated in similar manner as in the previous case since it is again  $L_0$  eigenstate. We can use Virasoro commutation relations to move positively moded generators that annihilate vacuum to the right.

The interaction term can be computed using conservation laws. For example

$$\langle c_1, L_{-2}^I c_1, c_1 \rangle = \langle c_1, c_1, c_1 \rangle \langle 1, L_{-2}^I 1, 1 \rangle = -\frac{5}{54} c \langle 1, 1, 1 \rangle = -\frac{5}{108} \quad (5.19)$$

since only the central term contributes and all the positively moded generators annihilate the identity insertions. It would not be the case if some other Virasoro generator appears at one of the three insertions. We would get contribution from the positively moded generators that we could commute to the right. In the case of ghost fields in  $SU(1,1)$  basis the algebra of ghost currents and their conservation laws are needed, but the procedure is totally analogous and a bit more tedious.

The same procedure leads to the action truncated to the level  $L = 2$ . Finding real solutions on this level leads to

$$t = 0.21084, \quad a = \pm 0.27990, \quad u = 0.08110, \quad v = -0.09947, \quad w = 0.03010 \quad (5.20)$$

with corresponding energy 0.75421 that approaches the expected value and differs only by 6.7 %.

The above procedure can be iterated and the coefficients converge to some fixed value. Example of such convergence for the two tachyonic modes is shown in the figure 5.1.

Moreover, we would like to find all the Ellwood invariants to interpret the solution. We get

$$\begin{aligned}
2\pi i \langle E[\tilde{\mathcal{V}}^\alpha] | c\phi_j \rangle &= 2\pi i (f'(0))^{h_j-1} \langle \tilde{V}^\alpha(i, -i) c\phi_j(0) \rangle_{UHP}^a \\
&= -\pi 2^{h_j+\Delta_\beta-1} \langle V^\beta(i, -i) \phi_j(0) \rangle_{UHP}^a \\
&= -\pi 2^{2h_j-1} B_{\alpha j}^a \langle \mathbb{1} \rangle_{UHP}^a
\end{aligned} \tag{5.21}$$

for each boundary primary  $\phi_i$ . In the expression above, we have used

$$\langle c(i)c(-i)c(0) \rangle = 2i, \quad \langle w^\beta(i, -i) \rangle_{UHP} = 2^{\Delta_\beta-2}, \tag{5.22}$$

where the first relation comes from 5.10 and the second one can be obtained mapping  $\langle w(0) \rangle_{disk} = 1$  to the UHP.

The only needed input into the above equation is the bulk-boundary correlator. We get for example

$$\langle \mathbb{1} \rangle_{UHP} = 1 \text{ and } \langle \epsilon(0) \rangle_{UHP} = 0 \tag{5.23}$$

for the identity insertion. In the case of  $\epsilon$  insertion, one finds

$$\langle \epsilon(i, -i) \rangle_{UHP} = -\frac{1}{2} \text{ and } \langle \epsilon(i, -i)\epsilon(0) \rangle_{UHP} = 0 \tag{5.24}$$

and in the third case

$$\langle \sigma(i, -i) \rangle_{UHP} = 0 \text{ and } \langle \sigma(i, -i)\epsilon(0) \rangle_{UHP} = 2^{1/8}. \tag{5.25}$$

At the level 0.5, we find for the first Ellwood invariant

$$n_\Psi^{\mathbb{1}} = -\frac{\pi}{2} [t \langle \mathbb{1} \rangle_{UHP} + a \langle \epsilon(0) \rangle_{UHP}] + 1 = -\frac{\pi}{2} t + 1. \tag{5.26}$$

where the additive constant corresponds to  $\Psi_{TV}$  term and ensures correct normalization. This term ensures that all the Ellwood invariants vanishes for the tachyon vacuum, where no open string modes are present.

For the two solutions, we receive numerical value  $n_\Psi^{\mathbb{1}} = 0.76729$  which differs only by 8.5 % from the expected value of the coefficient in front of the corresponding Ishibashi state  $|0\rangle\rangle$  in (5.1). Similar procedure can be done for the other two Ellwood invariants and we get  $n_\Psi^\epsilon = 0.76729$  and  $n_\Psi^\sigma = 0.64320$ . We can see big disagreement in the second coefficient, but things will go better if we move to the level 2.

Using conservation laws for the Ellwood invariants, we find for the new fields on the second level

$$\langle E[\mathbb{1}] | L_{-2}^I = \langle E[\mathbb{1}] | L_2^I + \frac{c_I}{2} \langle E[\mathbb{1}] | \tag{5.27}$$

and similarly for the other fields.

If we insert the coefficients of the found solutions, we find value  $n_\Psi^{\mathbb{1}} = 0.73370$  differing only by 3.8 % from the expected value. Moreover, we can find  $n_\Psi^\epsilon = 0.89339$  that is much closer to the expected value then in the case of level 0.5. General feature of the computation of boundary states using level truncation method is decreasing convergence for coefficients corresponding to the Ishibashi state associated with higher dimensional primaries.

Level	$2\pi^2\mathcal{V}(\Psi)$	$n_{\psi}^{\mathbb{1}}$	$n_{\psi}^{\epsilon}$	$n_{\psi}^{\sigma}$
2	0.74917	0.73370	0.89339	$\pm 0.73942$
4	0.72656	0.72213	0.48762	$\pm 0.77824$
6	0.71933	0.71585	0.72112	$\pm 0.80182$
8	0.71596	0.71401	0.62984	$\pm 0.81011$
10	0.71404	0.71216	0.70480	$\pm 0.81679$
12	0.71280	0.71154	0.66492	$\pm 0.82018$
14	0.71193	0.71065	0.70130	$\pm 0.82331$
16	0.71129	0.71035	0.67919	$\pm 0.82517$
18	0.71080	0.70983	0.70060	$\pm 0.82699$
20	0.71043	0.70978	0.69080	$\pm 0.82815$
$\infty$	0.70663	0.70688	0.70433	$\pm 0.83935$
Expected	0.70711	0.70711	0.70711	$\pm 0.84090$

Table 5.2: Boundary coefficients for the two solutions on the  $\sigma$ -brane. Extrapolated and precise values are mentioned.

Using computer code, the procedure can be performed to higher levels. With our code, we managed to hit the level 20 consisting of 29,772 fields. The boundary coefficients of the solution are listed in the table 5.2 below and in the figure 5.2.

In the table, linear extrapolation in  $1/L$  is performed to find the value, where the coefficients converge. We can see very good agreement with the analytical results since the first coefficient  $n_{\psi}^{\mathbb{1}}$  differs only by 0.03 % and the biggest disagreement can be again found in the field with the highest conformal weight  $n_{\psi}^{\epsilon}$ , where the difference from the correct value is 0.4 %.

Thus, we have found numerically the solutions with following boundary state coefficients:

$$\begin{array}{cccc}
\text{Energy}^{(\infty)} & n_{\Psi}^{\mathbb{1}(\infty)} & n_{\psi}^{\epsilon(\infty)} & n_{\psi}^{\sigma(\infty)} \\
\hline
0.70663 & 0.70688 & 0.70433 & \pm 0.83935
\end{array} \tag{5.28}$$

### 5.2.2 Solutions on the $\mathbb{1}$ -brane and $\epsilon$ -brane

The search for solutions on the  $\mathbb{1}$ -brane is more difficult. The boundary energy of the original D-brane is  $\frac{1}{\sqrt{2}}$  and the only configuration with lower energy is the tachyon vacuum. Therefore, we have to look for marginal or positive energy solutions.

On this brane, we have only one relevant boundary operator  $c_1|0\rangle$ . Equation of motion truncated to the level 0 with the only one field  $c_1|0\rangle$  leads only to the tachyon vacuum. To find a new solution, one has to move to the level  $L = 2$ . At this level the truncated string field has following form

$$|\Psi\rangle = tc_1|0\rangle + uL_{-2}^R c_1|0\rangle + vL_{-2}^I c_1|0\rangle + wL_{-2}^{Igh} c_1|0\rangle. \tag{5.29}$$

When solving the equations of motion, we find only following complex solution

$$\begin{aligned}
t &= 0.03383 - 0.31239i, & u &= 1.19000 + 0.52640i, \\
v &= 0.02453 - 0.04242i, & w &= 0.02532 - 0.12323i.
\end{aligned} \tag{5.30}$$

Notice that the non-diagonal primary  $L_{-2}^R - 51L_{-2}^I$  is excited.

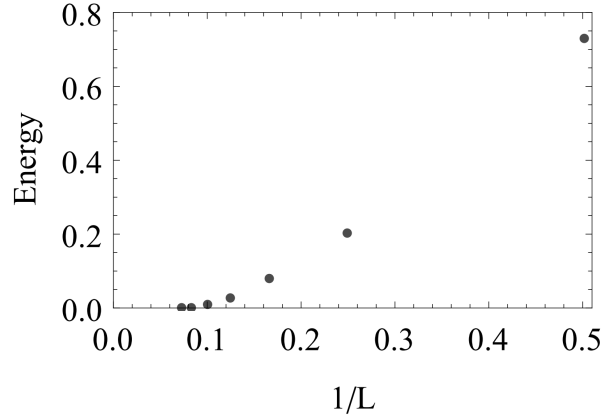


Figure 5.3: Decreasing imaginary part of the energy for the solution found on the 1-brane. It disappears completely at level  $L = 14$ .

Level	Energy	Im/Re
2	$1.59267 + 0.72688i$	0.78840
4	$1.41414 + 0.20152i$	0.43838
6	$1.28579 + 0.07668i$	0.30746
8	$1.21160 + 0.03054i$	0.22100
10	$1.16345 + 0.01007i$	0.15222
12	$1.12943 + 0.00123i$	0.07487
14	1.10568	0
16	1.09045	0
18	1.07936	0
20	1.07084	0
22	1.06405	0

Table 5.3: The energy and the imaginarity coefficient of the solution with positive energy on the 1-brane.

Although the solution looks pretty wild at the first sight, we find that it is stable under level truncation. The imaginary part of the solution is getting smaller as the level increases increase and surprisingly it disappears completely at level 14. We were able to evaluate the solution up to level 22 and the data are shown in the tables 5.3, 5.4 and the figure 5.4.

The last column shows the ratio between the imaginary and real part of the solution<sup>1</sup>. The energy of the solution is close to one, so its the most likely interpretation is a  $\sigma$ -brane. The components of boundary state do roughly agree with the expected values, but the agreement is not very good. Therefore, we would like to make an extrapolation to infinite level to see whether we can expect correct convergence. The dependence of the real part of energy and the invariants on level are plotted at figures 5.4. One can immediately see that the behavior of the invariants changes drastically at level 14. The best we can do is a linear fit using data from levels 14 to 22. Since the raw invariant  $n_{\psi}^{\epsilon}$  is oscillating, we have

<sup>1</sup>This ratio is computed as  $\sum_i \text{Re}[t_i] / \sum_i \text{Im}[t_i]$ , where  $t_i$  are the components of the string field. It is not an invariant quantity, but it gives a good idea how big the imaginary part of the solution is.

Level	$n_{\psi}^{\mathbb{1}}$	$n_{\psi}^{\epsilon}$	$n_{\psi}^{\sigma}$
2	$1.06048 - 0.18455i$	$-9.73471 - 5.23904i$	$-0.34358 - 0.97082i$
4	$0.96290 - 0.14267i$	$-0.66854 + 1.99191i$	$-0.36976 - 0.56423i$
6	$0.92262 - 0.11378i$	$-3.86207 - 0.37376i$	$-0.38933 - 0.39436i$
8	$0.90480 - 0.08685i$	$-0.57514 + 0.82266i$	$-0.37217 - 0.28194i$
10	$0.89256 - 0.06174i$	$-2.48552 + 0.00261i$	$-0.37629 - 0.19232i$
12	$0.88510 - 0.03109i$	$-0.56951 + 0.24561i$	$-0.36891 - 0.09399i$
14	0.91469	-1.93951	-0.26607
16	0.93044	-0.95087	-0.20633
18	0.93918	-1.69824	-0.17497
20	0.94538	-1.04849	-0.15003
22	0.94994	-1.55407	-0.13398
$\infty$	1.01265	-1.26593*	0.10153
Expected	1	-1	0

Table 5.4: Boundary coefficients for the solutions on the  $\mathbb{1}$ -brane. The coefficient labeled by \* corresponds to the value obtained using Padé-Borel approximation.

to modify it first by Padé-Borel approximation to suppress the oscillations. The approximated point are shown in the table below.

Level	$n_{\psi}^{\epsilon}{}_{PB}$	$L$	$n_{\psi}^{\epsilon}{}_{PB}$
4	$-4.36484 - 0.74899i$	14	-1.38446
6	$-2.90862 - 0.10512i$	16	-1.38544
8	$-1.88644 + 0.33130i$	18	-1.37157
10	$-1.57741 + 0.24252i$	20	-1.35608
12	$-1.43600 + 0.26176i$	22	-1.33856

(5.31)

The extrapolated values of energy and components of the boundary state are:

Energy <sup>(<math>\infty</math>)</sup>	$n_{\Psi}^{\mathbb{1}(\infty)}$	$n_{\psi}^{\epsilon(\infty)}$	$n_{\psi}^{\sigma(\infty)}$
0.9908	1.0127	-1.2659	0.1015

(5.32)

The energy and  $n_{\Psi}^{\mathbb{1}}$  are approximately 1% away from the expected value, which is quite good agreement. The other two invariants  $n_{\psi}^{\epsilon}$  and  $n_{\psi}^{\sigma}$  are more off the correct value. However, the reliability of the extrapolations is not very good due to small amount of points in the extrapolation. More data will be needed to make precise conclusion.

### 5.3 Algorithm details

In this section, we will discuss details of the algorithm used to perform computations to the higher levels.

First of all, we need to construct a string field. It consists of three sectors: the ghost sector, the Ising sector, and the rest sector. The ghost sector consists of  $L'^{gh}$  descendants of the state  $c_1|0\rangle$ . The rest sector is a subsector of the matter

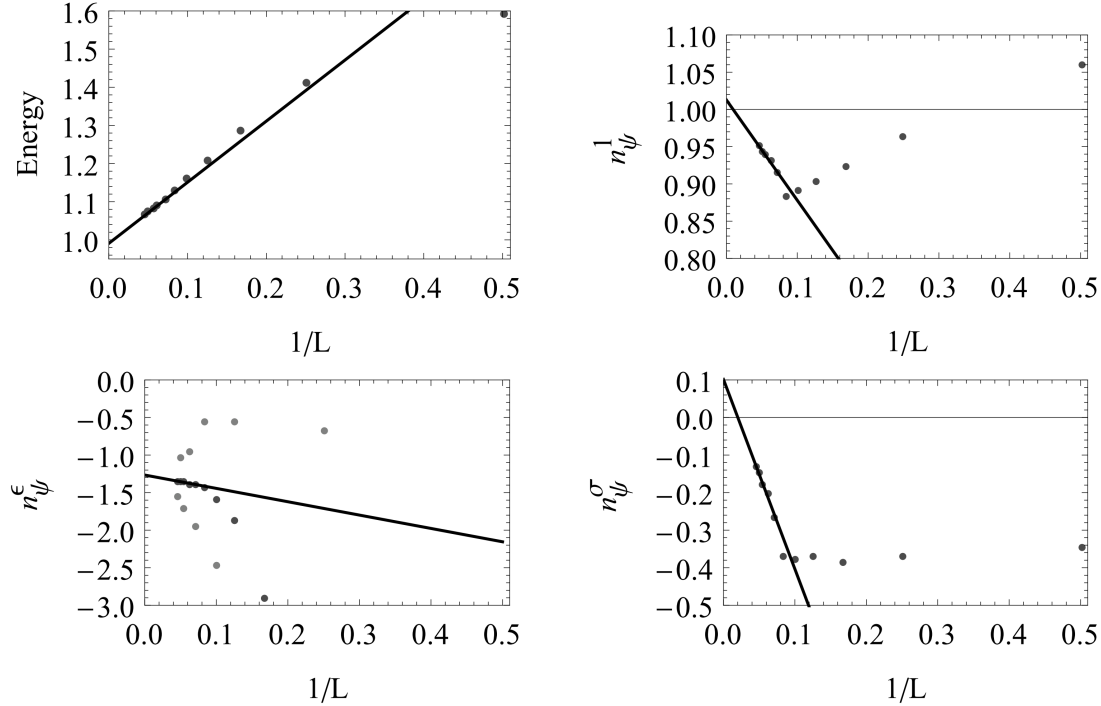


Figure 5.4: Convergence of the coefficients in the boundary state  $||\sigma\rangle\rangle$  corresponding to the solution found on the  $\mathbb{1}$ -brane.

sector with conformal weight  $c = 25.5$  and consists of the vacuum  $|0\rangle$  and its descendants. The Ising sector is a bit more difficult. If the field is living on the  $\mathbb{1}$ -brane or on the  $\epsilon$ -brane, only  $|0\rangle$  with its descendants is present in this sector, but if we are interested in solutions on the  $\sigma$ -brane, we need to include both  $\mathbb{1}$  and  $\epsilon$  Verma modules. Truncated field is then constructed as appropriate combination of states from these three sectors with the use of the Siegel gauge restriction, twist symmetry,  $SU(1,1)$  symmetry, and projecting the null states out.

Next step consist of the computation of the action of Virasoro generators  $L_n$  with positive mode  $n$  on the states constructed above in each sector. In the case of the ghost sector, also action of the ghost current  $j$  is needed to be computed. This procedure is easily performed using commutation relations of  $j_m$  and  $L_n$ . The resulting state is always a state constructed in the previous step multiplied by some constant. The number labeling the resulting state and the multiplier have to be stored in the memory.

Using previously computed actions of  $L_n$  on the states, one can find two-vertices in each sector simply finding BPZ-conjugate state and computing overlap with these conjugate states. Note that fields from different levels has vanishing BPZ-product.

Another needed ingredient is the 3-vertex. In the case of primary fields insertions, they have been computed previously from the knowledge of structure constants and definition of 3-vertex. The other vertices can be obtained using conservation laws. Not all vertices for all combinations of fields are needed to be stored due to its symmetry. If  $i$  is a positive integer labeling fields in given sector, only vertices  $\langle i, j, k \rangle$  for  $i \geq j \geq k$  are needed to be stored. All the other combinations are the same up to relative sign depending on the level of the inserted fields. We can also use subsector factorization of the correlator. The 3-vertex

can be computed as a product of vertices in each sector. This factorization saves memory dramatically but it slows the algorithm down since the evaluation of 3-vertex takes the most time during the computation.

First of all, we have to compute the coefficients in conservation laws for all the needed  $L_{-n}$ s. With this knowledge the manipulation is similar to the one in the previous chapter. Going to the next level gives us fields from the lower levels after application of some conservation laws and 3-vertices can be computed recursively.

The computation of the coefficients for the Ellwood invariants is straightforwardly implemented using conservation laws.

In the procedure that makes the result for the boundary state more precise, the Newton method can be conveniently used. The solutions can be easily found at the lower levels, but general solution at higher levels cannot be found since it would correspond to solving enormous system of quadratic equations with many non-physical solutions. Since we have a solution at some low level, we can use its coefficients as the starting point for the Newton method that converge to the new, more precise, truncated solution.

If we label the coefficients in front of the basis states in the string field by  $x_i$ , the SFT action has generally form

$$S(\{x_i\}_i) = \frac{1}{2} \sum_{i,j} A_{ij} x_i x_j + \frac{1}{3} \sum_{i,j,k} B_{ijk} x_i x_j x_k, \quad (5.33)$$

where  $A_{ij}$  and  $B_{ijk}$  are the 2- and 3-vertices computed previously. Equations of motion can be found as an extreme of this action

$$f_k(\{x_i\}_i) = \sum_i A_{ik} x_i + \sum_{i,j} B_{ijk} x_i x_j = 0, \quad (5.34)$$

where we have assumed without the loss of generality  $A$  and  $B$  to be symmetric. The solution to this set of equations can be found iteratively using

$$x_i^{(n+1)} = x_i^{(n)} - \sum_j M_{ij}^{-1}(\{x_i^{(n)}\}) f_j(\{x_i^{(n)}\}), \quad (5.35)$$

where  $f_j(\{x_i^{(n)}\})$  can be easily computed plugging above and we have denoted

$$M_{ij}(\{x_k^{(n)}\}) = \frac{\partial f_i}{\partial x_j}. \quad (5.36)$$

Specially, in the case of our quadratic system, we find from the equation (5.34)

$$M_{ij}(\{x_k^{(n)}\}) = A_{ij} + 2 \sum_k B_{ijk} x_k. \quad (5.37)$$

The iterated solution is then readily computable from the knowledge of the 3- and 2-vertices encoded in the coefficients  $A$  and  $B$ .

The iteration procedure stops when the wanted precision is achieved. In the case of our program the procedure stops if  $|x^{(n+1)} - x^{(n)}| < 10^{-12}$  or the number of iterations exceeds 20.

From the knowledge of the solution we can compute Ellwood invariants as combinations of the coefficients  $x_i$  with the use of the conservation laws.

## 5.4 Double Ising model

Let us move to the case of double Ising model. Tensor product of the original Ising model boundary states remains to be a boundary state in the doubled Ising model. In the following, we will restrict ourselves on these products. Finding other boundary states would be more difficult since complex solutions have to be analyzed and higher-weight primaries taken into account. Their convergence is getting worse and many difficulties would emerge as will be evident from the later discussion.

Starting with a background given by  $||\sigma\rangle\rangle \otimes ||\sigma\rangle\rangle$ , we look for a solution to the equations of motion. Clearly, solutions in each subsector that we have found in the previous section remain to be solutions and they correspond to  $||1\rangle\rangle \otimes ||\sigma\rangle\rangle$ ,  $||\epsilon\rangle\rangle \otimes ||\sigma\rangle\rangle$ ,  $||\sigma\rangle\rangle \otimes ||1\rangle\rangle$ , and  $||\sigma\rangle\rangle \otimes ||\epsilon\rangle\rangle$ . Ellwood invariants goes in the same fashion as in the case of the single Ising model and they are only multiplied by  $\pm 1$  or 0, which correspond to the appropriate multiplication with  $||\sigma\rangle\rangle$ . Looking at the table 3.4 we can see that these solutions correspond to the condensation into the fractional D1-brane in the orbifold picture.

Solution	1	2	3	4
$ B_\Psi\rangle$	$  1\rangle\rangle \otimes   1\rangle\rangle$	$  1\rangle\rangle \otimes   \epsilon\rangle\rangle$	$  \epsilon\rangle\rangle \otimes   1\rangle\rangle$	$  \epsilon\rangle\rangle \otimes   \epsilon\rangle\rangle$
$c_1 0\rangle$	0.23926	0.23926	0.23926	0.23926
$c_1 \epsilon^{(1)}\rangle$	-0.16828	0.16828	-0.16828	0.16828
$c_1 \epsilon^{(2)}\rangle$	-0.16828	-0.16828	0.16828	0.16828
$c_1 \epsilon^{(1)}\epsilon^{(2)}\rangle$	-0.11836	0.11836	0.11836	-0.11836

Table 5.5: Coefficients for the new D-branes found in the doubled Ising model at level one with the identification of corresponding boundary state.

If we look for the action for the field truncated to the level one

$$|\psi\rangle = tc_1|0\rangle + ac_1|\epsilon^{(1)}\rangle + bc_1|\epsilon^{(2)}\rangle + cc_1|\epsilon^{(1)}\epsilon^{(2)}\rangle, \quad (5.38)$$

we can easily find

$$\mathcal{V}(t, a) = -\frac{1}{2}t^2 - \frac{1}{4}(a^2 + b^2) + \frac{1}{3}K^3t^3 + K^2t(a^2 + b^2) + \frac{2}{K}abc + \frac{1}{K}tc^2. \quad (5.39)$$

From this truncated action the orbifold picture is apparent if we compare it with the action derived in [64] for an open string field living between parallel D-branes.

At the level one, new four solutions can be found. Their coefficients differ only by relative sign and they are mentioned in the table 5.5. Picking up one of the solutions and performing the computation up to the level 16, we find results from the table 5.6. Comparing the listed coefficients with the one obtained simply by tensor multiplication of the boundary states 5.1, this four new solutions can be interpreted as  $||1\rangle\rangle \otimes ||1\rangle\rangle$ ,  $||1\rangle\rangle \otimes ||\epsilon\rangle\rangle$ ,  $||\epsilon\rangle\rangle \otimes ||1\rangle\rangle$ , and  $||\epsilon\rangle\rangle \otimes ||\epsilon\rangle\rangle$  in double Ising model and their boundary states can be found simply by change of signs in some Ellwood invariants.

The extrapolated values have been obtained from the last eight coefficients. In the case of oscillating invariants Padé-Borel approximation has been used and



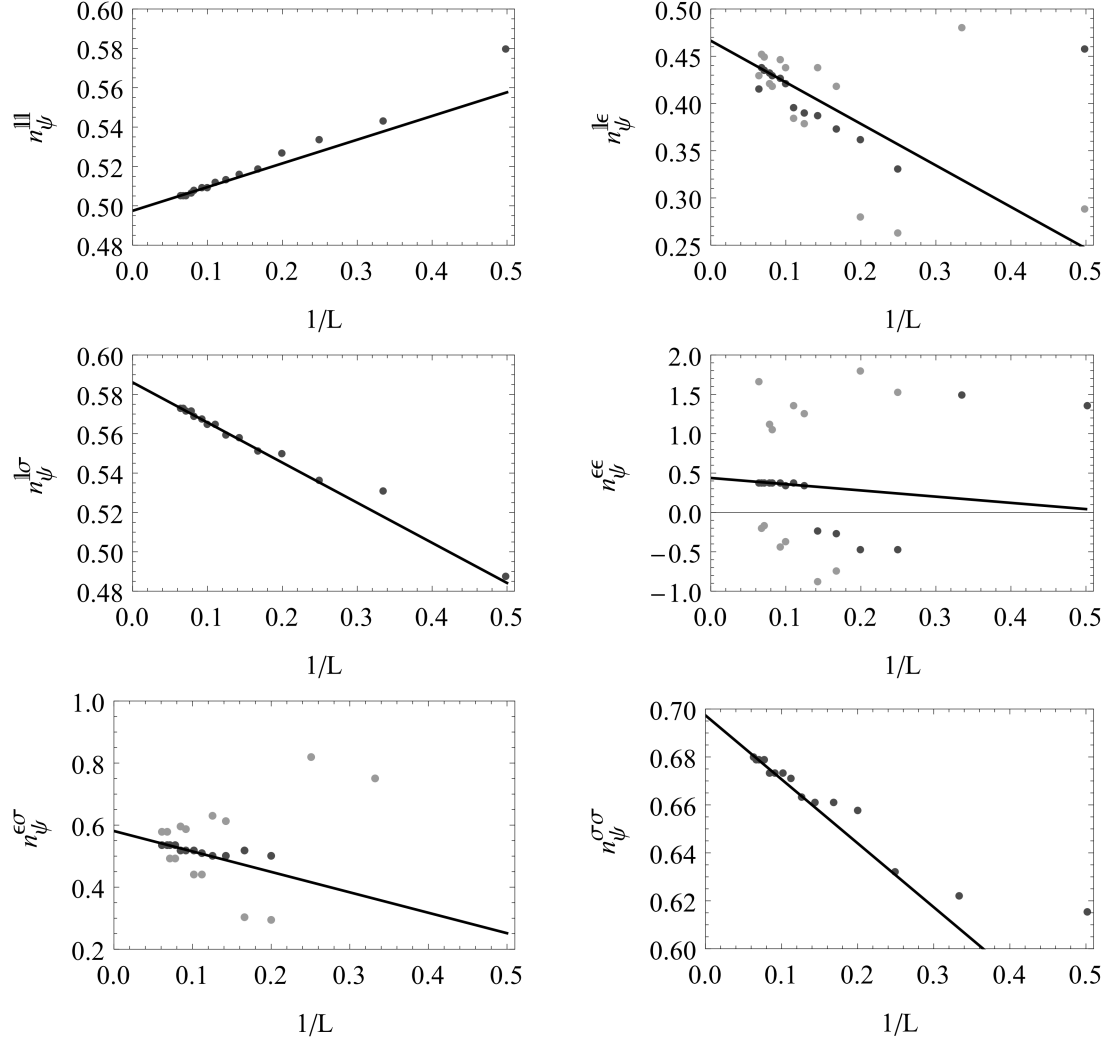


Figure 5.5: Convergence of the boundary state coefficients for the new solution found on the  $\sigma \otimes \sigma$ -brane. In the case of  $n_{\Psi}^{1e}$ ,  $n_{\Psi}^{ee}$ , and  $n_{\Psi}^{e\sigma}$ , Padé-Borrel approximation has been used to suppress oscillations. The black points correspond to the approximated values in this case.

Level	$2\pi^2\mathcal{V}(\Psi)$	$n_{\Psi}^{\mathbb{1}\mathbb{1}}$	$n_{\Psi}^{\mathbb{1}\epsilon}$	$n_{\Psi}^{\mathbb{1}\sigma}$	$n_{\Psi}^{\epsilon\epsilon}$	$n_{\Psi}^{\epsilon\sigma}$	$n_{\Psi}^{\sigma\sigma}$
2	0.60317	0.58024	0.28858	0.48785	-1.15740	-0.48785	0.61593
4	0.54447	0.53344	0.26231	0.53601	1.54237	0.81851	0.63243
6	0.52870	0.51879	0.41792	0.55168	-0.75631	0.29982	0.66158
8	0.52138	0.51333	0.37867	0.55949	1.25240	0.62768	0.66279
10	0.51714	0.50931	0.43869	0.56491	-0.38660	0.44261	0.67291
12	0.51435	0.50741	0.41674	0.56832	1.05267	0.59137	0.67384
14	0.51237	0.50559	0.44966	0.57120	-0.16680	0.49358	0.67917
16	0.51095	0.50544	0.42829	0.57314	1.64889	0.57983	0.67975
$\infty$	0.50021	0.49748	0.46636*	0.58607	0.43794*	0.58094*	0.69734
Exp.	0.5	0.5	0.5	0.59460	0.5	0.59460	0.70711

Table 5.6: Convergence of the boundary coefficients of the new solutions found in the double Ising model. \* labels coefficients that have been found using Padé-Borel approximation as in the previous section.

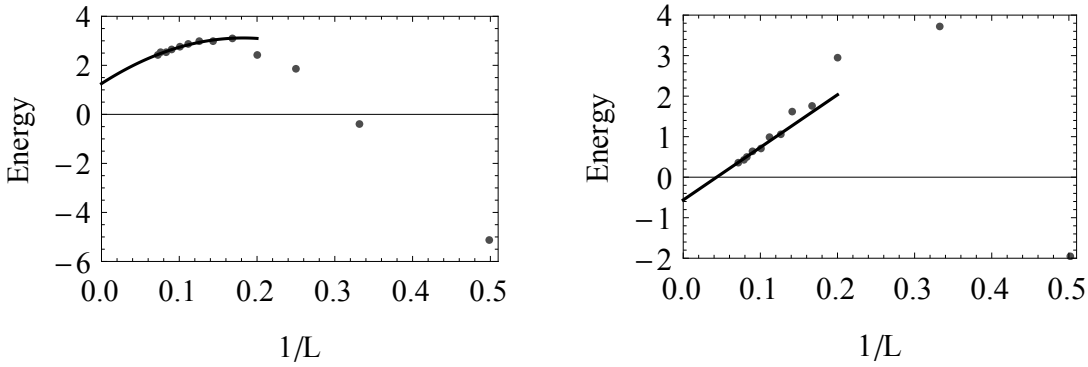


Figure 5.6: Real and imaginary part of the energy of the complex solution found on the  $\sigma \otimes \sigma$ -brane. We predict that the imaginary part vanishes above the level 23 from the linear extrapolation.

extrapolated data obtained with this approximation are labeled by \*. In the case of double Ising model a bit bigger disagreement emerges. In the case of  $n_{\Psi}^{\epsilon\epsilon}$  coefficient, it is about 16 %. The convergence is still good enough to surely interpret the solution. We can see that the oscillations grow with increasing conformal weight.

The solution shown in the table above can be interpreted as  $\|1\rangle \otimes \|1\rangle$  as can be checked comparing the boundary state coefficients. From the relations  $\sigma \otimes \sigma = \sqrt{2} \cos X / \sqrt{2}$  and  $\frac{1}{2}(\epsilon \otimes \mathbb{1} + \mathbb{1} \otimes \epsilon) = \cos \sqrt{2} X$  we can see that the nonzero coefficient  $n_{\Psi}^{\epsilon\epsilon}$  and vanishing difference  $n_{\Psi}^{\mathbb{1}\epsilon} - n_{\Psi}^{\epsilon\mathbb{1}} = 0$  is in correspondence with the statement that the position of the corresponding lumps is 0 or  $\pi R$  respectively. The lump profile can be easily drawn and the solution corresponds to the condensation of the original centered bulk D0-brane that interacts with its mirror image into the fractional D0-brane placed at the orbifold singularity.

Finally, we will discuss a complex solution found in the double Ising model that does not correspond to any of the above D-branes obtained as tensor multiplication of the Ising model boundary states. Moreover, it is conjectured not to be a solution corresponding to some integer combination of these solutions and

Level	$n_{\psi}^{\mathbb{1}\mathbb{1}}$	$n_{\psi}^{\mathbb{1}\epsilon}$	$n_{\psi}^{\mathbb{1}\sigma}$
2	$1.87205 - 0.65873i$	$2.76933 - 24.0032i$	$1.72340 - 0.58336i$
4	$1.41624 + 0.13575i$	$-9.42168 - 11.0881i$	$0.46075 - 0.78530i$
6	$1.30925 + 0.02542i$	$-12.08010 - 0.76995i$	$0.37338 - 0.45259i$
8	$1.29759 - 0.06266i$	$-11.07330 - 4.54310i$	$0.31235 - 0.31617i$
10	$1.27567 - 0.09428i$	$-6.22506 - 1.08487i$	$0.28629 - 0.23494i$
12	$1.26520 - 0.10277i$	$-6.28963 - 1.34765i$	$0.26587 - 0.18755i$
14	$1.24770 - 0.10742i$	$-4.00383 + 0.14905i$	$0.25303 - 0.15626i$
$\infty$	1.21095	2.65083*	0.13665

Level	$n_{\psi}^{\epsilon\epsilon}$	$n_{\psi}^{\epsilon\sigma}$	$n_{\psi}^{\sigma\sigma}$
2	$-7.4107 + 48.6651i$	$-1.72340 + 0.58336i$	$-3.06497 - 0.44089i$
4	$34.2795 - 22.1599i$	$9.52807 + 7.02241i$	$-2.23681 + 2.32752i$
6	$3.0951 + 54.2758i$	$-2.37738 + 5.62347i$	$-0.22515 + 3.16732i$
8	$28.1975 - 54.5559i$	$5.13751 - 0.27363i$	$-0.45171 + 2.77718i$
10	$-23.8878 + 44.0841i$	$-1.94025 + 1.20794i$	$-0.15413 + 2.28524i$
12	$32.2743 - 33.9938i$	$2.54769 + 0.14870i$	$0.01053 + 1.98463i$
14	$-29.0102 + 26.4553i$	$-1.28572 + 0.33440i$	$0.14835 + 1.73229i$
$\infty$	-3.3499*	-0.68618*	0.32273

Table 5.7: Boundary state coefficients of the complex solution in the double Ising model. The other coefficients that are not mentioned are  $n_{\psi}^{\mathbb{1}\epsilon} = n_{\psi}^{\epsilon\mathbb{1}}$ ,  $n_{\psi}^{\mathbb{1}\sigma} = n_{\psi}^{\sigma\mathbb{1}}$ , and  $n_{\psi}^{\sigma\epsilon} = n_{\psi}^{\epsilon\sigma}$ . It does not seem to be a solution corresponding to some integer combination of the nine D-branes discussed above. We conjecture the solution to be bulk D1-brane. To give precise interpretation, we would have to perform computations to higher levels and probably find Ellwood invariants for primary states with higher weights.

we conjecture that it corresponds to bulk D1-brane. In the figure 5.6, the real and imaginary part of the energy is mentioned. From the linear regression, we see that the imaginary part disappears above the level 23. We have performed extrapolation of the real part of the energy with the use of quadratic function to get better agreement with the coefficient  $n_{\psi}^{\mathbb{1}\mathbb{1}}$ . The extrapolated value is 1.25404. The Ellwood invariants computed for this solution are shown in the table 5.7. One may guess from the energy of this solution that it should correspond to some combination of fractional D0-brane and fractional D1-brane. Looking at corresponding boundary states,  $n_{\psi}^{\sigma\mathbb{1}}$  and  $n_{\psi}^{\mathbb{1}\sigma}$  of the combined boundary states is not equal for any of these boundary states. We conclude that the solution is not the combination of fractional D0-brane and fractional D1-brane since these coefficients are equal in our solution. Precise interpretation of this solution would need higher level computations and inclusion of the higher-weight Ellwood invariants. We can also expect that convergence of the Ellwood invariants change dramatically after the complex part disappears and it is not easy to make predictions.



# Conclusion

We have reviewed basics of the Ising model and discussed briefly methods used to solve it. We have also argued that lattice models can be described by means of CFT if we are at the critical point. In the case of two dimensions, CFT provides classification of universality classes of lattice models with central charge  $c \leq 1$ , where all unitary theories have been found. Conformal invariance gives constraints on the correlators of the fields present in the theory. If the theory is defined in two dimensions, conformal group becomes infinitely dimensional and the restrictions on the theory big enough to solve the model. Arbitrary correlator can be computed using sewings of 3-point amplitudes.

Boundary problems in two-dimensional CFT are reviewed and brief comments on sewing constraints are given. CFT approach to SFT is set up and method of level truncation and generalized Ellwood invariants are discussed.

String field theory and the Ellwood conjecture allows us to classify all BCFTs, i.e. find all boundary states of the theory. From each solution to SFT equations of motion we can construct a boundary state. The new method avoids solving difficult set of sewing constraints since it is believed that the equations of motion provide consistent solutions automatically.

Boundary states can be constructed numerically by means of level truncation. The only ingredient we need is the knowledge of structure constants in one BCFT background and all the other boundary states can be then constructed. Unlike RG methods limited by the  $g$ -theorem, boundary states with higher energy can be constructed.

We give details of the computations from our paper [1] in preparation and key statements are supported by pictures, graphs, and tables. The Ising model SFT is constructed and new solutions of the equations of motion are found in this theory numerically up to the level 20 and 22 respectively. Corresponding boundary states are constructed and agree quite well with analytical results.

We discuss the double Ising model and its duality with the free boson on an orbifold. We compare their spectra and find some of the boundary states using level truncation method again. Correspondence between double Ising model D-branes and free boson D-branes is clarified on the lower levels.

We conclude that level truncation and generally methods commonly used in SFT can be efficiently used in CFT and statistical physics.

Still many open questions remain. Let us list some of them. First of all, application of the methods for other minimal models to find boundary states would be interesting. Even more interesting are the questions concerning boundary states in folded models for higher minimal models that have not been yet understood. Tensor products of the simple boundary states still remain to be boundary states, but the solution for the most general boundary states. The application to the non-minimal model theories can be also interesting.

More fundamental questions are following. How can boundary and bulk-boundary structure constants on the new D-brane be extracted from SFT and are they also so easily computable? How are the sewing constraints encoded in the SFT equations of motion?

In the case of the Ising model, finding the solution analytically would probably

lead to a huge progress in SFT and hopefully the solution will be found soon. Also, it would be nice to complete our SFT level-truncation construction of Ising model boundary states by finding the solution for  $\mathbb{1}$ -brane on  $\epsilon$ -brane (and vice versa). The solution to this problem would complete our discussion on the Ising model boundary states obtained by means of level truncation.

In the double Ising model much more open questions remain. Finding and classifying solutions of string field theory corresponding to all boundary states has not been done here. The procedure has been hinted showing that at finite truncation level there are additional (complex) solutions that may in the infinite level limit converge to some new real D-brane solutions. There is a problem with convergence of the solutions and also with the convergence of higher Ellwood invariants, which only rarely converge if we get above conformal weight 1 of corresponding primary operator. Making the convergence better and accessing higher levels would enable us to find new solutions.

# Bibliography

- [1] M. Kudrna, M. Rapčák and M. Schnabl, “Ising model conformal boundary conditions from string field theory,” *in preparation*
- [2] E. Ising, “Beitrag zur Theorie des Ferromagnetismus,” Z. Phys. **31** (1925) 253
- [3] Baxter, J. Rodney, “Exactly solved models in statistical mechanics,” London (1982) Academic Press Inc.
- [4] C. Itzykson, J.M. Drouffe, “Statistical field theory,” Cambridge (1989) Cambridge University Press
- [5] G. Mussardo, “Statistical field theory,” Oxford (2009) Oxford University Press
- [6] H.E. Stanley, “Scalling, universality, and renormalization: Three pillars of modern critical phenomena” Rev. Mod. Phys. 71, no. 2 (1999) 358
- [7] A. M. Polyakov, A. A. Belavin and A. B. Zamolodchikov, “Infinite Conformal Symmetry of Critical Fluctuations in Two-Dimensions,” J. Statist. Phys. **34** (1984) 763.
- [8] P. H. Ginsparg, “Applied Conformal Field Theory,” hep-th/9108028.
- [9] J. Polchinski, “String theory,” Cambridge (1998) Cambridge University Press
- [10] J. L. Cardy, “Boundary conformal field theory,” hep-th/0411189.
- [11] J. Polchinski, “Dirichlet Branes and Ramond-Ramond charges,” Phys. Rev. Lett. **75** (1995) 4724 [hep-th/9510017].
- [12] J. L. Cardy, “Boundary Conditions, Fusion Rules and the Verlinde Formula,” Nucl. Phys. B **324** (1989) 581.
- [13] M. Oshikawa and I. Affleck, “Boundary conformal field theory approach to the critical two-dimensional Ising model with a defect line,” Nucl. Phys. B **495** (1997) 533 [cond-mat/9612187].
- [14] A. Recknagel, D. Roggenkamp and V. Schomerus, “On relevant boundary perturbations of unitary minimal models,” Nucl. Phys. B **588** (2000) 552 [hep-th/0003110].
- [15] M. Kormos, I. Runkel and G. M. T. Watts, “Defect flows in minimal models,” JHEP **0911** (2009) 057 [arXiv:0907.1497 [hep-th]].
- [16] E. Witten, “Noncommutative Geometry and String Field Theory,” Nucl. Phys. B **268** (1986) 253.
- [17] A. Sen, “Descent relations among bosonic D-branes,” Int. J. Mod. Phys. A **14** (1999) 4061 [hep-th/9902105].

- [18] A. Sen, “Universality of the tachyon potential,” JHEP **9912** (1999) 027 [hep-th/9911116].
- [19] N. Moeller, A. Sen and B. Zwiebach, “D-branes as tachyon lumps in string field theory,” JHEP **0008** (2000) 039 [hep-th/0005036].
- [20] D. Gaiotto, L. Rastelli, A. Sen and B. Zwiebach, “Ghost structure and closed strings in vacuum string field theory,” Adv. Theor. Math. Phys. **6** (2003) 403 [hep-th/0111129].
- [21] A. Hashimoto and N. Itzhaki, “Observables of string field theory,” JHEP **0201** (2002) 028 [hep-th/0111092].
- [22] I. Ellwood, “The Closed string tadpole in open string field theory,” JHEP **0808** (2008) 063 [arXiv:0804.1131 [hep-th]].
- [23] M. Kudrna, C. Maccaferri and M. Schnabl, “Boundary State from Ellwood Invariants,” arXiv:1207.4785 [hep-th].
- [24] M. Schnabl, “Analytic solution for tachyon condensation in open string field theory,” Adv. Theor. Math. Phys. **10** (2006) 433
- [25] M. Fisher, “The theory of equilibrium critical phenomena,” Rep. Prog. Phys. **30** (1967) 615
- [26] L.P. Kadanoff, et al., “Static Phenomena Near Critical Points: Theory and Experiment,” Rev. Mod. Phys. **39** (1967) 395
- [27] J.L. Cardy, “Scaling and renormalization in statistical physics,” Cambridge. (1996) Cambridge University Press
- [28] N. Goldenfeld, “Renormalization Group in Critical Phenomena,” Addison-Wesley (1994)
- [29] H.A.. Kramers, G.H. Wannier, “Statistics of the two-dimensional ferromagnet,” Physical Review **60** (1941) 252
- [30] L. Osanger, “Crystal Statistics I. A Two-Dimensional Model with an Order-Disorder Transition,” Physical Review **65** (1941) 117
- [31] A.B. Zamolodchikov, “Integrals of motion of the (scaled)  $T = T_c$  Ising model with magnetic field,” Mod. Phys. A **4** (1989) 4235
- [32] G. Delfino, P. Simonetti, “The spin-spin correlation function in the two-dimensional Ising model in a magnetic field at  $T = T_c$ ,” Phys. Lett. B **383** (1996) 450
- [33] G. Delfino, G. Mussardo, “Non-integrable quantum field theories as perturbations of certain integrable models,” Nucl. Phys. B **383** (1996) 724
- [34] M.E.J. Newman, G.T. Barkema “Monte Carlo methods in statistical physics,” Oxford, USA Oxford University Press (1999) 496 p



- [35] R.E. Peierls, “On Ising’s model of ferromagnetism,” *Proc. Camb. Philos. Soc.* **32** (1936) 477
- [36] H.A. Kramers, G.H. Wannier, “Statistics of the two-dimensional ferromagnet,” *Phys. Rev.* **60** (1936) 252 and 263
- [37] M. Kac, J.C. Ward, “A combinatorial solution of the two dimensional Ising model,” *Phys. Rev.* **88** (1952) 477
- [38] E. Wong and I. Affleck, “Tunneling in quantum wires: A Boundary conformal field theory approach,” *Nucl. Phys. B* **417** (1994) 403.
- [39] J. Ashkin, E. Teller, “Statistics of two-dimensional lattices with four components,” *Phys. Rev.* **64** (1943) 178.
- [40] J. Cardy, “Conformal Field Theory and Statistical Mechanics,” [arXiv:0807.3472]
- [41] T.D. Schultz, D.C. Mattis, E.H. Lieb, “Two-dimensional Ising model as a soluble problem of many fermions,” *Ann. Phys.* **16** (1964) 856
- [42] J. L. Cardy, “Conformal Invariance And Statistical Mechanics,”
- [43] P. Di Francesco, P. Mathieu and D. Senechal, “Conformal field theory,” New York, USA: Springer (1997) 890 p
- [44] E. Kiritsis, “String Theory in a Nutshell,” Princeton (2007) Princeton University Press.
- [45] D. Tong, arXiv:0908.0333 [hep-th].
- [46] A.M. Polyakov, “Conformal symmetry of critical fluctuations,” *JETP Lett.* **12** (1970) 381
- [47] A.A. Belavin, A.M. Polyakov, A.B. Zamolodchikov, “Infinite conformal symmetry in two-dimensional quantum field theory,” *Nucl. Phys. B* **241** (1984) 763
- [48] S. Fubini, A.J. Hanson, R. Jackiw, “New approach to field theory,” *Phys. Rev. D* **7** (1973) 1932
- [49] D. Friedan, “Introduction to Polyakov’s string theory,” (1984) New York
- [50] M.A. Virasoro, “Subsidiary conditions and ghosts in dual resonance models,” *Phys. Rev. D* **1** (1970) 2933
- [51] V.G. Kac, “Contravariant form for infinite dimensional Lie algebras and superalgebras,” Berlin (1979) Springer-Verlag
- [52] B.L. Feigin, E.V. Frenkel, “Skew-symmetric differential operators on the line and Verma modules over the Virasoro algebra,” *Funct. Anal. Phys.* **17** (1989) 114
- [53] D. Friedan, Z. Qiu, S. Shenker, “Conformal invariance, unitarity and critical exponents in two dimensions,” *Phys. Rev. Lett.* **52** (1984) 1575

- [54] M.R. Gaberdiel, “Boundary conformal field theory and D-branes,” Lecture notes (2003)
- [55] Ingo Runkell, “Boundary Problems in Conformal Field Theory,” Disertation (2000) University of London
- [56] J. Cardy, “Conformal Invariance and Surface Critical Behavior,” Nucl. Phys. **B240** (1984) 514
- [57] J. L. Cardy, “Operator Content of Two-Dimensional Conformally Invariant Theories,” Nucl. Phys. B **270** (1986) 186.
- [58] N. Ishibashi, “The Boundary and Crosscap States in Conformal Field Theories,” Mod. Phys. Lett. A **4** (1989) 251.
- [59] J. L. Cardy, “Effect of Boundary Conditions on the Operator Content of Two-Dimensional Conformally Invariant Theories,” Nucl. Phys. B **275** (1986) 200.
- [60] J. L. Cardy, “Boundary Conditions, Fusion Rules and the Verlinde Formula,” Nucl. Phys. B **324** (1989) 581.
- [61] D. C. Lewellen, “Sewing constraints for conformal field theories on surfaces with boundaries,” Nucl. Phys. B **372** (1992) 654.
- [62] H. Sonoda, “Sewing Conformal Field Theories,” Nucl. Phys. B **311** (1988) 401.
- [63] V. S. Dotsenko and V. A. Fateev, “Conformal Algebra and Multipoint Correlation Functions in Two-Dimensional Statistical Models,” Nucl. Phys. B **240** (1984) 312.
- [64] J. L. Karczmarek and M. Longton, “SFT on separated D-branes and D-brane translation,” JHEP **1208** (2012) 057 [arXiv:1203.3805 [hep-th]].
- [65] W. Taylor and B. Zwiebach, “D-branes, tachyons, and string field theory,” hep-th/0311017.
- [66] E. Fuchs and M. Kroyter, “Analytical Solutions of Open String Field Theory,” Phys. Rept. **502** (2011) 89 [arXiv:0807.4722 [hep-th]].
- [67] A. Sen, “Tachyon dynamics in open string theory,” Int. J. Mod. Phys. A **20** (2005) 5513 [hep-th/0410103].
- [68] A. LeClair, M. E. Peskin and C. R. Preitschopf, Nucl. Phys. B **317** (1989) 411.
- [69] A. LeClair, M. E. Peskin and C. R. Preitschopf, Nucl. Phys. B **317** (1989) 464.
- [70] K. Bardakci and M. B. Halpern, “Explicit Spontaneous Breakdown in a Dual Model. 2. N Point Functions,” Nucl. Phys. B **96** (1975) 285.

- [71] V. A. Kostelecky and S. Samuel, “On a Nonperturbative Vacuum for the Open Bosonic String,” Nucl. Phys. B **336** (1990) 263.
- [72] I. Ellwood and M. Schnabl, “Proof of vanishing cohomology at the tachyon vacuum,” JHEP **0702** (2007) 096 [hep-th/0606142].
- [73] A. Hashimoto and N. Itzhaki, “Observables of string field theory,” JHEP **0201** (2002) 028 [hep-th/0111092].
- [74] D. Gaiotto, L. Rastelli, A. Sen and B. Zwiebach, “Ghost structure and closed strings in vacuum string field theory,” Adv. Theor. Math. Phys. **6** (2003) 403 [hep-th/0111129].
- [75] S. B. Giddings and E. J. Martinec, “Conformal Geometry and String Field Theory,” Nucl. Phys. B **278** (1986) 91.
- [76] S. B. Giddings, E. J. Martinec and E. Witten, “Modular Invariance in String Field Theory,” Phys. Lett. B **176** (1986) 362.
- [77] I. Ellwood and W. Taylor, “Gauge invariance and tachyon condensation in open string field theory,” hep-th/0105156.
- [78] L. Rastelli and B. Zwiebach, “Tachyon potentials, star products and universality,” JHEP **0109** (2001) 038 [hep-th/0006240].
- [79] D. Gaiotto, L. Rastelli, A. Sen and B. Zwiebach, “Ghost structure and closed strings in vacuum string field theory,” Adv. Theor. Math. Phys. **6** (2003) 403 [hep-th/0111129].
- [80] D. Gaiotto and L. Rastelli, “Experimental string field theory,” JHEP **0308** (2003) 048 [hep-th/0211012].
- [81] N. Moeller, A. Sen and B. Zwiebach, “D-branes as tachyon lumps in string field theory,” JHEP **0008** (2000) 039 [hep-th/0005036].



# List of Tables

1.1	All the critical exponents introduced for ferromagnets. . . . .	12
2.1	Four fundamental conformal transformations that generate whole conformal group for $d > 2$ dimensions. . . . .	28
2.2	First few states in the chiral representation of Virasoro algebra with corresponding conformal weights (levels). . . . .	38
2.3	Spectrum of primary operators in non-twisted sector of the free boson on the orbifold $S/Z_2$ with radius $R$ . . . . .	45
2.4	Characters of the three irreducible representations appearing in the Ising model CFT. . . . .	49
2.5	Primary fields in the double Ising model $CFT_I \otimes CFT_I$ with conformal weights equal or less than two. . . . .	51
3.1	Bulk structure constants for the Ising model. . . . .	66
3.2	Boundary structure constants for the Ising model. . . . .	66
3.3	Bulk-boundary structure constants for the Ising model. . . . .	66
3.4	Correspondence between D-branes in the double Ising model and in the free boson theory. The energy $\langle \mathbb{1} \rangle_B$ , coefficient characterizing type of the boundary condition $\langle \partial X \bar{\partial} X \rangle / \langle \mathbb{1} \rangle$ , and the position of the corresponding D-brane is mentioned. . . . .	68
5.1	Boundary spectrum of the Ising D-branes. . . . .	88
5.2	Boundary coefficients for the two solutions on the $\sigma$ -brane. Extrapolated and precise values are mentioned. . . . .	93
5.3	The energy and the imaginarity coefficient of the solution with positive energy on the $\mathbb{1}$ -brane. . . . .	94
5.4	Boundary coefficients for the the solutions on the $\mathbb{1}$ -brane. The coefficient labeled by $*$ corresponds to the value obtained using Padé-Borel approximation. . . . .	95
5.5	Coefficients for the new D-branes found in the doubled Ising model at level one with the identification of corresponding boundary state. . . . .	98
5.6	Convergence of the boundary coefficients of the new solutions found in the double Ising model. $*$ labels coefficients that have been found using Padé-Borel approximation as in the previous section. . . . .	100
5.7	Boundary state coefficients of the complex solution in the double Ising model. The other coefficients that are not mentioned are $n_{\psi}^{\mathbb{1}\epsilon} = n_{\psi}^{\epsilon\mathbb{1}}$ , $n_{\psi}^{\mathbb{1}\sigma} = n_{\psi}^{\sigma\mathbb{1}}$ , and $n_{\psi}^{\sigma\epsilon} = n_{\psi}^{\epsilon\sigma}$ . It does not seems to be a solution corresponding to some integer combination of the nine D-branes discussed above. We conjecture the solution to be bulk D1-brane. To give precise interpretation, we would have to perform computations to higher levels and probably find Ellwood invariants for primary states with higher weights. . . . .	101



# List of Abbreviations

CFT	Conformal Field Theory
BCFT	Boundary Conformal Field Theory
SFT	String Field Theory
RG	Renormalization Group
QFT	Quantum Field Theory
OPE	Operator Product Expansion
BPZ	Belavin-Polyakov-Zamolodchikov
NS	Neveu-Schwarz
R	Ramond
UHP	Upper Half Plane
BRST	Becchi-Rouet-Stora-Tyutin

